Role of Rieske FeS and SBPase in stomatal behaviour

Amnah M S Alamri

A thesis submitted for the degree of Doctor of Philosophy

School of Life Sciences
University of Essex
October 2021

Abstract

The biomass of a crop depends on the cumulative rate of photosynthesis and the rate of carbon fixation can be limited by the flux of CO_2 in to the leaf. Stomata regulate gaseous exchange between the leaf interior and the external air surrounding the leaf, thereby, controlling CO_2 uptake for photosynthesis, and simultaneously water loss and evaporative cooling through transpiration. Both stomatal conductance (g_s) and photosynthesis (A) respond to changes in environmental conditions and a close correlation between A and g_s is often reported. However, the mechanism(s) that co-ordinate stomatal behavior with A is not clear.

This study was conducted to investigate the role of guard cell chloroplast in stomatal function and in particular their role in the coordination between stomatal behaviour and mesophyll photosynthesis. For that, we have examined transgenic tobacco (Nicotiana tabacum) plants with altered expression levels of the Calvin cycle enzyme Sedoheptulose-1,7, bis-phosphatase (SBPase), and the electron transport protein, Rieske FeS specifically in guard cells under the control of promoter AGPase. Expression levels were quantified using an epidermal peel enrichment prep for guard cells and qPCR. High-resolution chlorophyll fluorescence imaging and infra-red gas analysis were used to assess the influence of these manipulations on photosynthesis efficiency and stomatal kinetics.

Our results revealed that the increase in Rieske FeS in guard cells resulted in a increased operating efficiency of PSII in guard cells when compared to the WT. Moreover, overexpression Rieske FeS plants showed higher stomatal

conductance and shoot biomass increased significantly (5%-10%). On other hand, significant variation in the operating efficiency of PSII in guard cells was observed in plants with altered SBPase expression. Furthermore, stomatal conductance and assimilation rates have been affected, this suggests that the greatest effect in terms of stomatal behaviour is realised by manipulation of Calvin cycle enzymes.

Acknowledgments

First, my most heartfelt thanks go to Allah for giving me the power, patience and guidance to complete my studies. I would like to express my sincere gratitude to Professor Tracy Lawson, for her continued support, help, and encouragement during my PhD studies. I will always be proud that I worked with such an exceptional supervisor and a superb scientist. Additionally, I would like to thank Dr. Ulrike Bechtold for the comments and suggestions given at all meetings. Also, I would like to thank Professor Philip Mullineaux and Dr Matthew Jones for valuable feedback during supervisory meetings. Likewise, my thankfulness goes to Dr Patricia Lopez-Calcagno for her kindness, assistance and invaluable advice.

Of course, I would also like to thank all the other members of the Plant productivity group, for their technical expertise and help in the lab. It is difficult to express in words the gratitude and the thankfulness I feel towards my family for their endless love and support. A very special thank you goes to my mother who kept motivating me, pushing me, and providing all the support. I am extremely grateful to my husband Saeed, who has stood beside me all this time and provided me with strength and support throughout my academic journey. None of this would have been possible without you. My endless thanks and gratitude also go to my brothers and sisters for always being there for me and pushing me towards hard work.

I am also grateful to King Abdul Aziz University in Jeddah, Saudi Arabia for giving me the opportunity to complete my PhD in the UK. I am truly grateful to everyone who so generously supported me and inspired me.

Table of contents

	Abstract	i
	acknowledgment	ii
	Table of contents	iv
	List of Figures	vii
	List of Tables	xiii
	List of Abbreviations	xiv

CHAPTER1

1	**Introduction**	1
1.1	Global food security	1
1.2	Major factors influencing global food security	1
2	Evolution of stomata	4
2.1	Stomata anatomy and distribution	4
2.2	Stomata function	8
2.3	Stomata responses to environmental parameters	9
2.3.1	Stomatal responses to CO_2 concentration	9
2.3.2	Stomatal responses to light	10
3	Guard cell chloroplasts	13
3.1	Guard cell osmoregulation	14
3.2	The role of guard cell chloroplasts in stomatal movement	16
3.2.1	Electron transport in guard cells	17
3.2.2	Calvin cycle activity in guard cells	18
4	Co-ordination of stomatal behavior and mesophyll photosynthesis	19
5	A role for guard cell chloroplasts and photosynthesis in coordinating mesophyll photosynthesis and stomatal behaviour	20
6	Manipulation of guard cells to understand stomatal function	22
7	Genetic manipulation of photosynthetic enzymes	25
8	Aims of the Project	27

CHAPTER 2

	Materials and Methods	28
2.1	Plant Material and Growth Conditions	29
2.2	Seed sterilisation	29
2.3	DNA Extraction	32

2.4	Polymerase chain reaction (PCR)	32
2.5	Agarose gel electrophoresis of nucleic acids	35
2.6	Isolation of Guard-cell Enriched Tissue for RNA Extraction	35
2.7	Quantitative real-time PCR	38
2.7.1	RNA extraction and DNase treatment of extracted total RNA	38
2.7.2	cDNA synthesis	39
2.7.3	Real-time quantitative RT-PCR (qRT-PCR)	40
2.8	Plant Phenotyping techniques	42
2.8.1	Thermal imaging phenotyping and porometry measurements of stomatal conductance	42
2.8.2	Chlorophyll fluorescence imaging of photosystem II operating efficiency	43
2.9	Leaf gas exchange	44
2.9.1	Intracellular CO_2 response curves (A/C_i)	44
2.9.2	PPFD-step measurements	45
2.10	Modelling gas exchange parameters	45
2.10.1	Determining the rapidity of stomatal conductance response	45
2.10.2	Determining the rapidity of net CO_2 assimilation response	46
2.11	High resolution imaging of photosynthetic efficiency in guard and mesophyll cells	47
2.12	Growth Analysis	47
2.12.1	Plant growth characteristics	47
2.13	Statistical analysis	48

CHAPTER 3

The effect of Overexpression of the Rieske FeS of the cytochrome b_6f complex in guard cells on stomatal and photosynthetic behaviour

3.1	Introduction	50
3.2	Results	54
3.2.1	Screening for primary transgenics	54
3.2.2	Molecular Biology techniques	54
3.2.2.1	DNA analysis of T3 generation plants	54
3.2.2.2	Gene expression analysis of transgenic tobacco plants using qPCR	57
3.2.3	Plant phenotyping techniques	58
3.2.3.1	Thermal imaging and stomatal conductance	58
3.2.3.2	Chlorophyll fluorescence of PSII operative efficiency	60
3.2.4	Leaf gas exchange	65
3.2.4.1	Intracellular CO_2 (A/C_i) response curves	65
3.2.4.2	Kinetics responses of g_s and A to a step change in PPFD	68
3.2.4.3	Speed of g_s response to a step change in light intensity	70
3.2.5	Photosynthetic efficiencies in guard and mesophyll cells	74

3.2.6	Plant growth characteristics	76
3.3	Discussion	78

CHAPTER 4

Alter expressing levels Sedoheptulose-1, 7-bisphosphatase (SBPase) on guard cell photosynthesis and stomatal behaviour

4.1	Introduction	83
4.2	Results	88
4.2.1	Screening for primary transgenics	88
4.2.2	Molecular Biology techniques	89
4.2.2.1	DNA analysis of T3 generation plants	89
4.2.2.2	Gene expression analysis of transgenic tobacco plants using qPCR	92
4.2.3	Plant phenotyping techniques	94
4.2.3.1	Thermal imaging and stomatal conductance	94
4.2.3.2	Chlorophyll fluorescence of PSII operative efficiency	97
4.2.4	Leaf gas exchange	105
4.2.4.1	Intracellular CO_2 (A/C_i) response curves	105
4.2.4.2	Kinetics responses of g_s and A to a step change in PPFD	111
4.2.4.3	Speed of g_s response to a step change in light intensity	114
4.2.5	Photosynthetic efficiencies in guard and mesophyll cells	118
4.2.6	Plant growth characteristics	121
4.3	Discussion	123

CHAPTER 5

General Discussion

5.1	Overall aim and main findings	129
5.2	Impact of Increased Rieske FeS protein on photosynthetic efficiency of PSII electron transport	131
5.3	Influence of altering expression levels of SBPase on guard cell quantum efficiency of PSII	132
5.4	Influence of increased Rieske FeS protein on stomatal and photosynthetic behaviour	133
5.5	The impact of manipulation of the Calvin cycle activity on stomatal responses and photosynthetic CO_2 assimilation	135
5.6	Conclusion and future works	137
	References	139
	Appendix A	168
	Appendix B	169
	Appendix C	170

List of Figures

Figure 1.1	Different stomatal morphologies.	7
Figure 2.1	Process of isolation of Guard-cell Enriched Tissue.	37
Figure 3.1	Herbicide (BASTA) screening of transgenic seeds and wild type seeds.	54
Figure 3.2	Genomic DNA screening of transformants for the presence of the transgene.	56
Figure 3.3	Quantitative PCR (qPCR) analysis of the expression of AtRieske FeS transgenic plants.	57
Figure 3.4	A comparison of leaf temperatures between wild-type (WT) and AtRieske FeS transgenic plants.	59
Figure 3.5	Stomatal conductance (g_s) of wild-type (WT) and AtRieske FeS transgenic plants.	59
Figure 3.6	Photosynthetic efficiency of wild-type (WT) and AtRieske FeS transgenic plants at two different light intensities.	62
Figure 3.7	PSII operating efficiency of the light response curves of wild-type (WT) and AtRieske transgenic plants.	63
Figure 3.8	PSII operating efficiency, *Fq'/Fm'*, at PPFD 500µmol m^{-2} s^{-1}**,** and *Fv/Fm*, at PPFD 0µmol m^{-2} s^{-1}	64
Figure 3.9	The response of net CO_2 assimilation (*A*) to intercellular [CO_2] (C_i) between 50 µmol m^{-2} s^{-1}	65

	and 1500 µmol m^{-2} s^{-1} under saturating PPFD (1500 µmol m^{-2} s^{-1}) of AtRieske FeS and WT tobacco plants.	
Figure 3.10	Photosynthetic parameters (Vc_{max}, J_{max}, A_{max}) estimated from the response of A to Ci of AtRieske FeS plants	67
Figure 3.11	Temporal response of stomatal conductance (g_s), net CO_2 assimilation (A), and intrinsic water use efficiency (W_i), to a step increase in light intensity (100-1500 µmol m^{-2} s^{-1}) for WT and AtRieske FeS tobacco plants	69
Figure 3.12	Time constants for the increases in gs (τ_{gs}) in minutes, the final value of the g_s response at 1500 µmol m^{-2} s^{-1} PPFD (g_{sF}), and difference in g_s between 100 µmol m^{-2} s^{-1} PPFD and 1500 µmol m^{-2} s^{-1} PPFD (Δg_s) following the step increase in light intensity.	71
Figure 3.13	Time constants for the increases in A (τ_A) in minutes, the final value of the A response at 1500 µmol m^{-2} s^{-1} PPFD after an increased step change in light intensity (A_F), and the difference in A between 100 µmol m^{-2} s^{-1} PPFD and 1500 µmol m^{-2} s^{-1} PPFD (ΔA) following the step increase in light intensity.	73
Figure 3.14	Comparison of guard cell and mesophyll cell photosynthetic efficiency (estimated by *Fq'/Fm'*) in leaves of wild-type (WT) and AtRieske FeS transgenic plants.	75
Figure 3.15	Growth properties of the wild-type (WT) and AtRieske FeS transgenic plants including: **(A)** leaf area and **(B)** dry weight.	77

Figure 4.1	Herbicide (BASTA) screening of transgenic seeds and wild type seeds.	88
Figure 4.2	Genomic DNA screening of transformants for the presence of the transgene of construct (2-pL2B-BAR-(pAGPase)-ASNtSBPase)	90
Figure 4.3	Genomic DNA screening of transformants for the presence of the transgene of construct (3-pL2B-BAR-(pAGPase)-AtSBPase)	91
Figure 4.4	Quantitative PCR (qPCR) analysis. The expression of antisense SBPase of construct (2-pL2B-BAR-(pAGPase)- ASNtSBPase) **(A)** and the expression of SBPase of construct (3-pL2B-BAR-(pAGPase)- AtSBPase) **(B)** in tobacco plants.	93
Figure 4.5	A comparison of leaf temperatures between wild-type (WT), transgenic plans. Construct (2-pL2B-BAR-(pAGPase)-ASNtSBPase) **(A)** and construct (3-pL2B-BAR-(pAGPase)-AtSBPase) **(B),** at two different light intensities.	95
Figure 4.6	Stomatal conductance (g_s) of wild-type (WT) and transgenic plants. **(A)** construct (2-(pL2B-BAR-(pAGPase) ASNtSBPase), and **(B)** construct (3-pL2B-BAR-(pAGPase)-AtSBPase.	96
Figure 4.7	Photosynthetic efficiency of wild-type (WT) and ASNtSBPase transgenic plants (construct (2-pL2B-BAR-(pAGPase)- ASNtSBPase) at two different light intensities	99
Figure 4.8	Photosynthetic efficiency of wild-type (WT) and AtSBPase transgenic plants of construct (3-pL2B-BAR-(pAGPase)- AtSBPase) at two different light intensities.	100

Figure 4.9	PSII operating efficiency of the light response curves of wild-type (WT) and ASNtSBPase transgenic plants of (construct 2-pL2B-BAR-(pAGPase)-ASNtSBPase).	101
Figure. 4.10	PSII operating efficiency, *Fq'/Fm'*, at PPFD 500µmol m^{-2} s^{-1}**(A),** and the maximum quantum efficiency of PSII photochemistry, *Fv'/Fm'*, at PPFD 0µmol m^{-2} s^{-1}	102
Figure 4.11	PSII operating efficiency of the light response curves of wild-type (WT) and AtSBPase transgenic plants of construct 3-pL2B-BAR-(pAGPase)-AtSBPase.	103
Figure. 4.12	PSII operating efficiency, *Fq'/Fm'*, at PPFD 500µmol m^{-2} s^{-1}**(A),** and the maximum quantum efficiency of PSII photochemistry, *Fv/Fm*, at PPFD 0 µmol m^{-2} s^{-1}	104
Figure 4.13	The response of net CO_2 assimilation (*A*) to intercellular [CO_2] (C_i) between 50 µmol m^{-2} s^{-1} and 1500 µmol m^{-2} s^{-1} under saturating PPFD (1500 µmol m^{-2} s^{-1}) of antisense SBPase and WT tobacco plants.	105
Figure 4.14	The maximum rate of carboxylation (Vc_{max}) and maximum rate of electron transport (J_{max}) estimated from the response of *A* to C_i, and the light and CO_2 saturated rate of photosynthesis (A_{max}) determined for the four independent lines of ASNtSBPase and WT tobacco plants.	107
Figure 4.15	The response of net CO_2 assimilation (*A*) to intercellular [CO_2] (C_i) between 50 µmol m^{-2} s^{-1} and 1500 µmol m^{-2} s^{-1} under saturating PPFD (1500 µmol m^{-2} s^{-1}) for overexpressing SBPase and WT tobacco plants	109

Figure 4.16	The maximum rate of carboxylation (Vc_{max}) and maximum rate of electron transport (J_{max}) estimated from the response of A to C_i, and the light and CO_2 saturated rate of photosynthesis (A_{max}) determined for the three independent lines of AtSBPase and WT tobacco plants	110
Figure. 4.17	Temporal response of stomatal conductance (g_s), net CO_2 assimilation (A), and intrinsic water use efficiency (W_i), to a step increase in light intensity (from 100 µmol m^{-2} s^{-1} to 1500 µmol m^{-2} s^{-1}) for WT and transgenic tobacco plants (ASNtSBPase & AtSBPase).	113
Figure 4.18	Time constants for the increases in gs (τ_{gs}) in minutes, the final value of the g_s response at 1500 µmol m^{-2} s^{-1} PPFD after an increased step change in light intensity (g_sF), and difference in g_s between 100 µmol m^{-2} s^{-1} PPFD and 1500 µmol m^{-2} s^{-1} PPFD (Δg_s) following the step increase in light intensity. All results for 4 independent lines of ASNtSBPase, three independent lines of AtSBPase, and WT tobacco plants.	116
Figure 4.19	Time constants for the increases in A (τ_A) in minutes, the final value of the A response at 1500 µmol m^{-2} s^{-1} PPFD after an increased step change in light intensity (A_F), and the difference in A between 100 µmol m^{-2} s^{-1} PPFD and 1500 µmol m^{-2} s^{-1} PPFD (ΔA) following the step increase in light intensity All results for 4 independent lines of ASNtSBPase, three independent lines of AtSBPase, and WT tobacco plants	117

Figure 4.20	Variation (box and whisper plots displaying distribution of biological replicates) and mean (central black line) of photosynthetic efficiency (estimated by *Fq'/Fm'*) of wild-type (WT) and transgenic tobacco plants (ASNtSBPase and AtSBPase)	120
Figure 4.21	Growth properties of transgenic tobacco plants (ASNtSBPase & AtSBPase) and WT plants, including: **(A+B)** leaf area and **(C+D)** dry weight	122

List of Tables

Table 2.1	summarises the names, descriptions and abbreviations of the *Nicotiana tabacum* mutants used in this study	31
Table 2.2	List of primers used for the presence of the construct.	34
Table 2.3	Primers sequences used for qPCR	41

List of abbreviations

A	Net CO_2 assimilation rate per unit leaf area
AGPase	ADP-glucose pyrophosphorylase
ATP	Adenosine triphosphate
A_F	The final value of the *A* response at 1500 µmol m^{-2} s^{-1} PPFD after an increased step change in light intensity
A_{max}	Light and CO_2 saturated rate of CO_2 assimilation
ANOVA	A One-way Analysis of Variance
A/C_i	Net CO_2 assimilation rate (*A*) as a function of [CO_2]
BASTA	glufosinate-ammonium herbicide
bp	base pair
cDNA	Complementary DNA
cm^2	Centimeter
CO_2	Carbon dioxide
Cyt_{b6f}	Cytochrome b_6f
CF	Chlorophyll fluorescence
Ca	external atmospheric CO_2 concentrations
C_i	Intercellular CO2 concentration
dH_2O	Distilled water
DNA	Deoxyribonucleic Acid
dNTPs	deoxyribonucleotide triphosphate
E	Transpiration
EDTA	Ethylenediaminetetraacetic Acid Tetasodium Salt
Fq'/Fm'	PSII operating efficiency
Fv/Fm	The maximum efficiency of photosystem II
G	gram
g_{sF}	The final value of the g_s response at 1500 µmol m^{-2} s^{-1} PPFD after an increased step change in light intensity
GFP	green fluorescent protein
GUS	β-glucuronidase
g_s	Stomatal conductance to water vapour
HXK	hexokinase
J_{max}	Maximum electron transport demand for RuBP regeneration
NADP	Nicotinamide adenine dinucleotide phosphate

NADPH	Nicotinamide adenine dinucleotide phosphate
NADP-MDH	NADP-malate dehydrogenase
NtSUS2	sucrose synthase 2
OAA	oxaloacetate
PCR	Polymerase chain reaction
PEPc	phosphoenolpyruvate carboxylase
pKST	K+ influx channel of guard cells in potato
PPFD	photosynthetically active photon flux density
PSI	Photosystem I
PSII	Photosystem II
qPCR	Quantitative Polymerase chain reaction
RNA	Ribonucleic acid
RuBP	Ribulose 1,5-bisphosphate
SUT1	Sucrose Transporter 1
T	Time
T3	Third generation
TAE	Tris-acetate EDTA
T-DNA	transfer DNA
Tris	Tris-(hydroxymethyl)aminomethane
τ_{gs}	Time constants for the increases in g_s
τ_A	Time constants for the increases in A
µL	Microliter
µmol m^{-2} s^{-1}	Micromole: per second and square meter
V_{Cmax}	Maximum rate of carboxylation by Rubisco
VPD	vapour pressure deficit
W_i	Intrinsic water use efficiency
WT	Wild type

CHAPTER 1

Introduction

1. Introduction

1.1 Global food security

Food security has four key elements: the availability of food; physical and economic access to food; its utilization and the stability of its provision under any circumstances (Maggio *et al.*, 2015). The production of food supply is not just the quantity but also the quality and diversity of food. Increases in the yield potential of the major crops has radically contributed to a rise in food supply over the past 50 years, which until recently has more than kept pace with rising global food demand (Zhu *et al.*, 2010; Long *et al.*, 2015). Previous studies indicate that the world demand for food will increase by between 70 and 100% by 2050, therefore, producing more food is a grand challenge for crop scientists and agronomists (Braun *et al.*, 2010; Godfray *et al.*, 2010). In the last few decades, discussions about ensure food security have largely focused on agricultural production and its associated main challenges for the agricultural system (Maggio *et al.*, 2015). Photosynthesis is the basis for all metabolic processes and therefore has the potential to be improved to keep pace with the demand for increasing plant biomass (Raines, 2006; Feng *et al.*, 2007; Zhu *et al.*, 2010; Driever *et al.*, 2017a).

1.2 Major factors influencing global food security

The expanding global population and changing climate are major factors influencing the growing demand to find suitable crop plants with increased yields for sustainable food and fuel production for future generations (Zhu *et al.*, 2010; Ray & Foley, 2013). The growing population is predicted to reach 9.5 billion by 2050, more than 34 % higher than today (FAO, 2015). The United Nations

expected that the proportion of world population will rise at an annual rate of 0.96 % from now until 2030 and at a rate of 0.63 % per year from 2030 to 2050. Based on these estimates, the world will have to feed an extra 1.62 billion by 2030 and an additional 2.38 billion people by 2050 (Maggio *et al.*, 2015). Population growth will occur mostly in urban areas, with more than 70% of the world's population concentrated in cities, compared to 49% today. The increase in population growth and urbanization with also result in less land available for agricultural use (FAO, 2015; Maggio *et al.*, 2015). Furthermore, this population growth is also associated with increasing dietary changes from staples to processed food such as meat and fresh produce, with more resources required to feed livestock than directly feeding people. These changes will have a significant impact on global demand for food and agricultural products by 50 % in 2030 and possibly by 60 %-110 % by 2050 (Von Braun *et al.*, 2005; Long *et al.*, 2015).

Climate change is an additional contributing factor influencing suitable crop production and a threat to world food security (Slingo *et al.*, 2005). Agriculture covers about 20% of cultivated land and accounts for 40% of global food production. Moreover, agriculture accounts for 70% of global fresh water use. By 2030, it is predicted that freshwater demand for agricultural use will increase by 13%, but if there is less water available due to increased agricultural, urban and industrial uses and more demand due to rapid population growth, water scarcity can cut production and adversely impact food security (Unesco, 2009; Hanjra & Qureshi, 2010). High global temperatures as a result of climate change will increase crop water requirements due to a rise in evapotranspiration and together with more erratic patterns of annual precipitation will put more pressure on increasing irrigation to sustain crop yields (Tubiello *et al.*, 2007). Drought has been

one of the major abiotic constraints of crop yield, accounting for losses of up to 40% in maize (Boyer, 1982; Harrison *et al.*, 2014) and 15% in wheat (Foulkes *et al.*, 2002, 2007). As a result of climate change, temperature is also predicted to increase between 1.8º- 4.9º C per year over the 21st century (IPPC, 2007). Future temperature increases are predicted to negatively affect global yields of key sensitive crops, including wheat (*Triticum aestivum*), maize (*Zea mays*), rice (*Oryza sativa*), and soybean (*Glycine max*)(Zhao *et al.*, 2017). Crop plant in the future must, therefore, have the capability of maintaining productivity in growth environments that are predicted to have less available water (Lawson *et al.*, 2002). With this in mind finding ways to improve plant water use efficiency (WUE) is important. WUE is defined as the ratio of carbon gained per unit of water loss, and can be calculated by the ratio of [CO_2] assimilation (*A*) to transpiration (E), WUE = *A*/*E*, intrinsic WUE can be calculated by replacing transpiration (*E*) with stomatal conductance (g_s) WUEi = *A*/ g_s (Bacon, 2009; Beer *et al.*, 2009). As stomata regulate whole plant water usage as well as CO_2 uptake for photosynthesis they are considered key targets for promoting WUE through improving CO_2 diffusion to the mesophyll while conserving water (Lawson & Blatt, 2014), and their behavior have profound impacts on the global water cycles (Keenan *et al.*, 2014; Blatt *et al.*, 2017). Over the last few decades, numerous models of stomatal, especially stomatal conductance models, were studied to explore and predict plant-environment interactions in response to the ongoing global changing climate (Buckley & Mott, 2013; Buckley, 2017; Franks *et al.*, 2018).

2. Evolution of stomata

The aerial parts of most plants have stomatal pores on their surface that are thought to have developed more than 400 million years ago (Edwards *et al.*, 1998). Stomatal evolution predates that of flowers, leaves, roots and even a vascular system, indicating their importance in the adaptation of plants to life on land and the widely fluctuating environmental conditions (Raven, 2002; Hetherington & Woodward, 2003; Peterson *et al.*, 2010). Although stomatal pores occupy only a small fraction of the total leaf surface, nearly all CO_2 absorbed and water lost pass through these pores; therefore, stomatal behaviour has a major impact on the global carbon and hydrological cycles (Lawson & Blatt, 2014). It is estimated that over 98% of water taken up by plant is lost to the atmosphere through the stomatal pores (Hetherington & Woodward, 2003; Lawson, 2009). Selecting plants which optimise the balance between water loss and carbon gain is not only essential in order to reduce the fresh water allocated to crop irrigation but also to maintain yields under increasingly unpredictable field environments (Lawson & Blatt, 2014).

2.1 Stomata anatomy and distribution

Stomata have been observed more frequently on the lower surface of leaves but their occurrence on both surfaces has also been commonly reported (Kramer & Boyer, 1995). Herbaceous plants are often amphistomatous meaning stomata are found on both adaxial (upper) and abaxial (lower) leaf surfaces although the ratio is not always equal between the two leaf surfaces, with more stomata often found on the abaxial surface of the leaf (Tichá, 1982). In some species for example trees, stomata can be present on the lower leaf surface and the leaf is known as

hypostomatous, while other species have stomata on the upper surface and the leaf is termed epistomatous (Lawson, 2009).

A stoma is formed by a pair of guard cells which change in shape to alter the pore aperture and therefore play a key role in controlling CO_2 uptake for photosynthesis, relative to water loss via transpiration (Farquhar & Sharkey, 1982). Morphologically, guard cells can be classified by their shape, into either elliptical (kidney-shaped) or graminaceous (dumbbell-shaped)(Hetherington & Woodward, 2003). Elliptical ,or kidney-shaped guard cells were the first to evolve and found in the first land plant 400 Mya, while graminaceous, or dumbbell-shaped guard cells evolved within the last 55-70 million years (Kellogg, 2001; Peterson *et al.*, 2010). Stomatal anatomical characteristics play an essential role in the aperture size of stomata, functioning as hydraulic valves that respond to the environment (Hetherington & Woodward, 2003; Franks & Farquhar, 2007). The characteristic graminaceous (dumbbell-shaped) guard cells have bulbous ends and a long slit located between the two 'handles' of the dumbbells, while the elliptical (kidney-shaped) guard cells have an obvious elliptical curve with the pore at its center (Figure 1). A distinctive feature of the guard cell is the structure and thickening of the cell walls, which is 2-3 times bigger than that of the adjacent epidermal cells, often with thicker ventral walls (nearer the pores) which are inelastic and thinner dorsal walls (nearer the epidermal cells) (Evert, 2006; Taiz & Zeiger, 2010; Carter *et al.*, 2017). Elliptical guard cells are connected at the two ends and have cellulose microfibrils fanning out radially from the pore, reinforcing the girth, causing the cells to curve during opening, which results in the aperture of the exposed pore (Evert, 2006). Whereas dumbbell shaped guard cells function like beams, with bulbous inflatable ends. When the bulbous ends of the cells

increase in volume and swell, the beams are separated from each other and the slits between them widen. The adaptation of the dumbbell guard cells relative to the elliptical guard cells is the uses of a smaller amount of change in water to swell and therefore a reduced response time which could support higher WUE particularly in dynamic environments (Hetherington & Woodward, 2003; Evert, 2006; Taiz & Zeiger, 2010; Vialet-Chabrand *et al.*, 2017a). In some species, the guard cells are associated with subsidiary cells, and the pair of guard cells and subsidiary cells form the stomatal complex. Subsidiary cells are believed to play a role in regulation of stomatal aperture either mechanically or as ion reserves (Franks & Farquhar, 2007; Chen *et al.*, 2017).

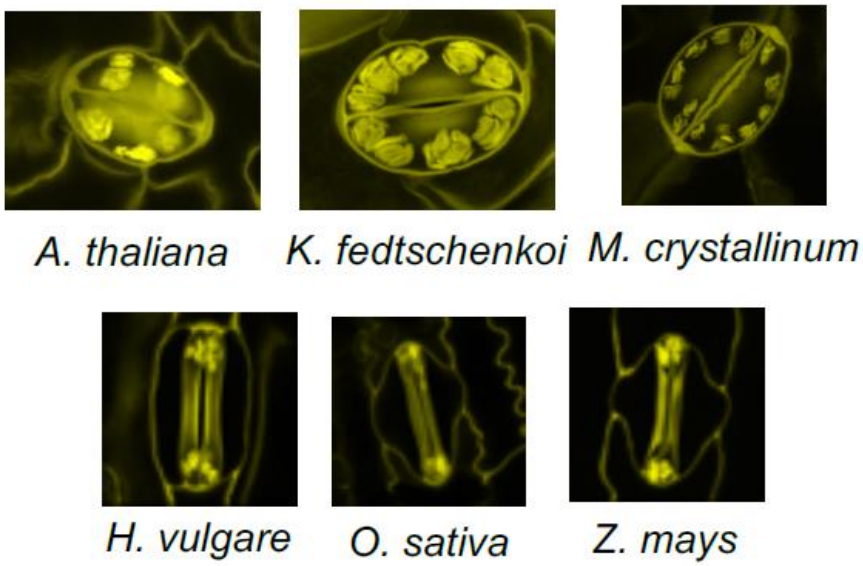

Figure 1.1 Different stomatal morphologies. The upper panel shows kidney-shaped stomata of dicot species; for example (***Arabidopsis thaliana***, ***Kalanchoe fedtschenkoi*** and ***Mesembryanthemum crystallinum***), the lower panel shows dumb-bell-shaped stomata of monocot species; for example (***Hordeum vulgare***, ***Oryza sativa*** and ***Zea mays***). Pictures are taken from (Flütsch & Santelia, 2021).

2.2 Stomata function

Stomata control the gaseous exchange between the interior of the leaf and the external environment and therefore control CO_2 uptake for photosynthesis and water loss through transpiration (Farquhar & Sharkey, 1982). Early studies (Wong *et al.*, 1979; Hosy *et al.*, 2003; Fischer & Edmeades, 2010) showed that reduced stomatal conductance has major implications for the photosynthetic assimilation rates (*A*). It is known that stomatal conductance correlates closely with the rate of photosynthetic assimilation, even under conditions of differing nutrient levels, light intensities and of [CO_2] (Wong *et al.*, 1979; Hetherington & Woodward, 2003). However, although this relationship appears constant in the long-term, short-term dynamic changes in the environment can bring about a disconnect between photosynthesis and stomata behavior (Farquhar & Sharkey, 1982; Lawson, 2009). This is mostly due to the fact that the response time of stomata are often an order of magnitude slower than photosynthetic responses and result in a lag in stomatal behaviour. For instance, photosynthetic response rates are typically measured in terms of just a few seconds, whereas stomatal response rates vary between a number of seconds and tens of minutes (Lawson *et al.*, 2010). With increased light intensity, the slow response rate of stomata can cause low g_s that restricts the diffusion of CO_2 and restricts photosynthesis (McAusland *et al.*, 2016). This restriction will influence the biomass negatively with consequences for crop yield. For instance, studies of C3 crop species have confirmed that well-watered plants that have lower g_s can experience a 20% reduction in rates of photosynthesis (Fischer *et al.*, 1998), and it is quite possible that this observation is attributable to

the time required for stomata to respond (Lawson & Blatt, 2014; Mcausland *et al.*, 2017).

2.3 Stomata responses to environmental parameters

As discussed above, stomata respond to changes in external environmental factors such as light intensity, [CO_2] temperature and vapour pressure deficit (VPD) either directly or indirectly and therefore influence photosynthetic rates, transpiration and evaporative leaf cooling (Huxman & Monson, 2003; Lawson *et al.*, 2010). In general, stomatal opening is stimulated under light, low CO_2 and high humidity, whereas closure occurs under conditions of darkness, high CO_2, low humidity and high temperatures (Outlaw & William, 2003; Lawson *et al.*, 2010). The typical responses outlined above are customary for stomata of C_3 and C_4 plants. However, plants with crassulacean acid metabolism (CAM) are an exception to this with stomata opening in darkness and close during the day when light is present (Black & Osmond, 2003).

2.3.1 Stomatal responses to CO_2 concentration

In order to ensure that plants are best able to manage their use of water and demand for carbon, stomatal conductance is responsive to [CO_2]. Under short-term exposure, stomata tend to respond to low [CO_2] by opening while closure is induced by high [CO_2] (in both darkness and light) (Lawson *et al.*, 2010). Long term exposure may lead to physiological acclimation of stomata, for example reduced sensitivity to CO_2 when compared to those exposed under short term (Lodge *et al.*, 2001; Maherali *et al.*, 2002; Ainsworth & Rogers, 2007).

Growth conditions also influence the responses of stomata. For instance, when *Vicia faba* plants are placed in a growth chamber and subjected to ambient CO_2 concentrations, they demonstrated more pronounced responses relative to plants that had been grown in a greenhouse. This was attributed to the acclimation process is intrinsic to the guard cell (Frechilla *et al.*, 2002). However, it is quite possible that changes in humidity or light levels could also have influenced these observations. Additionally, sensitivity to CO_2 has been shown to have decrease either under well-watered conditions or in regions associated with low evaporative demands (Lawson *et al.*, 2010). It is thought that the guard cells are responsible for sensing CO_2 concentration in the atmosphere because epidermal peels have revealed evidence of responses to CO_2 (Fitzsimons & Weyers, 1986) and it is widely believed that guard cells might sense intercellular CO_2 concentration (*Ci*) instead of external atmospheric CO_2 concentrations (*Ca*)(Mott, 1988). However, some research on transgenic plants has indicated that stomata might respond to *Ca* and not *Ci* (von Caemmerer *et al.*, 2004). Plants subjected to an increase in *Ca* concentrations closed their stomata, while at ambient *Ca* stomatal conductance was similar in both transgenic plants and wild type (WT) even when *Ci* concentrations were increased as a result of reduced photosynthetic rates (von Caemmerer *et al.*, 2004; Baroli *et al.*, 2008).

2.3.2 Stomatal responses to light

Light is one of the most dynamic environmental parameters that directly affects plant performance. Leaves experience a range of light environments over their lifetime, and therefore plants acclimate to the light environment under which they are grown to maintain performance and fitness and this is known as photosynthetic

acclimation (Vialet-Chabrand *et al.*, 2017b). Long-term, they can acclimate to these conditions by modifying leaf anatomy and morphology and, in particular, stomatal characters (Lawson *et al.*, 2010). Short-term changes to fluctuating environmental conditions result in changes to the plant physiology, in particular to dynamic photosynthetic and stomatal responses (Casson & Gray, 2008; Casson & Hetherington, 2010; Matthews *et al.*, 2018). There are two elements to the response of stomata to light: the photosynthetic dependent red light response and the photosynthesis-independent blue light response (Hiyama *et al.*, 2017; Inoue & Kinoshita, 2017; Matthews *et al.*, 2020).

The photosynthesis-independent blue light response, which is sensed by guard cells results in rapid opening (Zeiger, 2000; Shimazaki *et al.*, 2007). It has been proposed that the blue light response of guard cells is of special importance for morning pore opening, facilitating photosynthesis when the light spectrum is enriched in blue wavelengths (Schwartz & Zeiger, 1984). Blue light receptors (phototropins 1 and 2) trigger the plasma membrane H+-ATPase by means of phosphorylation, therefore stomatal opening (Inoue & Kinoshita, 2017). Guard cells are able to take up K^+ through the K^+-channels due to a change in membrane potential. The uptake of K^+ is related to the synthesis of malate^{2-} and/or the uptake of Cl^-. When there is blue light, malate^{2-} is produced as a result of starch in the guard cells being broken down (Shimazaki *et al.*, 2007). Accumulation of these ions support osmotic adjustment of guard cells and thus lead to stomatal movement (Shimazaki *et al.*, 2007; Kim *et al.*, 2010; Marten *et al.*, 2010; Horrer *et al.*, 2016; Inoue & Kinoshita, 2017). Possible blue light receptors put forward have included zeaxanthin and phototropins. The reason why zeaxanthin was thought to

be a receptor is because of research conducted into epidermal peels of Arabidopsis mutants lacking zeaxanthin that were unresponsive when subjected to blue light (Zeiger1 & Zhu, 1998; Frechilla *et al.*, 1999). However, when this experiment was repeated with whole leaves, it was not possible to achieve the same result (Eckert & Kaldenhoff, 2000), and it is now accepted that zeaxanthin is most likely not the blue light receptor (Roelfsema *et al.*, 2006).

The second component of light is the photosynthesis-dependent red-light response which refers to the response driven by photosynthesis (Sharkey & Raschke, 1981). In red light conditions, the opening of stomata could be caused by a reduction in intercellular CO_2 concentration caused by the process of photosynthesis (Roelfsema *et al.*, 2002). However, experiments using entire leaves reveal that the stomata open in response to red light even if the intracellular concentration of CO_2 is maintained at a certain level (Messinger *et al.*, 2006). Furthermore, it is not thought that the red-light response is indirect and caused when red light brings about mesophyll photosynthesis and *Ci*. It is likely to also come about because of the direct response of guard cells when subjected to red light (Shimazaki *et al.*, 2007). Numerous studies have demonstrated that stomata open in the isolated epidermis when red light is present, and thus this response is determined by the guard cell chloroplasts, and also is suppressed by DCMU, an inhibitor of electron transport. No red response was observed in the epidermis of the orchid, *Paphiopedilum*, which has chlorophyll-free guard cells and (Schwartz & Zeiger, 1984; Tominaga *et al.*, 2001; Olsen *et al.*, 2002). If red and blue light are used in combination, stomatal conductance is greater than the sum of the stomatal conductance when red or blue light are used in isolation. Therefore, this indicates that there is a synergistic action when the stomata in whole leaves open.

This synergistic effect for the movement of stomata is likely to rely on both *Ci* and guard cell chloroplasts. When *Ci* is adjusted using gas exchange techniques, this changes the extent of the response to blue light. This suggests that a stomatal response to the reduction of *Ci* caused by mesophyll photosynthesis could lie behind why blue and red light are synergistic (Shimazaki *et al.*, 2007).

3. Guard cell chloroplasts

Guard cells in most species of plant have chloroplasts. Palisade mesophyll cells have between 30-70 chloroplasts compared with 10-15 chloroplasts per guard cell (Willmer & FRicker 1990; Lawson, 2009). However, the number of chloroplasts varies depending on species, in some species, e.g. *Selaginella*, each guard cell has only 3-6 chloroplasts, whilst up to 100 can be found in *Polypodium vulgare* (Stevens & Martin, 1978). Moreover, some species, e.g. *Paphiopedilum* species, guard cells still maintain functional stomata although these cells lack chloroplasts (Nelson & Mayo, 1975). Another feature of chloroplasts in guard cells, is that they are often smaller and less well-developed than those in mesophyll cells, although this feature also depends on species. Moreover, guard cell chloroplasts have a reduced thylakoid network and chlorophyll content compared to mesophyll cells (Shimazaki & Okayama, 1990), however guard cell chloroplasts have been shown to have functional photosystems I and II, electron transport, oxygen evolution and photophosphorylation (Zeiger *et al.*, 1980; Outlaw *et al.*, 1981; Shimazaki *et al.*, 1982; Hipkins *et al.*, 1983; Lawson *et al.*, 2002). Furthermore, guard cell chloroplasts have been observed to accumulate starch in the dark that is rapidly degraded within 30 min of light. Whereas the reverse is true in mesophyll cells (Horrer *et al.*, 2016).

Controversies regarding the function of guard cell chloroplasts and the contribution of mesophyll in stomatal movements have persisted for several decades. This could be due to multiple roles for guard cell chloroplasts in photosynthetic carbon fixation for osmoregulatory processes or acting as a sensing and signaling mechanism (Zeiger *et al.*, 2002). However, before discuss guard cell photosynthesis, it is important to elucidate the guard cell osmoregulation and the role of solute contents in guard cells.

3.1. Guard cell osmoregulation

In the last decades, stomatal physiology researches have focused on the mechanisms of guard cell osmoregulation and the relationship between photosynthesis of guard cells and stomatal movements (Gotow *et al.*, 1988; Poffenroth *et al.*, 1992; Santelia & Lawson, 2016). Changes in stomatal aperture are associated with an increase or decrease in guard cell turgor, which is achieved by the osmolytes in these cells (Daloso *et al.*, 2017) and several different osmoregulatory pathways have been proposed.

The starch-sugar hypothesis was put forward in 1908 when Lloyd realised that starch levels in stomata were higher when the stomata were closed during the night (dark conditions) than they were when the stomata were open during the day (light conditions). This theory relates to the interconversion of starch to sugar that brings about osmotic changes which, in turn, changes osmotic potential and results in the update of water into the guard cells that leads to alterations in cell turgor. The starch-sugar hypothesis remained the most widely-recognized theory of osmoregulatory mechanisms throughout much of the twentieth century

(MacRobbie & Lettau, 1980). It was in the 1960s that the starch-sugar theory was superseded by the K^+-malate^{2-} theory when Fischer recognised the role that potassium uptake plays in the opening of stomata (Fischer, 1968; Fischer & Hsiao, 1968). More specifically, Fischer confirmed that the uptake of potassium in guard cells was associated with the opening of stomata, with the counterion being either malate^{2-}, chloride (Cl^-) or both (Fischer, 1968; Willmer & Fricker, 1996; Asai *et al.*, 2000). In the majority of cases, it is malate that acts as the counterion to balance the uptake of potassium. However, there are certain species in which starch is not found (e.g. *Allium cepa*) and these rely solely on chloride as their counterion (Schnabl & Raschke, 1980).

It was not until several years later that researchers realised that potassium and its counterions could not be responsible for sufficient osmoticum to support stomatal apertures in *Commelina communis* (MacRobbie & Lettau, 1980). This resulted in recognition of the role that sucrose plays in guard cell osmoregulation because soluble sugars provide the extra osmoticum required to facilitate the opening mechanism, and therefore, the osmotica required for guard cell osmoregulation comprise K^+-malate^{2-} but also sugars (Talbott & Zeiger, 1993; Talbott, 1998). Daloso *et al.*, (2015) supported an important role for sucrose in the control of stomatal opening, but the mechanism by which it does so remains far from clear and needs to be further dissected.

Over the course of the day, K^+ concentrations fall whereas sucrose concentrations increase in the guard cell. This resulted in a hypothesis being proposed that K^+ was responsible for stomata opening in the early morning. From midday, sucrose becomes the main osmolyte that is responsible for maintaining stomatal aperture

(see Lawson, 2009). In the case of sucrose in epidermal peels of *Vicia faba* and *Commelina cyanea*, Pearson (1973) found a consistent increase that mid-afternoon however the relationship between aperture and the concentration of sucrose was quite weak, questioning the contribution of sugar to the guard cells osmoticum. Therefore, the role of sucrose as a major osmolyte has not been accepted by researchers. Several researchers have hypothesised that sucrose could play a role in coordinating and stomatal behaviour and mesophyll via the apoplast (Lu *et al.*, 1995, 1997; Kang *et al.*, 2007; Lawson *et al.*, 2014). It has been shown that sucrose released from the mesophyll is accumulated in the apoplast and transported into guard cells via the transpiration stream (Lawson *et al.*, 2003; Kang *et al.*, 2007; Daloso *et al.*, 2016a). It has been suggested that during stomata opening, the concentration of sucrose within the guard cell's apoplast could be absorbed and replace potassium and malate as the osmoticum under high photosynthesis and transpiration rates (Kang *et al.*, 2007).

3.2 The role of guard cell chloroplasts in stomatal movement

It has been determined that stomatal function could be influenced by guard cell chloroplasts in four possible ways, by (i) providing ATP generated by electron transport for H^+-ATPase in guard cells; (ii) participating in blue light signaling and response; (iii) converting starch stored in the chloroplasts to malate or sucrose; and (iv) producing osmotically active sugars as a result of the assimilation of photosynthetic carbon in guard cells (Lawson, 2009).

3.2.1 Electron transport in guard cells

Studies have provided evidence for linear electron transport, photophosphorylation and oxygen evolution in the guard cells and that the rates of these processes can be modulated by CO_2 concentrations (Schwartz & Zeiger, 1984; Mawson & Zeiger, 1991; Lawson *et al.*, 2002). Several studies have reported high rates of cyclic electron flow observed in guard cell protoplasts of *Vicia faba* supported by increase PSI activity compared with the mesophyll cells, suggesting that electron transport in guard cells could result in greater ATP production (Lurie, 1977). This however did not agree with the work of Shimazaki & Zeiger (1985) who did not observe an unusually increase PSl activity in guard cells of *Vicia faba* and linear electron transport has been reported to be 80% of the mesophyll (Lawson *et al.*, 2002). Such electron transport rates could provide sufficient energy to drive ions for stomatal opening in the absence of CO_2 fixation. Goh *et al.*, (2002) have demonstrated that K^+-uptake channel activity at the guard cell plasma membrane and the photosynthetic electron transport in chloroplasts of guard cell are dependent on cystolic ATP, thus providing evidence for ATP as an important regulator linking guard cell photosynthesis and ion transport activity. It has been showed that guard cells provid ATP to the cytosol under red light, which is used for H^+ pumping by the plasma membrane H^+-ATPase and opening of stomata (Tominaga *et al.*, 2001).

3.2.2 Calvin cycle activity in guard cells

There is no consensus in the empirical literature regarding the capacity of guard cell chloroplasts to achieve photosynthetic carbon reduction. Nor is there agreement about the role it plays in stomatal function (Shimazaki *et al.*, 1989; Lawson, 2009). Early research found little to indicate Calvin cycle activity in guard cells and concluded that CO_2 is incorporated as malate (Raschke & Dittrich, 1977). Raschke and Dittrich (1977) found evidence of Calvin cycle activity and demonstrated that radioactive 3-PGA/Rubisco activity was evident when epidermal peels came into contact with $^{14}CO_2$. Subsequent research confirmed that guard cell chloroplasts were unsuited to the photosynthetic carbon reduction pathway owing to a paucity of ribulose-1,5-bisphosphate carboxylase(RuBPC) and ribulose-5-phosphate kinase (Ru5PK) activity (Outlaw & Manchester, 1979), as well as other enzymes that are required for the pathway (Outlaw *et al.*, 1979; Schnabl, 1981). These findings concluded that there was insignificant Rubisco activity, thereby supporting the previous conclusion of Hampp *et al.*, (1982) that guard cells showed no indication of photoreduction of CO_2. The early literature pointed to a lack of carbon fixation in guard cell chloroplasts but studies in the last two decades have shown that photosynthetic carbon fixation does takes place in the guard cells (Lawson, 2009).

Numerous studies have shown various Calvin cycle enzymes are present in guard cells of intact leaves (Zeiger *et al.*, 1980). Cardon & Berry, (1992) observed that guard cell chloroplasts are capable of fixing CO_2 as chlorophyll fluorescence kinetics were altered by different O_2, suggesting that the end produces of electron transport are used in photorespiration as well as CO_2 fixation in guard cells.

Additionally, photosynthetic dependence of sucrose accumulation was demonstrated when dichlorophenyl dimethyl urea (DCMU) was applied to epidermal peels incubated under red light (Poffenroth *et al.*, 1992). Some researchers do not believe that the rates of CO_2 fixation in the guard cells could be sufficiently high to have any functional bearing, however, the contribution to osmotic requirements for open the stomata has been shown to vary from 2%- 40% (Hampp *et al.*, 1982; Outlaw, 1983; Reckmann *et al.*, 1990; Poffenroth *et al.*, 1992). Other researchers believe that the Calvin cycle acts as a sink for the output from photosynthetic electron transport (Cardon & Berry, 1992; Lawson *et al.*, 2002, 2003; Zeiger *et al.*, 2002). Evidence for guard cell production of sucrose has been obtained during red light-induced stomatal opening in *V. faba.* This research found no evidence of starch breakdown and confirmed that sugar was not being imported as a result of the use of epidermal peels (Tallman & Zeiger, 1988; Talbott & Zeiger, 1993).

4. Co-ordination of stomatal behavior and mesophyll photosynthesis

Studies have suggested that synchrony of stomatal behaviour with mesophyll photosynthetic rates can improve water use efficiency (WUE) in plants grown in a dynamic environment (Lawson *et al.*, 2012; Lawson & Blatt, 2014). It has been reported in the empirical literature that stomata conductance and photosynthetic assimilation rates are highly correlated across a variety of light levels and CO_2 concentrations (Wong *et al.*, 1979; Farquhar & Sharkey, 1982; Hetherington & Woodward, 2003; Buckley & Mott, 2013). For a long time it was thought that the [CO_2] within the leaf helped maintain the relationship between stomatal aperture and mesophyll photosynthesis as it was often reported in the literature that

stomata adjust to maintained in a steady ratio of internal to external [CO_2] (*Ci:Ca* ratio) (Ball & Berry, 1988; Mott, 1988).

As the light intensity varies, mesophyll consumption of CO_2 also changes and it is this that stimulates a response by the stomata. However, some researchers have cast doubt on whether the stomatal responses to *Ci* would be sufficiently to account for the large changes in g_s that have been observed in the presence of light (Farquhar & Raschke, 1978; Sharkey & Raschke, 1981; Farquhar & Sharkey, 1982). This is an agreement with earlier literature using epidermal peels which suggested that *Ci* alone would be insufficient if it were the only signal. Some recent studies have demonstrated that stomata in a number of plant species are responsive to light even when *Ci* is held constant (Messinger *et al.*, 2006; Lawson *et al.*, 2008; Wang & Song, 2008). These findings confirm studies of transgenic plants which have revealed that even when CO_2 uptake is limited and *Ci* is at elevated levels, g_s rises when the intensity of light is increased (von Caemmerer *et al.*, 2004; Baroli *et al.*, 2008; Lawson *et al.*, 2008). In the case of transgenic plants, however, there is no correlation between *A* and g_s and, therefore, empirical studies suggest that a mesophyll driven signal coordinating *A* and g_s is unlikely, and von Caemmerer *et al.*, (2004) suggested that it is external CO_2 and not internal *Ci* to which stomata are responsive.

5. A role for guard cell chloroplasts and photosynthesis in co-ordinating mesophyll photosynthesis and stomatal behaviour

It has been suggested in previous literature that the regulation and coordination of stomatal responses with mesophyll photosynthesis was in some way related to

photosynthesis in the guard cells (Messinger *et al.*, 2006; Wang *et al.*, 2011; Lawson *et al.*, 2014). Furthermore, it is understood that the relationship between stomatal responses and mesophyll photosynthesis could be explained by high rates of photosynthetic electron transport within guard cell chloroplasts (Lawson *et al.*, 2002, 2003; Lawson, 2009). Guard cells photosynthesis has been shown to respond to similar stimuli as mesophyll photosynthesis (Lawson *et al.*, 2002) and therefore one could envisage that a link could be drawn in terms of coordination between carbon fixation or electron transport in both cell types help to ensure that responses are coordinated. Early research has demonstrated that red light triggers plasma membrane proton pumping. As such, it was understood that the energy required for opening and/or the photosynthetic signalling product NADPH may be provided by guard cell photosynthesis (Serrano *et al.*, 1988; Wu & Assmann, 1993). Later studies were unable to confirm these findings (Roelfsema *et al.*, 2001; Taylor & Assmann, 2001).

Daloso *et al.* (2015) found evidence to support the notion that ribulosebisphosphate carboxylase oxygenase and phosphoenol pyruvate carboxylase are both responsible for carbon dioxide fixation in guard cells. In the absence of any CO_2 fixation in guard cells, stomata could still open because the necessary energy for ATP-driven ion exchange could be derived from guard cell electron transport (Shimazaki & Zeiger, 1985). Azoulay-Shemer *et al.* (2015) studied stomata in transgenic *Arabidopsis thaliana* and was able to rule out guard cell photosynthesis playing a part in stomatal responses to CO_2 concentration. They were able to demonstrate that stomata, which lack chlorophyll content, still closed in response to CO_2 elevation and abscisic acid (ABA). However, these studies revealed that chlorophyll-less stomata had a “deflated thin-shaped

phenotype". This was considered to indicate that turgor relied upon guard cell photosynthesis. Furthermore, it has been suggested that the redox state of photosynthetic electron transport chain components is highly correlated with stomatal conductance (g_s) over the entire range of intensities of red light (Busch, 2014). The accumulation of reducing substances might function as the possible signal stimulating stomatal opening. Once again, it would indicate a connection between mesophyll photosynthesis and the response of stomata. However, researchers have yet to confirm the role played by the chloroplasts of guard cells and photosynthesis and this is an area of on-going avenue of research.

6. Manipulation of guard cells to understand stomatal function

Over the last 10 years considerable progress has been made in understanding the underlying mechanisms controlling the opening and closing of stomata as well as the proteins require for guard cell functions and interactions between the mesophyll and stomata (Lawson *et al.*, 2014). Genetic engineering provides valuable insight into the association between mesophyll and guard cell metabolism. More specifically, genetic engineering can be used to better understand the physiology of stomata, the way in which they operate and the function of the various cell types for determining photosynthetic capacity and water use efficiency (Nilson & Assmann, 2006; Lawson *et al.*, 2014). Lawson and Blatt, (2014) assessed changes in the number and size of stomata and the impact this has on WUE. They concluded that the activity of guard cells is able to offset anatomical developments. Lawson and Blatt also suggested that WUE could be increased through the manipulation of guard cell metabolism while simultaneously holding the rate of photosynthesis constant.

Cell-specific metabolism can be influenced using various new tools and methods including guard and mesophyll cells. To do that, it is possible to elucidate mesophyll-derived signals that coordinate mesophyll CO_2 demands with the behaviour of stomata. WUE and crop yields can be enhanced using tools derived from improvements to molecular and transgenic techniques (Webb & Baker, 2002; Lawson & Blatt, 2014). Hudson *et al.*, (1992) examined transgenic plants with impaired photosynthesis and found that Rubisco concentration had only a little effect on photosynthesis and the response of stomata. Meanwhile, Ruuska *et al.*, (1998) examined tobacco plants (*Nicotiana tabacum*) that are known to have reduced Rieske FeS protein and revealed that there was no effect on stomatal conductance, and they concluded that photosynthetic electron transport is not required for stomata to set conductance. However, Gehlen *et al.*, (1996) studied transgenic antisense PEPc plants and confirmed the role played by malate and PEPc activity in guard cells. Potato plants with reduced PEPc activity were found to have delayed stomatal opening responses, but rapid opening when there was overexpression.

Certain cell metabolisms in mesophyll and guard cells can be used to demonstrate how guard cell metabolism and stomatal response can be manipulated using the available tools. Lawson *et al.*, (2008) observed a relationship between the rate of CO_2 assimilation and the conductance of stomata when subjecting tobacco antisense SBPase plants to red light and a combination of both red and blue light. Lawson *et al.*, (2008) also confirmed that stomata open more quickly in transgenic plants than in the wild type controls. In addition, antisense plants with small reductions in SBPase activity exhibited greater stomatal conductance.

Meanwhile, stomatal conductance was decreased when there was a reduction in NADP-Malic enzyme expression, although photosynthesis was not measured no negative impact on the growth was reported (Laporte *et al.*, 2002).

Numerous empirical studies have emphasised the importance of identifying genes that determine the density or patterning of stomata and how genetic alterations can improve the efficiency of how water is used by the plant. Eisenach *et al.*, (2012) observed that stomatal conductance in an Arabidopsis mutant with a non-operational trafficking protein SYP121 resulted in greater WUE but lower CO_2 assimilation that had a detrimental effect on growth. Tanaka *et al.*, (2013) have shown that stomagen (EPLF9) increased the density of stomata and bring about a thirty percent improvement in the rate of assimilation. However, there was also a fifty percent increase in the rate of transpiration and this caused WUE to decline.

Under stress conditions, manipulating gene function specifically in guard cells offers advantages over manipulation at the entire plant level to improve plant performance (Yang *et al.*, 2008). Guard cell-specific promoters have been developed that enable the expression of transcripts in guard cells. This opportunity to manipulate guard cell-specific metabolisms or certain stomatal features to be controlled without disrupting mesophyll photosynthetic metabolism (Lawson, 2009). Several promoters have been examined for the expression of guard cells utilizing reporter genes such as green fluorescent protein (GFP) and β-glucuronidase (GUS)(Kelly *et al.*, 2017). It has been confirmed that guard cell-specific promoters combined with specific organelle transit peptides enable the roles of certain transcripts involved in electron transport, carbohydrate biosynthesis and ion channel function to be evaluated on a cell-by-cell basis

(Lawson *et al.*, 2014). For example, the guard cell-specific KST1 promoter (Müller-Röber *et al.*, 1995) has been used to alter expression of HXK in tomato plants (*Solanum lycopersicum*. This study has shown that WUE can be effectively enhanced by the expression of HXK by this specific promoter. Kelly *et al.*, (2013) found that the time required for stomatal closure can be reduced if the rate at which HXK is expressed in guard cells is increased. The closure of the stomata is caused by excess sucrose that travels to the stomata by means of the transpiration stream. Consequently, this helps to avoid water being lost. Furthermore, Wang *et al.*, (2014) demonstrated an enhanced light-induced stomatal opening, improved photosynthesis and thereby increase growth rate in transgenic Arabidopsis plants overexpressing H^+ ATPase under the control of the GC1 promoter. These studies suggest that the guard cell-specific promoter activity might be universal. However, Rusconi and colleagues (2013) pointed out that there is a promoter limitation between monocots and dicots, as the MYB60 promoter isolated from Arabidopsis showed a lack of activity in rice, but succeed to drive expression in guard cells of tomato and tobacco.

7. Genetic manipulation of photosynthetic enzymes

It is possible to control the rate of photosynthesis in plants by controlling the photosynthetic enzymes responsible for carbon metabolism (Lefebvre *et al.*, 2005; Lawson, 2009; Raines, 2011; Simkin *et al.*, 2015; Driever *et al.*, 2017a). Several studies have previously explored the regulation of carbohydrate metabolism during the photosynthetic fixation of CO_2. The advances made as a result of these studies have helped to enhance photosynthetic capacity thereby benefiting crop

yields (Raines & Paul, 2006; Feng *et al.*, 2007; von Caemmerer & Evans, 2010; Zhu *et al.*, 2010; Raines, 2011).

As a result of extensive research into stomata over many decades, it has become apparent that the guard cells feature an extensive network of signaling and osmoregulatory pathways (Li *et al.*, 2014). It is possible to control the main photosynthetic transcripts such as SBPase and FBPaldolase, and electron transport proteins in the mesophyll or guard cells so as to clarify a number of matters including the role of mesophyll metabolism in stomatal behaviour. Moreover, the contribution they make to coordinating how plants respond to external stimuli in the environment (possibly involving ion channels or guard cell photosynthesis); and how electron transport and guard cell photosynthesis influence guard cell function. For example, previous research relating to antisense SBPase plants indicates that carbon reduction and guard cell photosynthesis possibly influence how stomata respond to the introduction of red light (Lawson *et al.*, 2008). Conversely, other research carried out on antisense Rubisco and b_6f plants suggests that guard cell photosynthesis does not perform any function response to the presence of red light (Baroli *et al.*, 2008). Furthermore, it has been established that using overexpression of the SLAC1 protein to control the operation of the SLAC1 channel could reduce the time taken for stomata to open in the presence of light or other stimuli (Laanemets *et al.*, 2013). Previous research has demonstrated that it is possible to control how stomata behave by exerting influence over ion channels. Therefore, it remains unclear what function mesophyll signaling plays regarding such responses and in activating ion channels.

8. Aims of the Project

The overall aim of this project is to use molecular and physiological approaches to elucidate the role of the guard cell chloroplast in stomatal function and in particular their role in the coordination of stomatal behaviour with mesophyll photosynthesis.

The aims were addressed by the following objectives:

- Examine transgenic tobacco plants (*Nicotiana tabacum*) with altered expression levels (antisense and sense technology) of key enzymes of Calvin cycle activity (SBPase) and electron transport (Rieske FeS) in guard cell photosynthesis under the control of promoter AGPase.
- Use high-resolution chlorophyll fluorescence imaging to quantify alterations in guard and mesophyll photosynthesis efficiency in transgenic and non-transgenic tobacco (*Nicotiana tabacum*) plants.
- Conduct infra-red gas analysis to examine stomatal Kinetics such as stomatal conductance/ assimilation (A/g_s) and assimilation/ internal CO_2 (A/Ci).

CHAPTER 2

Materials and Methods

2.1 Plant Material and Growth Conditions

Wild type (Col-0), guard cell-specific overexpression of AtRieske (**pL2B-BAR-(pAGPase)-AtRieske**), guard cell-specific expression of ASNtSBPase (**pL2B-BAR-(pAGPase)-ASNtSBPase**) and guard cell-specific overexpression of AtSBPase (**pL2B-BAR-(pAGPase)-AtSBPase**), transgenic tobacco *(Nicotiana tabacum*) were used. All of the transgenic plants used in this study contained guard cell enriched promotors (AGPase promoter). ADP-glucose pyrophosphorylase (AGPase) performs a central function in photosynthetic plant tissues and the biosynthesis of starch (Preiss, 1991). AGPase also facilitates exclusive expression in transgenic potato and tobacco plants' guard cells (Müller-Röber *et al.*, 1994). Table 2.1 summarises the mutants investigated in this study.

2.2 Seed sterilisation

Tobacco seeds were sterilised for 10 min by washing in 20% bleach plus Tween 20 (1 drop in ml). Following this, the seeds were washed three times with distilled water for 5 min. In the flow hood, seeds were placed on sterile filter papers and allowed to dry. To select BASTA-resistant seedlings, seeds were germinated on 0.8% (w/v) agar containing 0.44% Murashige and Skoog medium (MS) with 0.51 mM of herbicide glufosinate-ammonium (BASTA; Sigma-Aldrich, UK) and with the pH level adjusted to pH 5.7 using 1M KOH solution. The plates were placed in a growth chamber at 22°C, 8-hour photoperiod, light level of 150 µmol m^{-2} s^{-1} and allowed to germinate for 2-3 weeks. After three weeks, eight-ten replicates of each genotype and WT plants were transferred to individual100 cm^3 pots containing compost (Levington's F2S, Everris, Ipswich, UK) and grown under the same

conditions for a further two weeks. A leaf disk was taken from the WT and transgenic lines in a 2.0 ml microfuge and sent for iDNA molecular genetic screening. This is a professional service used to screen plants in order to identify the copy numbers of BASTA gene present in the plants' chromosomes. The technology is novel, but the exact principle is the intellectual property of iDNA Genetics Ltd, The Norwich BioIncubator, Norwich Research Park, Norfolk, Norwich, UK, NR4 7UH. The iDNA screening result was used to identify plants with 2 copy numbers of BASTA and re-potted into 350 cm^3 pots containing compost and left to grow in the greenhouse for seed (T2) collection. The plants were maintained under well-watered conditions and regularly moved to minimise spatial variation in growth conditions. The T2 seeds were germinated on selective media the plates with 100% growth could be homozygous. The plates were placed in a growth chamber at 22°C, 8-hour photoperiod, light level of 150 µmol m^{-2} s^{-1} and allowed to germinate for 2-3 weeks. Transporting these plants in 350 cm^3 pots containing compost was done and moved into the greenhouse for T3 seeds collection.

Table 2.1 summarises the names, descriptions and abbreviations of the *Nicotiana tabacum* mutants used in this study.

Name	Description	Abbreviation
pL2B-BAR-(pAGPase)-AtRieske	Guard cell overexpression of AtRieske FeS	GCFeS4.1
		GCFeS4.2
		GCFeS4.10
		GCFeS4.22
pL2B-BAR-(pAGPase)-ASNtSBPase	Guard cell antisense of ASNtSBPase	GCAsSBP2.5
		GCAsSBP2.6
		GCAsSBP2.15
		GCAsSBP2.16
pL2B-BAR-(pAGPase)-AtSBPase	Guard cell overexpression of AtSBPase	GCSBP3.3
		GCSBP3.4
		GCSBP3.19

2.3 DNA Extraction

Leaf samples were collected in 1.5 ml microcentrifuge tube on dry ice and subsequently stored at -80 ^{o}C. DNA extraction was prepared by grinding a frozen leaf disc in liquid nitrogen with a mortar and pestle. To each tube, 200µL of Extraction Buffer (200 mM Tris-HC1 pH7.5, 250 mM NaCl, 25 mM EDTA, 0.5% SDS) was added to it. This was incubated for 2 min at room temperature and then centrifuged at maximum speed (usually around 13K) for 10 min. To precipitate nucleic acids, the supernatant was transferred to a clean 1.5 mL microcentrifuge tube containing 150µL isopropanol and mixed by brief vortexing the tube several times and precipitate pelleted by centrifuged at maximum speed for 15 min. The pellet was washed by adding 200µL 70% ethanol (prepared in dH_2O) and then centrifuged at maximum speed for 10 min, and supernatant removed using pipettes. Pellets were dried by incubating open microcentrifuge tubes at room temperature on the bench for 30 min. Finally, the DNA was resuspended in 50µL of TE Buffer (10 mM Tris-CI, pH 7.5. 1mM EDTA). This DNA was either used immediately or stored at -20^{o}C.

2.4 Polymerase chain reaction (PCR)

Plants were screened for the presence of the construct from isolated DNA by Polymerase chain reaction (PCR). PCR reactions were performed using an Applied Biosystems 2720 Thermal Cycler (Thermo Fisher Scientific, UK). PCR reactions were performed in 0.2 ml PCR tubes using in 25µL volumes consisting of 2.5µL Dream Taq Buffer, 0.3µL 10mM dNTP mix, 1.3µL 10µM forward primer, 1.3µL 10µM reverse primer, 0.3µL Taq polymerase,1µL template DNA, and

volume was made up to 25 µL with dH_2O. The condition used for the PCR reactions were varied depending on the expected size fragments to be amplified. Table 2.2 represents information on the annealing temperature and the expected fragments size.

The condition was used in most of the PCR reactions were as following: an initial denaturation at 95˚C for 3 minutes; 35 cycle of denaturation at 95˚C for 30 seconds, primer annealing at 60˚C for 30 seconds and extension at 72°C for 1 min per 1Kb template; final extension at 72˚C for 10 min.

Table 2.2: List of primers used for the presence of the construct.

Primer names	Sequences	Annealing Temperature	Expected fragment size
scr-AtRieske-FP	ACTGGCTACATGCTTGTCCC	60°C	690bp
scr-AtRieske-RP	ATTCCGCTGCAACTACATCG		
NtSBPase-FP1	GGAGGAATGGTGCCTGATGTTA	58°C	1269bp
NtSBPase-RP1	ACCCTACCAAATATTTAACGG		
scr-AtSBPase-FP	TACACACTGCGATACACCGG	60°C	1182bp
scr-AtSBPase-RP	CTTCCACTGGACCTCCCATG		

2.5 Agarose gel electrophoresis of nucleic acids

The PCR products were combined with 6x DNA Loading Buffer and resolved on a 0.8% agarose gel containing SafeView Nucleic Acid Stain (NBS Biologicals) in TAE buffer (40 mM Tris ultrapure, 1 mM EDTA, 20 mM acetic acid) ran at 100 volts for 30 min. 10µL GeneRuler 1kb DNA Ladder (Thermo Fisher Scientific) or MassRuler DNA Ladder Mix (Thermo Fisher Scientific) was analysed alongside 20µL of the sample. Gels were visualised under blue light using the Gene Genius Bioimaging system (Syngene, Synoptics Ltd., Cambridge, UK) per the manufacturer's instructions.

2.6 Isolation of Guard-cell Enriched Tissue for RNA Extraction

Three or four leaves were collected from each plant and the central vein (midrib) was removed using a razor blade. The cut leaf blades were put in the blender with 250 ml cold dH_2O and a handful of crushed ice (additional mechanical force to the disrupt tissue) and then the contents were blended at max speed for 1 min. The blended material was poured through a 200 µm nylon mesh placed in a plastic embroidery hoop. After that, the retained epidermal peels were rinsed with dH_2O. The remaining dark green tissue fragments (small leaf pieces that have not been blended) from the light green epidermal fraction were removed. This method was repeated twice after which the light green epidermal fraction was collected. The material was dried using filter paper and immediately ground in liquid nitrogen using a mortar and pestles. Then the powder was transferred to the prepared 1.5

ml Eppendorf tube and stored immediately in liquid nitrogen until used for RNA isolation. Isolated guard cell enriched fragments can be visualised with a microscope, and no mesophyll fragments (green tissue) should be present (Figure 2.1).

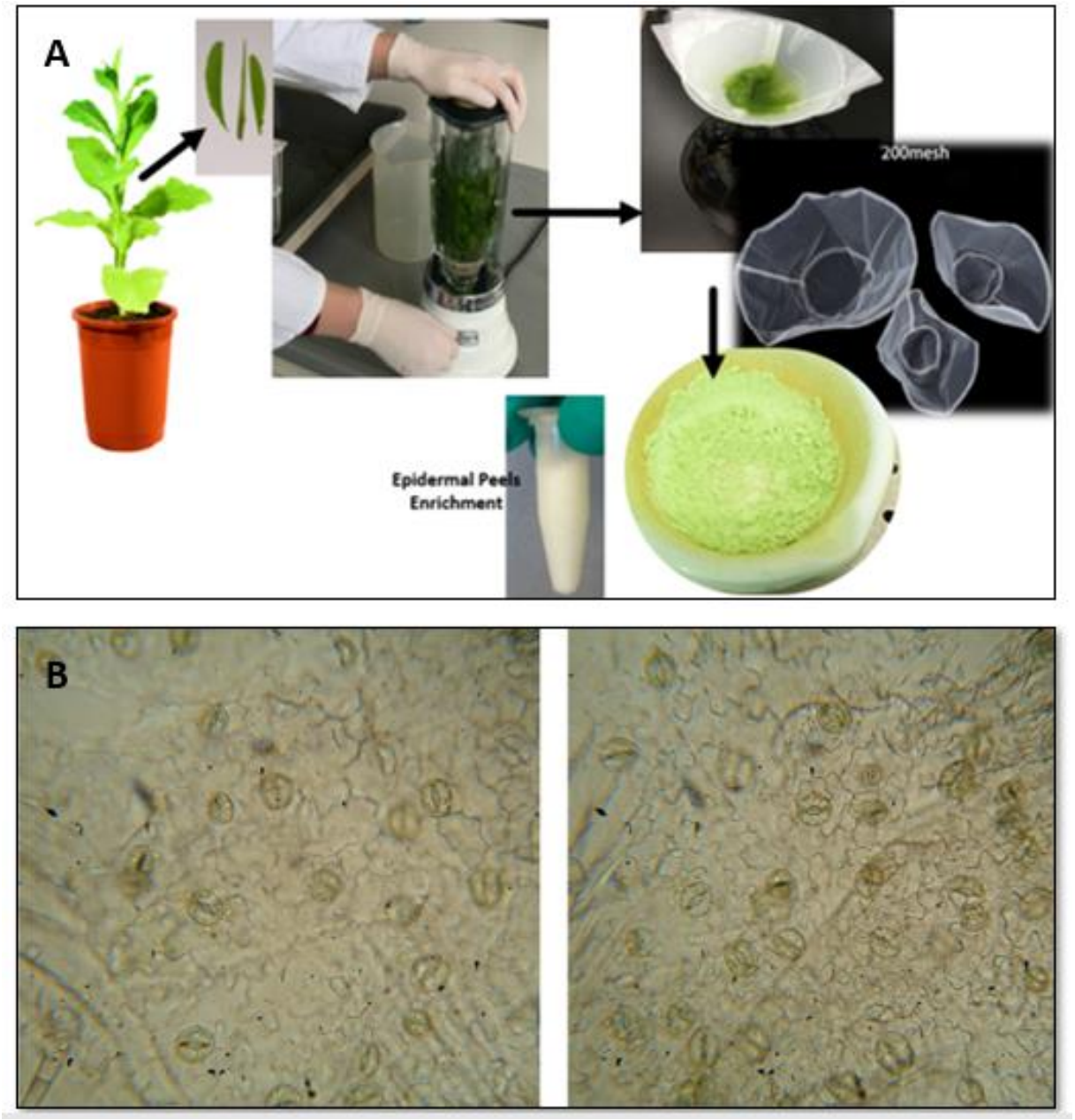

Figure 2.1 **(A)** Process of isolation of Guard-cell Enriched Tissue for RNA Extraction using the blender method**, (B)** Isolated guard cell enriched fragments under a microscope, illustrating limited mesophyll contamination.

2.7 Quantitative real-time PCR

2.7.1 RNA extraction and DNase treatment of extracted total RNA

Frozen leaf material was resuspended in 1000µL TRI Reagent® by brief vortexing and incubated on ice for 2 min. 200µL chloroform was added to each tube and the samples were mixed gently by inversion for 20 seconds, followed by incubation at room temperature for 5 minutes and subsequent centrifugation at 13,000 rpm for 15 min at 4°C. The upper aqueous phase was transferred (approx. 600µL) to a new 1.5 mL microcentrifuge tube containing 500µL isopropanol, mixing gently by inversion in the tube and incubated at room temperature for 2 min. The precipitate was collected by centrifugation at 13,000 rpm for 20 min at 4°C, and care was taken to remove all supernatant using pipettes without disturbing the pellet. The RNA pellets were then washed by adding 500 µL 70% ethanol with repeated pipette aspirations until the pellet was free-floating, followed by centrifugation at 13,000 rpm for 5 min at 4°C with all supernatant removed using pipettes. The wash step was repeated using 500 µL 100% ethanol and samples were centrifuged again at 13,000 rpm for 5 min at 4°C. Subsequently, all supernatant was removed using pipettes. Pellets were allowed to dry by incubating in open microcentrifuge tubes on the bench at room temperature for 30 min. Finally, the pellets were resuspended in 26 µL RNase-free water.

Genomic DNA was removed from total RNA preparations by DNase treatment using Recombinant DNase I, RNase-free (DNase I, Thermo Fisher Scientific, UK). The reactions were set up in microcentrifuge as follows: 26µL total RNA, 3µL 10x Reaction Buffer with $MgCl_2$ and 1µL DNase I. The reactions were gently mixed

and incubated at 37°C for 30 min. Following incubation, 1.8µL 50 mM EDTA solution was added to each reaction, mixed and DNase I inactivated by incubation at 65°C for 10 min.

The purity and concentration of the extracted total RNA were quantified using an absorbance measurement at 260 nm using a NanoDrop spectrophotometer, and RNA was re-precipitated using ethanol if not pure. For re-precipitation of total RNA, 3µL 3M sodium acetate and 90µL 100% ethanol were added to the RNA preparation, the reactions were mixed and briefly centrifuged, and incubated at -80°C overnight. Precipitates were pelleted by centrifugation at 13,000 rpm for 30 min at 4°C and supernatant was removed using pipettes. Precipitates were washed with 1000 µl 100% ethanol with repeated pipette aspirations until the pellet was free-floating, followed by centrifugation at 13,000 rpm for 3 min at 4°C and all supernatant was removed using pipettes. Following total removal of supernatant using pipettes, pellets were dried at room temperature for 30 min and resuspended in 30µL RNase-free water. Pure RNA preparations were used immediately or stored at -80°C for later use.

2.7.2 cDNA synthesis

RNA was quantified using a NanoDrop™ ND-1000 spectrophotometer (Thermo Fisher Scientific), and 500 ng (0.5µg) of RNA was taken into a separate tube to convert to cDNA using RevertAid reverse transcriptase (Thermo Scientific). Synthesis was performed by adding 1µL Oligo(dT)^{18} primer for each tube and total RNA was diluted to 11µL (RNA- free water) to make a final 12µL. Reactions were gently mixed, briefly centrifuged and incubated at 65°C for 5 min, after which it was immediately placed on ice. To each reaction 4µL 5x Reaction Buffer, 2µL

dNTPs mix (Thermo Scientific),1µL reverse transcriptase was added and 1µL of water making a total volume of 20µL. The reaction was centrifuged (30 sec) one more time and incubated at 42°C for 60 min followed by inactivation of the enzyme by incubating at 70°C for 10 min. This cDNA was used as a template for PCR amplification (semiquantitative RT-PCR or qRT-PCR) immediately or stored at -20°C.

2.7.3 Real-time quantitative RT-PCR (qRT-PCR)

To study gene expression, first the sequence of the homolog reference genes was found in tobacco and designed the primers for them (sequence information in Appendix A). Then, the synthesised cDNAs were amplified using quantitative reverse transcription PCR (qRT-PCR) to identify whether or not the transformed genes were expressed. Reactions were performed using qPCRBIO SyGreen (PCR Biosystem) and run in triplicate on 96-well plates (Greiner, UK) using the CFX96 Touch Real-Time PCR Detection System (Bio-Rad, UK). Reactions were prepared in a total volume of 20µL containing the following: 2µL of cDNA (equivalent to 0.05 ug/µL of RNA), 2x qPCRBIO SyGreen Mix 10µL (PCR Biosystem),1.6µL each of forward and reverse primers. Finally, the volume was made up to 20µL with RNA- free water. The sequence information for each primer is presented in Table 2.3. Blank controls were run in triplicate for each master mix. The cycling conditions were set as follows: initial denaturation step of 95°C for 2 min to activate the polymerase, followed by 40 cycles of denaturation at 95°C for 5 seconds and annealing at 65°C for 30 seconds. The amplification process was followed by a melting curve analysis, ranging from 60°C to 90°C, with temperature increasing steps of 0.1°C every 10s.

Table 2.3: Primers sequences used for qPCR

Primer names	Sequences		
qPCR-Nt14-CER2-RP	AGTCATGGTCACAACCCTTCC	qPCR	Reference gene
qPCR-Nt14-CER2-FP	GGATTTGACTGGGAGGGACA	qPCR	
qPCR-Nt13-GORK-RP	ACTCCACTTGCTTCACACGA	qPCR	Reference gene
qPCR-Nt13-GORK-FP	TCCGTGTTTGTGAACTCTGC	qPCR	
qPCR-NtSBPase-RP2	GTCTTGGAGCTCAGGTACTTCC	qPCR	
qPCR-NtSBPase-FP2	ACAAGTTGCTTTTCGACGCATT	qPCR	
qPCR-AtSBPase-R3	GCTTGCTGTATTCGGAGTTGTC	qPCR	
qPCR-AtSBPase-F3	ATGGCAGCATGTAAAGGAGACA	qPCR	
qPCR-AtRieske-RP	ACCACCATGGAGCATCACCA	qPCR	
qPCR-AtRieske-FP	AACGCCCAAGGAAGAGTCGT	qPCR	

2.8 Plant Phenotyping techniques

2.8.1 Thermal imaging phenotyping and porometry measurements of stomatal conductance

Leaf temperature depends on the aperture of the stomata and also on various environmental and plant variables (Guilioni *et al.*, 2008). Leaf temperature depends on evaporative cooling and this has been found to be a function of g_s (Jones, 2013). When the stomata close, this has the effect of reducing the loss of water via evaporation, thereby increasing the temperature of the leaf. It is possible to screen genotypic variation in g_s by means of thermography (Wang *et al.*, 2004) or diagnosing developments in g_s brought about by drought stress (Morison *et al.*, 2008a).

In this study, differences in leaf temperature were used to identify stomatal phenotype using thermal images obtained with a thermal imager (TH7100 Thermal Tracer, NEC Avio Infra-red Technologies Co. Ltd, Japan). The plants were placed in a controlled environmental chamber and maintained under well-watered conditions. The plants were left for 30 min at a light intensity of 275µmol m^{-2} s^{-1}, after which a thermal image was taken. Light was then decreased to 117µmol m^{-2} s^{-1} and the plants left for 15 min before a thermal image was captured. Transgenic and wild type plants were measured simultaneously and at different times of day in the morning (09:00 am), at midday (12:00 pm) and late afternoon (15:00 pm). Stomatal conductance (g_s) was also measured using a leaf porometer (SC-1 Leaf Porometer, Decagon Devices, Pullman, WA, USA) with an accuracy of ± 5%. The instrument was calibrated prior to taking each set of measurements. The measurements were taken in a controlled environmental chamber. Three

measurements were taken per leaf on the abaxial side and averaged to represent g_s of that leaf.

2.8.2 Chlorophyll fluorescence imaging of photosystem II operating efficiency

Chlorophyll fluorescence PSII operating efficiency was performed using a chlorophyll fluorescence (CF) imaging system (Technologica, Colchester, UK) on all replicates of each genotype. Measurements were performed on 3-week-old tobacco seedlings. The operating efficiency of photosystem II, *Fq'/Fm'*, was determined from the measurements of steady-state fluorescence in the actinic light (*F'*) and maximum fluorescence in the light (*Fm'*) using the following equation *Fq'/Fm'*= (*Fm' - F')/Fm'*. Images of *F'* were taken when fluorescence was stable at the desired PPFD, whilst images of *Fm'* were obtained after a saturating 800 ms pulse of 6200 µmol m^{-2} s^{-1} PPFD (Baker et al., 2001; Oxborough and Baker, 1997).

After three weeks, the seedlings were placed in chlorophyll fluorescence (CF) imaging in order to further elucidate the growth phenotype. Two different light intensities were used to estimate the photosystem II operating efficiency (*Fq'/Fm'*), under stable PPFD of 200 µmol m^{-2} s^{-1} and a PPFD of 800 µmol m^{-2} s^{-1}, then *Fq'/Fm'* images were taken.

Moreover, a further protocol comprising of the induction of steady state, light response curve and relaxation response of transgenic lines and wild type plants was applied. Plants were dark adapted for 20 min before induction, increasing light and relaxation protocol were measured. At photosynthetic photon flux density (PPFD) of 0 µmol m^{-2} s^{-1}, a record of the minimum fluorescence (F_o) was taken.

After 20 sec a saturating pulse of light (PPFD 6200µmol m^{-2} s^{-1}) was applied to obtain maximum fluorescence (*Fm*). The plants were then maintained under actinic light (PPFD 500µmol m^{-2} s^{-1}) and *Fm'* was taken by applying saturating light pulses (PPFD 6200µmol m^{-2} s^{-1}) every 2 min for a total of 20 min. The actinic light was then changed every 3 min (PPFD 100, 200, 300, 400, 600, 800, 1000, 1200, 1400, 1600, 1800 µmol m^{-2} s^{-1}) and *Fm'* measurements were taken by applying saturating light pulses (PPFD 6200 µmol m^{-2} s^{-1}) every 3 min for a total of 25 min. To determine relaxation of non-photochemical quenching (NPQ) plants were returned to the dark (PPFD 0 µmol m^{-2} s^{-1}) and *Fm* and *Fo* were determined again every 2 min with a saturating pulse for a total of 20 min. Three plants were measured simultaneously (two transgenic and one wild type) for each determination of fluorescence parameters.

2.9 Leaf gas exchange

2.9.1 Intracellular CO_2 response curves (A/C_i)

The response of net CO_2 assimilation rate (A) to intercellular CO_2 concentration (C_i) was measured at a saturating light intensity of 1500 µmol m^{-2} s^{-1}, a VPD of 1 kPa at 25^{o}C and 400 µmol mol^{-1} Ca until a steady state A and g_s were achieved. The fully expanded leaves were initially stabilised at an ambient CO_2 concentration of 400µmol mol^{-1}. Upon reaching a stable signal, measurements were taken before ambient CO_2 was decreased to 250, 150, 100, and 50µmol mol^{-1}, before returning to the initial concentration (400µmol mol^{-1}). An ambient CO_2 concentration was then increased to 550, 700, 900, 1100, 1300, and 1500µmol mol^{-1}, and each time A was allowed to stabilise before taking a recording. The

maximum velocity of Rubisco for carboxylation (V_{Cmax}; μmol m^{-1} s^{-1}) and the maximum rate of electron transport demand for RuBP regeneration (J_{max}; μmol m^{-1} s^{-1}) were estimated using the curve fitting method described by Sharkey et al., (2007). Maximum rates of CO_2 assimilation (A_{max}) were determined from the recorded values at 1500μmol mol^{-1} CO_2 concentration and 1500μmol m^{-2} s^{-1} PPFD.

2.9.2 PPFD-step measurements

Stomatal conductance (g_s) and CO_2 assimilation (A) were measured using a portable gas exchange system (LI-COR 6800). The fully expanded leaves were placed in the Li-COR cuvette and equilibrated at a PPFD of 100 μmol m^{-2} s^{-1} until both A and g_s were at steady state between 10 to 30 min, then PPFD was increased in a single step to 1500 μmol m^{-2} s^{-1} until A and g_s again reached a steady state for 60 min. All measurements were allowed to stabilise under 1 ±0.2 kPa VPD at 25 °C and 400 μmol mol^{-1} CO_2 concentration. The leaves were measured for all plants between 8am and 3pm to ensure a high degree of stomatal opening and photosynthetic activation.

2.10 Modelling gas exchange parameters

2.10.1 Determining the rapidity of stomatal conductance response

The rapidity of the stomatal response following a step change in light intensity was estimated as a function of time (t) using a custom exponential equation (Vialet-

Chabrand et al., 2013) including a slow linear increase of the steady state target (*G*):

$$g_s = (G + S_l t) + \left(g_0 - (G + S_l t)\right)e^{-t/\tau}$$

where S_l is the slope of the slow linear increase of *G* observed during the response, g_0 is the initial value of g_s, and τ is the time constant to reach 63% of *G*

$$\left(\text{when } \tau = t, \frac{g_s - g_0}{((G+S_l t) - g_0)} = 1 - e^{-1} \sim 0.63\right).$$

Due to the asymmetry of response shown during a step change in light intensity, a different value of τ was used in each condition (τ_i and τ_d). The model was able to predict the final asymptotic response even if gs did not reach a plateau within the time period and, therefore, the time constant (τ_i and τ_d). Parameters *G,* g_0 and S_l were assumed to vary at the individual level (random effects) and τ was assumed to vary only at the treatment level (fixed effect). R package was used to perform the analysis. Confidence intervals at 95% were reported at the treatment level.

2.10.2 Determining the rapidity of net CO_2 assimilation response

The rapidity of the photosynthesis response following a step change in light intensity was estimated as a function of time (*t*):

$$A_t = (A_s + S_l t) + \left(A_0 - (A_s + S_l t)\right)e^{-t/\tau}$$

where A_t is *A* at time *t*, A_s is the plateau of *A* reached in the steady state, S_l is the slope of the slow linear increase of *A,* A_0 the initial value of *A*, and τ is the time

constant to reach 63% of A_S. This equation was adjusted on response curves using the same method described above for g_S.

2.11 High resolution imaging of photosynthetic efficiency in guard and mesophyll cells

To compare guard and mesophyll cells photosynthetic performance in transgenic and WT plants, the leaves were placed in the Fluorescence Kinetic Microscope (Photon Systems Instruments; Brno, Czech Republic). The microscope was focused on the Arduino sensor at the height shown on the microscope (z=21.5501 mm) using a high-resolution CCD camera. The real distance between the microscope and sample was 0.71mm with x40 objective. Guard and mesophyll cells were isolated from images using the ends-in search and editing tools of the FluorCam 7 software as described in the instruction manual and user's guide. Images of *Fq'/Fm'* were taken at different light intensities (61µmol m^{-2} s^{-1},130µmol m^{-2} s^{-1}, and 300µmol m^{-2} s^{-1} PPFD), and the sensor was calibrated using a Licor model Li-250 light meter.

2.12 Growth Analysis

2.12.1 Plant growth characteristics

Total leaf area (cm^2) and dry weight (g) were measured using fully expanded leaves. For dry weight, the leaves were placed individually in labelled paper bags and set in an oven at 50°C until completely dry, then weighed using electronic precision scales (Kern, Northamptonshire, UK). Leaf area was calculated by

passing leaves through a bench-top LI-3100C area meter (Li-Cor, Lincoln, Nebraska, USA). An average leaf area was calculated.

2.13 Statistical analysis

Statistics were performed using SPSS (Version 25, SPSS Inc., Chicago) and R software (www.r-project.org; version 3.5.3). A One-way Analysis of Variance (ANOVA) was used to test for single factor differences where more than one group existed, when comparing more than one group, two-way ANOVA was used. a Tukey post-hoc test was used to identify where differences lay. Statistical significance was determined when P-value <0.05.

CHAPTER 3

The effect of Overexpression of the Rieske FeS of the cytochrome *b_6f* complex in guard cells on stomatal and photosynthetic behaviour

3.1 Introduction

Stomata have a significant influence on photosynthetic rates and therefore, plant productivity (Hosy *et al.*, 2003; Fischer & Edmeades, 2010). It is the metabolism of the guard cells surrounding the pore that are responsible for regulating stomatal aperture. In turn, environmental and endogenous signals have a bearing on the guard cell behaviour (Santelia & Lawson, 2016). The rate of photosynthesis and/or water-use efficiency can be enhanced by manipulating certain genes responsible for regulating the A–g_s trade-off, such as Hexokinase (HXK; Kelly *et al.*, 2013; Lugassi *et al.*, 2015). Consequently, there is a need to understand how stomatal regulation is impacted by the surrounding mesophyll cells and environmental conditions in order to produce plants with improved A and WUE (Lawson & Blatt, 2014; Flexas, 2016; Nunes-Nesi *et al.*, 2016).

It has been established that guard cell chloroplasts contain a number of the Calvin cycle enzymes and that photosynthetic electron transport are relatively high rates, and it has been suggested that this could be the link between mesophyll photosynthesis and stomatal responses. Photosynthesis in guard cells has been shown to respond to similar stimuli as mesophyll photosynthesis (Lawson *et al.*, 2010). Based on this, it is possible to imagine that the co-ordination of responses is assisted by the coordination of carbon fixation or electron transport in these types of cells. Although, there is consensus that the Calvin cycle activity is present in the guard cells but there is an on-going arguments regarding the extent that photosynthetic carbon fixation makes to function in these cells (Lawson, 2009; Daloso *et al.*, 2015, 2016b). It could provide osmotica for the movement of the

stomata or trigger signals that coordination mesophyll photosynthesis and the aperture of the stomata. Daloso *et al.*, (2015) has supplied further evidence for fixation of CO_2 by ribulose bisphosphate carboxylase oxygenase (as well as via phosphoenol pyruvate carboxylase) in guard cells. In the absence of any CO_2 fixation in guard cells, the energy required for ATP driven ion exchange to open the stomata could be provided from the end products of electron transport (Shimazaki & Zeiger, 1985; Lawson et al., 2002).

In addition, it has been shown that cystolic ATP is required for the activity of K^+-uptake channels at the plasma membrane of the guard cell and photosynthetic electron transport in guard cell chloroplasts (Goh *et al.*, 2002). This suggests that ATP plays an important regulatory role in connecting the activity of ion transport with guard cell photosynthesis (Goh *et al.*, 2002). Moreover, the process of the stomata opening in response to blue light requires H^+-ATPases to be activated as well as the accumulation of ions in the guard cells (Kinoshita *et al.*, 2014). Furthermore, leaves with relatively little guard cell chlorophyll have been shown to have lower g_s (Azoulay-Shemer *et al.*, 2015) suggesting that chlorophyll and light capture is important for guard cell function. Although not confirmed, it is believed that the electron transport chain performs a central role in energy production (ATP/NADPH) required for guard cell function. However, the regulation of these processes is considerably different from the approach in mesophyll cells (Daloso *et al.*, 2017).

One way to enhance the assimilation of photosynthetic carbon and yield is to manipulate the guard cell chloroplast electron transport chain and stomatal

behaviour. Electrons are transferred from donors to acceptors as a result of the photosynthetic electron transport chain which entails a series of complex reactions. In addition, this chain is also responsible for transferring proton ions (H^+) across the thylakoid member from the stroma to the lumen. Electron transfer between the photosynthetic reaction centres (Photosystem I (PSI) and Photosystem II (PSII)) is mediated by the membrane bound protein complex cytochrome *b_6f* complex. NADPH is the end product of linear electron flow and ATP is produced from the buildup of the proton gradient that is released through the ATP synthase, both of which used for photosynthetic carbon fixation (Stroebel *et al.*, 2003; Engle *et al.*, 2008) as well as other key processes including non-photochemical quenching (Baker, 2008). There are eight separate sub-units that comprise the cytochrome *b_6f* complex. Two of these are found in the nucleus (Rieske FeS and PetM) with the other six being in the chloroplast genome (cyt f, cyt b6, PetD, PetG, PetL and PetN) (Kurisu *et al.*, 2003; Simkin *et al.*, 2017a). The cyt *b_6f* complex functions in both linear electron flow between the PSII and PSI for production of NADPH and ATP and cyclic flow through PSI for generation of the transmembrane proton gradient for ATP synthesis. The electron flow through the cyt *b_6f* complex is considered to be a key rate-limiting step for RuBP regeneration (Yamori *et al.*, 2011a). Despite the complexity of the cytochrome *b_6f* complex in terms of its genetics and structure, manipulation has been achieved as a result of the Rieske FeS protein being subjected to antisense expression. Reducing this protein resulted in lower rates of electron transport and a decrease in plant biomass and seed yield (Yamori *et al.*, 2011a, 2016). It has been established that the activity of the cyt *b_6f* complex plays a central role in the electron transport functioning efficiency and this knowledge has been derived from transgenic

antisense studies the accumulation of the Rieske FeS protein as well as being inferred based on cytochrome b_6f inhibitors (Kirchhoff *et al.*, 2000, 2017). When the Rieske FeS protein in Arabidopsis was overexpressed, plant yields improve considerably because it results in markedly greater CO_2 assimilation and relative electron transport rates, and, importantly, resulted in increased (27–72%) biomass and seed yield by 51% (Simkin *et al.*, 2017a). More recently it has been shown that by increasing Rieske FeS protein in *Setaria viridis*, significant increased the content of Cytochrome b_6f in both mesophyll and bundle sheath cells (Ermakova *et al.*, 2019), and these increases in Rieske FeS protein resulted in an increase in photosynthetic rates without marked changes of Rubisco and chlorophyll content.

The aims of this chapter were to

1). Identify expression levels of the Rieske FeS gene in the guard cells of transgenic tobacco plants using an epidermal peel enrichment prep for guard cells and qPCR. 2). To carry out photosynthesis and growth analyses on identified and selected transgenic *Nicotiana tabacum* with increased Rieske FeS levels.

3). To assess the influence of increased in Rieske FeS on stomatal function and stomatal co-ordination with photosynthetic rates.

3.2 Results

3.2.1 Screening for primary transgenics

All lines of overexpression of Rieske FeS (AtRieske FeS) were grown on selective media and selected by watering with 0.51 mM of herbicide glufosinate-ammonium (BASTA; Sigma-Aldrich, UK) in order to obtain the BASTA-resistant seedlings. A clear observation between herbicide sensitive (wild type) and herbicide-tolerant (transgenic) seeds was achieved (Figure 3.1). WT seedlings completely died on media with BASTA, while transgenic seedlings were grown.

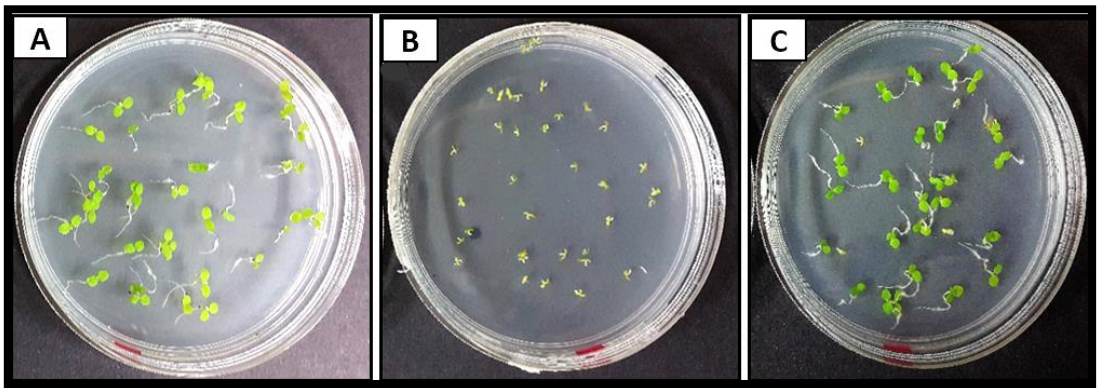

Figure 3.1 Herbicide (BASTA) screening of transgenic seeds and wild type seeds. (A) WT seeds grown without BASTA, (B) WT showing complete death of seeds grown on media with BASTA, and (C) transgenic seeds grown on media with BASTA. Plants were grown in controlled environment conditions (22 °C, 8 h light/16 h dark cycle).

3.2.2 Molecular Biology techniques

3.2.2.1 DNA analysis of T3 generation plants

PCR analysis was undertaken to check the presence of the transgene for each line. An insertion specific primer for all AtRieske FeS genes were used to amplify the T-DNA insert. The result of PCR bands in the following AtRieske FeS mutant

lines, GCFeS4.1, GGFeS4.2, GCFeS4.10, and GCFeS4.22 is shown in Figure 3.2. The band with the insertion specific primers at 690 bp was the size of the expected fragment, and no band was observed in WT plants with the insertion specific primers. At least 10 replicates for each line were analysed and insertion specific primers for AtRieske FeS gene were used to amplify the T DNA insert. (Figure 3.2). After the PCR analysis, only plants that showed a band were selected from each line, and the seeds collected for the next generation.

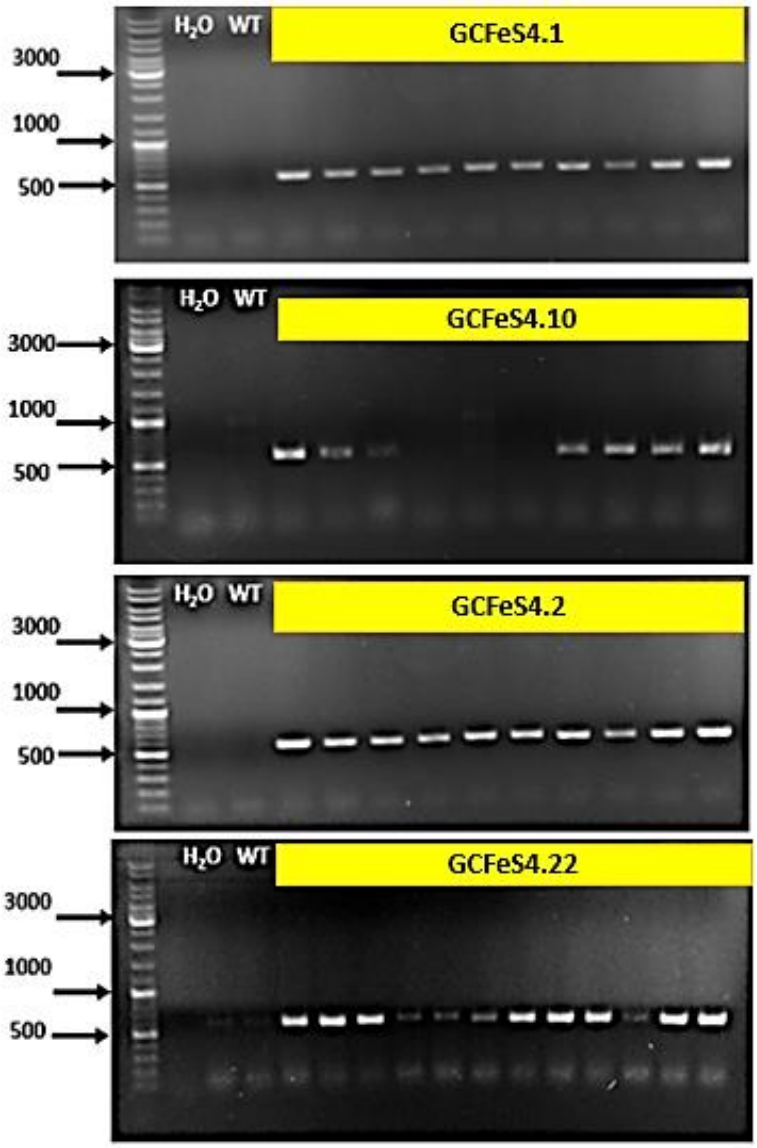

Figure 3.2 Genomic DNA screening of transformants for the presence of the transgene. PCR analysis was used to confirm the presence of construct (4-(pL2B-BAR-(pAGPase) AtRieske) at the selected lines. Yellow bars represent the names of independents lines.

3.2.2.2 Gene expression analysis of transgenic tobacco plants using qPCR

To analyse the expression of the AtRieske FeS gene in transgenic tobacco plants, total RNA was extracted from epidermal peel enrichment preps taken from four biological replicates from each independent line. In the next step, cDNA was produced for use in the quantification of the expression of the gene of interest transcript using qPCR. The results shown in Figure 3.3 clearly indicate different increases in AtRieske FeS gene expression levels compared to wild-type plants. The comparison between the four mutant lines revealed that the GCFeS4.2 line had the highest values of AtRieske FeS gene expression (47.1 ± 13.2) which were significantly greater ($P < 0.05$) than those of the wild-type (1.19 ± 0.14). A comparison of gene expressions between mesophyll and guard cells in WT and transgenic lines can be found in Appendix B.

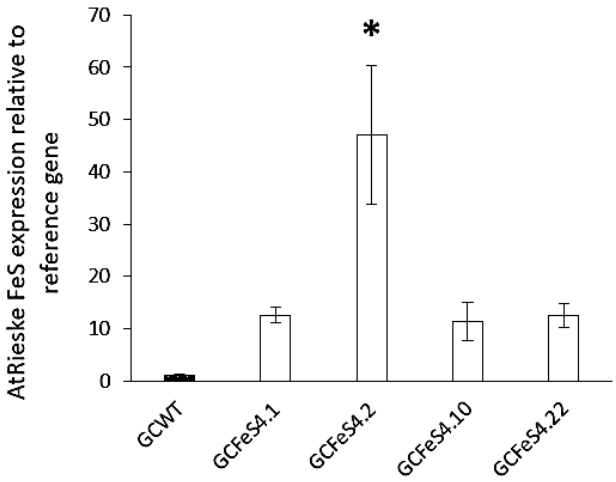

Figure 3.3 Quantitative PCR (qPCR) analysis of the expression of AtRieske FeS transgenic plants of construct (4-pL2B-BAR-(pAGPase)-AtRieske). RNA was extracted from extractions of epidermal peel enrichments. AtRieske FeS gene was amplified using specific primers (Chapter 2, Table 2.2). The expression was normalised against the reference gene (CER2 &GORK). Data are the means with standard error (n = 3 to 4). Asterisks (*) indicate significant differences ($P < 0.05$).

3.2.3 Plant phenotyping techniques

3.2.3.1 Thermal imaging and stomatal conductance

Thermal images were obtained using a thermal camera to determine differences in leaf temperature as a rapid phenotyping method to identify differences in stomatal behaviour. At two light intensities (130-600 µmol m^{-2} s^{-1}), the leaf temperature was responded to change in the light intensities, where the increased light led to a decrease in leaf temperature and vice versa. The results show that no differences in leaf temperature were observed between AtRieske FeS plants and wild-type plants, irrespective of when measurements were captured during the day (morning, mid-day, and afternoon) (Figure 3.4). Although the values of leaf temperature at mid-day were lower in all lines relative to the wild-type, this decline was not significant (Figure 3.4B).

On the other hand, when stomatal conductance (g_s) was measured using a leaf porometer, the Rieske FeS overexpressing plants had higher values of g_s than the wild-type plants and the g_s values were significantly different between the lines ($F_{(5,104)}$ = 2.354, P < 0.05), with the highest values being observed in line GCFeS4.22 (161.5 ± 9.91) which were significantly greater than those of the wild-type plants which had the lowest values of g_s (122 ± 7.55) (Figure 3.5).

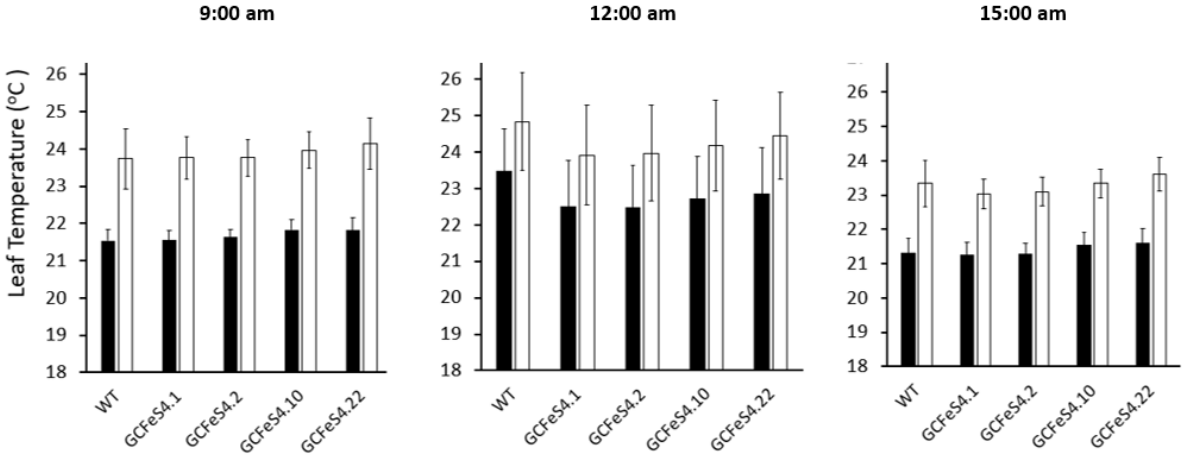

Figure 3.4 A comparison of leaf temperatures between wild-type (WT) and AtRieske FeS transgenic plants of construct (4-pL2B-BAR-(pAGPase)-AtRieske) was made at low light intensity at 130µmol m^{-2} s^{-1} (White bars) and at 600µmol m^{-2} s^{-1} high light intensity (Black bars). The measurements were taken during the daytime period. Plants were grown in controlled environment conditions (22°C, 8h light/16h dark cycle). Mean values ± SE were indicated (n=20).

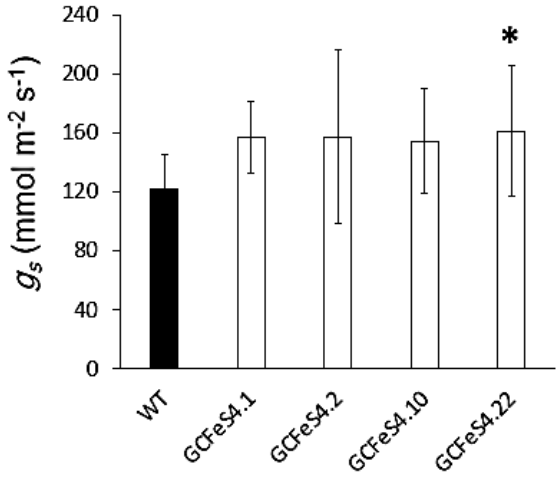

Figure 3.5 Stomatal conductance (g_s) of wild-type (WT) and AtRieske FeS transgenic plants of construct (4-pL2B-BAR-(pAGPase)-AtRieske) was measured. Plants were grown in controlled environment conditions (22°C, 8h light/16h dark cycle). Mean values ± SE were indicated (n=20). A significant difference was observed between lines and asterisks are used to indicate a significant difference from WT plants (P> 0.05).

3.2.3.2 Chlorophyll fluorescence of PSII operative efficiency

The operating efficiency of photosystem II (*Fq'/Fm'*) was determined from simultaneous images of chlorophyll fluorescence in whole plants. Rieske FeS overexpression (from four independent transgenic lines) and wild-type tobacco plants were grown in a controlled environment chamber until they had four to five leaves. A comparison between the AtRieske FeS lines and WT plants showed that *Fq'/Fm'* values of the AtRieske FeS lines decreased at both 200 and 800µmol m^{-2} s^{-1} PPFD when compared to WT plants (see Figure 3.6). GCFeS4.22 demonstrated significantly lower ($P < 0.05$) values of *Fq'/Fm'* at both low and high light intensities (see Figures 3.6A and 3.6B). Meanwhile, the GCFeS4.10 line had significantly lower ($P < 0.05$) values of *Fq'/Fm'* at 200µmol m^{-2} s^{-1} PPFD (see Figure 3.6A).

To investigate further the response of photosynthesis to the overexpression of AtRieske FeS, the induction of steady state chlorophyll fluorescence, light response curve and relaxation responses of transgenic lines and wild-type plants were measured. Ten replicates of T3 plants were assessed for each transgenic line and WT. The response of *Fq'/Fm'* to increasing PPFD revealed no significant differences in the operating efficiency of PSII (*Fq'/Fm'*) between transgenic and wild-type plants (Figure 3.7). In the light-adapted state at PPFD 500 µmol m^{-2} s^{-1} there was a tendency for *Fq'/Fm'* values to be higher in the transgenic lines compared to the WT control. The highest values of *Fq'/Fm'* were calculated for line GCFeS4.2 (Figure 3.8A). In the dark-adapted state, *Fv/Fm* values, which are indicative of the maximum quantum efficiency of PSII photochemistry,

considerable variation was observed between AtRieske FeS lines. Line GCFeS4.2 and line GCFeS4.10 had higher values of *Fv/Fm* than the wild-type plants (Figure 3.8B).

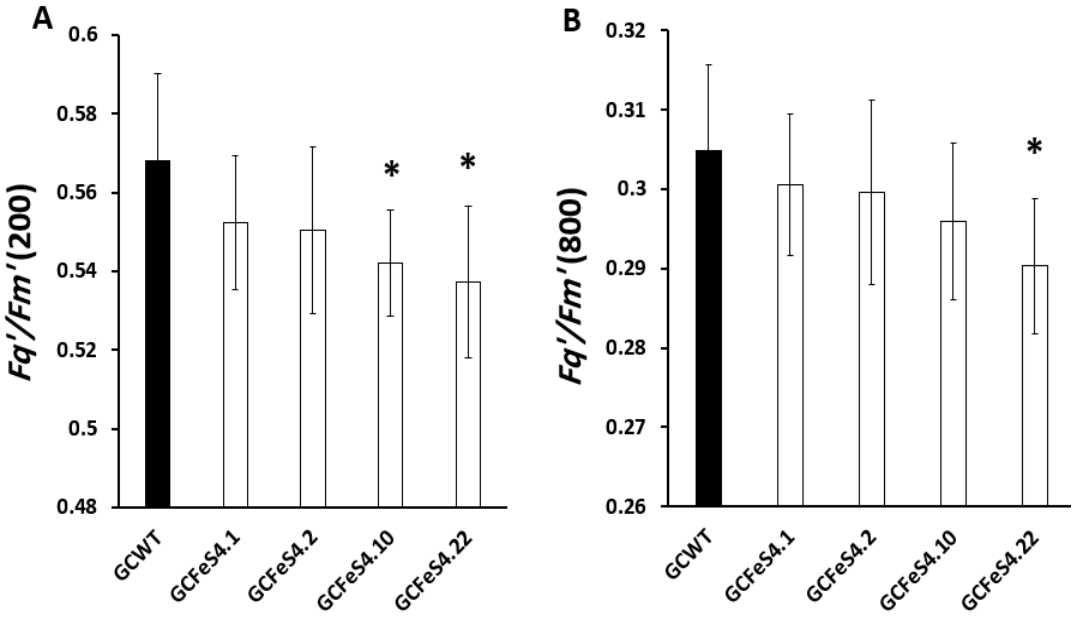

Figure 3.6 Photosynthetic efficiency of wild-type (WT) and AtRieske FeS transgenic plants of construct (4-pL2B-BAR-(pAGPase)-AtRieske) at two different light intensities. The operating efficiency of PSII (*Fq'/Fm'*) was determined at: **(A)** 200μmol m^{-2} s^{-1} and **(B)** 800μmol m^{-2} s^{-1}. Plants were grown in controlled environment conditions (22°C, 8h light/16h dark cycle). Mean values ± SE were indicated (n=10). Asterisks (*) indicate significant differences ($P < 0.05$) using the results of a Tukey post-hoc test following a one-way ANOVA.

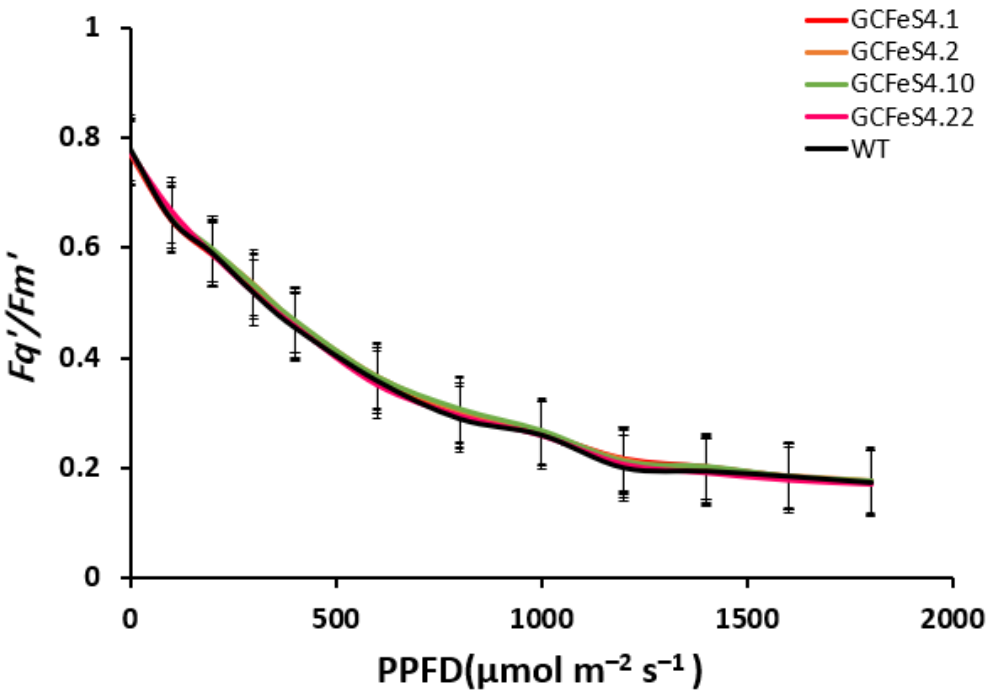

Figure 3.7 PSII operating efficiency of the light response curves of wild-type (WT) and AtRieske FeS transgenic plants of construct (4-pL2B-BAR-(pAGPase)-AtRieske). The chlorophyll fluorescence was used to determine *Fq'/Fm'* at different light intensities: 100, 200, 300, 400, 600, 800, 1000, 1200, 1400, 1600, and 1800 µmol m^{-2} s^{-1}. Plants were grown in controlled environment conditions (22°C, 8h light. 16h dark cycle). Mean values ± SE were indicated (n=10).

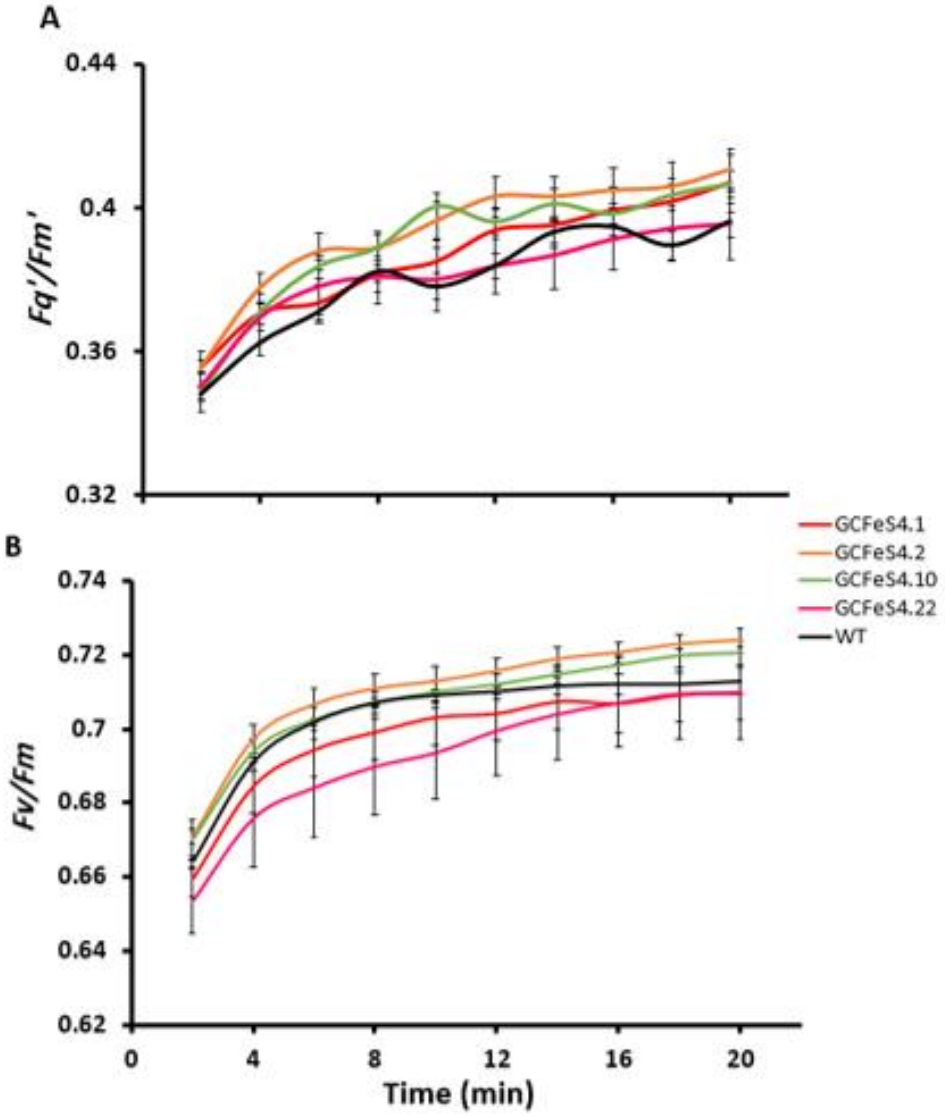

Figure. 3.8 PSII operating efficiency, *Fq'/Fm'*, at PPFD 500µmol m^{-2} s^{-1}**(A),** and the maximum quantum efficiency of PSII photochemistry, *Fv/Fm*, at PPFD 0µmol m^{-2} s^{-1} **(B)** were estimated. AtRieske FeS tobacco and WT seedlings were grown in controlled environment conditions (22°C, 8h light. 16 h dark cycle). Error bars represent mean ± SE (n=10).

3.2.4 Leaf gas exchange

3.2.4.1 Intracellular CO_2 (A/C_i) response curves

Photosynthesis as a function of internal [CO_2] (C_i), known as A/C_i curves, was used to determine any difference in photosynthetic capacity in plants overexpressing Rieske FeS compared to wild-type plants. All plants exhibited the expected increase in A with increased C_i up to a certain point before reaching a plateau. The results obtained from the A/C_i response analysis revealed that the transgenic plants overexpressing Rieske FeS achieved lower rates of photosynthetic carbon fixation than the wild-type plants. Line GCFeS4.22 achieved the greatest values of A (19.9 ± 0.77) compared with other transgenic lines but it was lower than the wild-type plants (Figure 3.9).

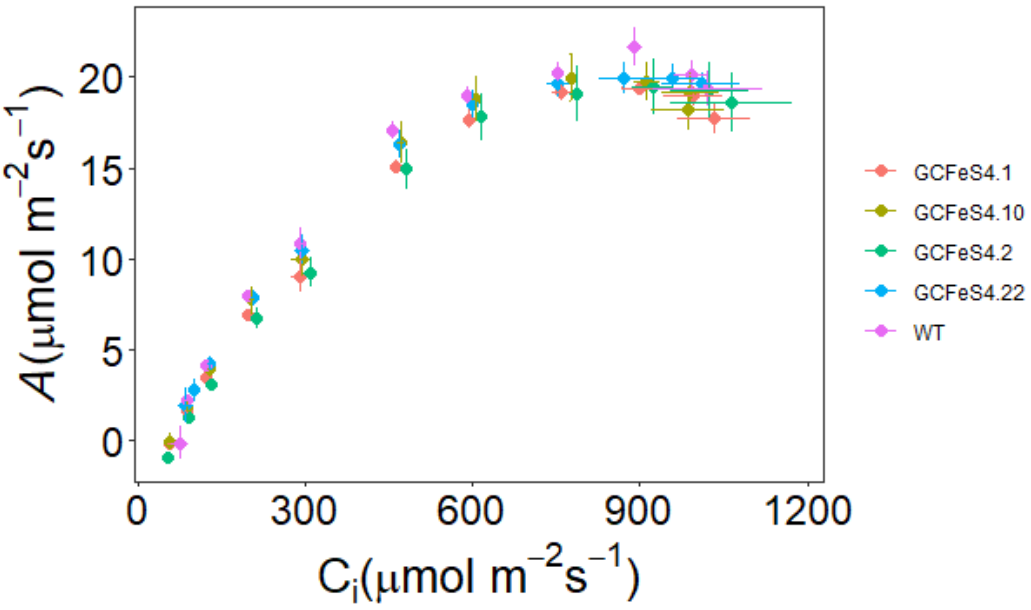

Figure 3.9 The response of net CO_2 assimilation (A) to intercellular [CO_2] (C_i) between 50 µmol m^{-2} s^{-1} and 1500 µmol m^{-2} s^{-1} under saturating PPFD (1500 µmol m^{-2} s^{-1}) for 4 independent lines of AtRieske FeS and WT tobacco plants. Error bars represent mean ± SE (n = 6-8).

The *A/C*$_i$ curves were used to calculate the maximum carboxylation capacity of Rubisco (*Vcmax*; Figure 3.10A), the maximum rate of electron transport for RuBP regeneration (J_{max}; Figure 3.10B) to determine any differences in photosynthetic capacity between the mutants, and the light and CO_2 saturated assimilation rate (A_{max}; Figure 3.10C) at 1500 µmol m^{-2} s^{-1} CO_2 under 1500 µmol m^{-2} s^{-1} PPFD. Overexpression Rieske FeS plants showed no significant differences in terms of the maximum rate of carboxylation (V_{Cmax}) compared to wild-type plants. The values of V_{cmax} were observed to be lower for line GCFeS4.1 and line GCFeS4.2 than for the wild-type (Figure 3.10A). All J_{max} values were observed to be lower for overexpression Rieske FeS plants when compared to the wild-type plants (Figure 3.10B), but this decrease was not significant. AtRieske FeS transgenic plants had lower photosynthetic rates compared to wild-type plants, except line GCFeS4.1 (20.44± 0.97), but no significant differences in A_{max} between transgenic and WT plants. (Figure 3.10C).

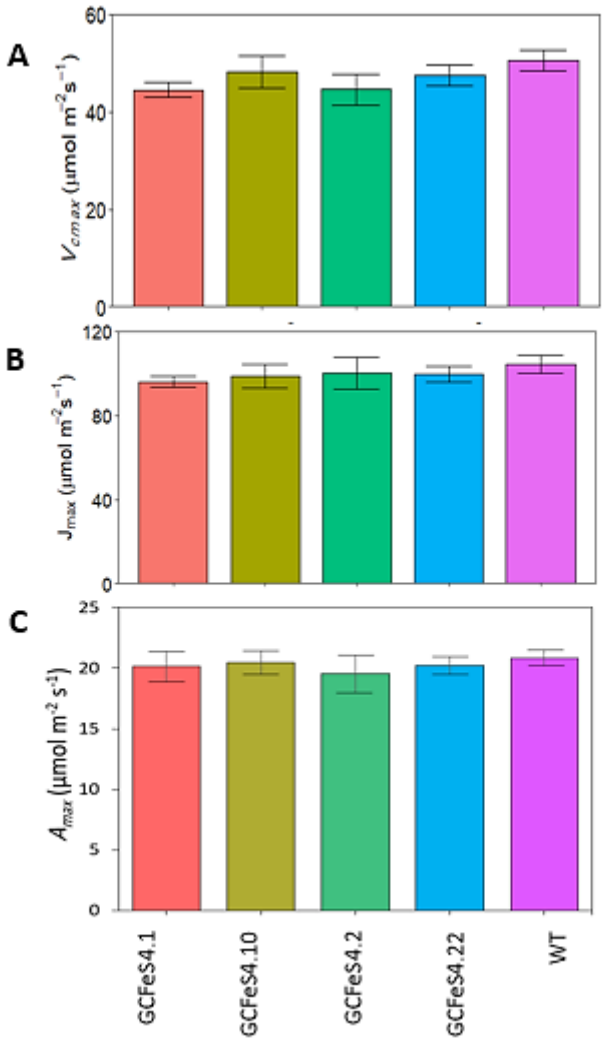

Figure 3.10 The maximum rate of carboxylation (V_{Cmax}; **A**) and maximum rate of electron transport (J_{max}; **B**) estimated from the response of *A* to C_i, and the light and CO_2 saturated rate of photosynthesis (A_{max}; **C**) determined for the four independent lines of AtRieske FeS and WT tobacco plants. Error bars represent mean ± SE (n=6-8).

3.2.4.2 Kinetics responses of g_s and A to a step change in PPFD

To assess the impact of the overexpression of Rieske FeS on photosynthesis and stomatal behaviour between the four lines and the WT, gas exchange measurements were taken. To assess the speed of response of g_s and plants were subjected to a step increase in light intensity (100-1500 µmol m^{-2} s^{-1}). Gas exchange parameters were measured for each genotype, including: stomatal conductance (g_s; Figure 3.11A), net CO_2 assimilation (A; Figure 3.11 B), and intrinsic water use efficiency (W_i; Figure 3.11C) calculated from the values of A and g_s ($W_i = A/g_s$).

Considerable variation was observed in the A and g_s responses to step-changes in PPFD between the transgenic lines measured and compared to WT plants. In general, the increase in PPFD to 1500µmol m^{-2} s^{-1} led to an immediate and rapid increase in A compared to g_s for all lines. G_s continued to increase for all AtRieske FeS lines, except line GCFeS4.1 (see Figure 3.11A). Despite A having reached near steady state levels, A was lower for transgenic plants compared to WT plants (see Figure 3.11B). Intrinsic water use efficiency (W_i) declined over the course of a step increase in light intensity (100µmol m^{-2} s^{-1} to 1500µmol m^{-2} s^{-1}) (see Figure 3.11C), predominantly driven by the slow increase in g_s at the same time period.

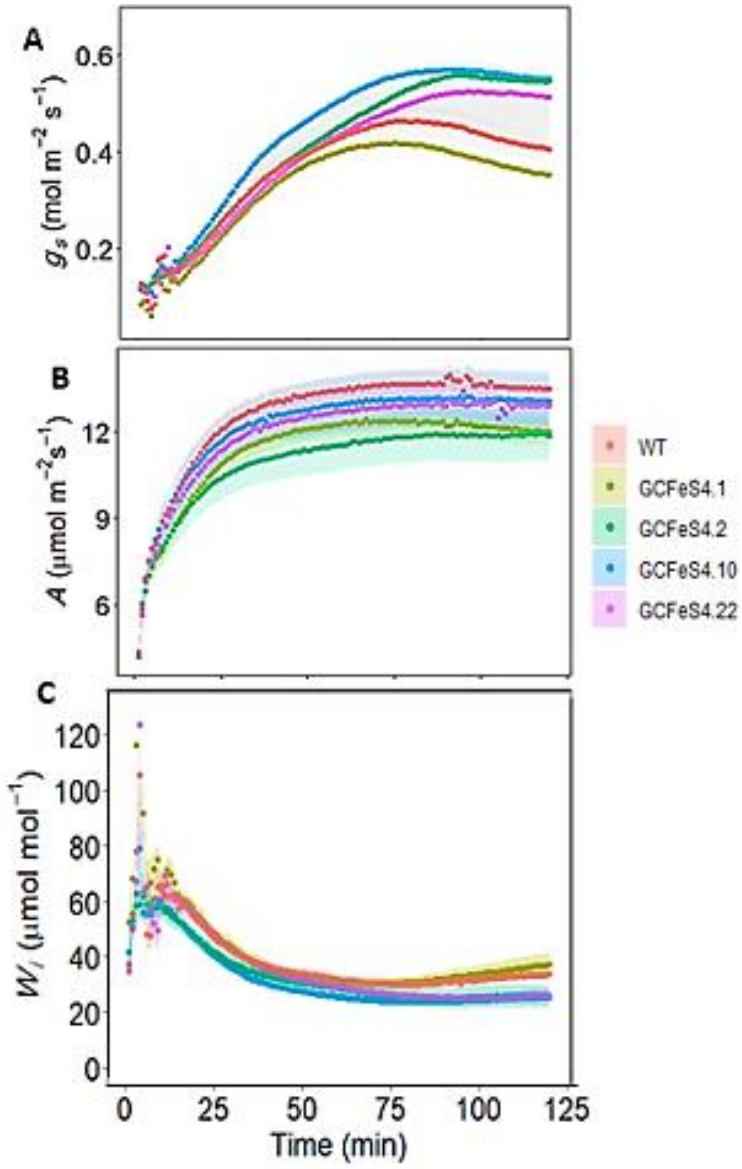

Figure. 3.11 Temporal response of stomatal conductance (g_s; **A**), net CO_2 assimilation (A; **B**), and intrinsic water use efficiency (W_i; **C**), to a step increase in light intensity (from 100 µmol m^{-2} s^{-1} for 10 minutes to 1500 µmol m^{-2} s^{-1} for 60 minutes) for WT and AtRieske FeS tobacco plants. Gas exchange parameters (g_s and A) were recorded at 30s intervals, leaf temperature maintained at 25°C, and leaf VPD at 1 ± 0.2 KPa. The data represent mean ± SE (n=6-8).

3.2.4.3 Speed of g_s response to a step change in light intensity

To determine the rapidity of the g_s and A responses to a step increase in PPFD a model was used to determine the following parameters: the time constants for the increases in g_s (τ_{gs}; Figure 3.12A), the final value of the g_s response at 1500 µmol m^{-2} s^{-1} PPFD (g_{sF}; Figure 3.12B), and the magnitude of change in g_s between steady state values at 100 PPFD to 1500 PPFD (Δg_s; Figure 3.12C). Figure 3.13 displays the time constants to reach 63 % of the final value for A (τ_A; Figure 3.13A), the final value of the A response at 1500 µmol m^{-2} s^{-1} PPFD (A_F; Figure 3.13B), and finally the magnitude of change in A between steady state values at 100 PPFD to 1500 PPFD (ΔA; Figure 3.13C).

Time constants for the increase in g_s (τ_{gs}; Figure 3.12A) were significant in the AtRieske FeS lines compared with the wild-type plants, line GCFeS4.2 and line GCFeS4.22 took a long time for stomatal opening. The final value of the g_s was higher in all transgenic lines of AtRieske FeS (except line GCFeS 4.1) compared to the wild-type plants. The highest g_{sF} observed was line GCFeS4.2, followed by line GCFeS4.22 and the same results for τ_{gs} was observed (Figure 3.12B). The magnitude of change in g_s (Δg_s; Figure 3.12C) between steady state values at 100 PPFD to 1500 PPFD displayed higher values in the transgenic lines of AtRieske FeS. The highest were line GCFeS4.2 and line GCFeS4.10; there was a ~100% difference between the highest value of Δg_s compared to the wild-type value.

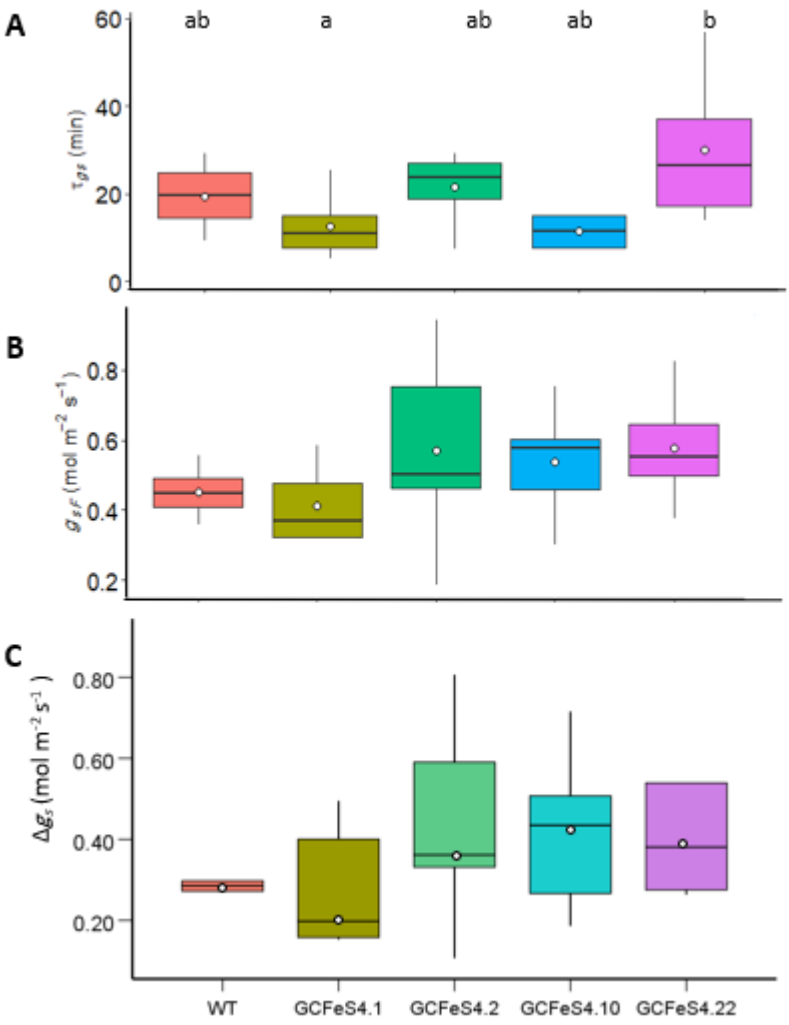

Figure 3.12 Time constants for the increases in gs (τ_{gs}; **A**) in minutes, the final value of the g_s response at 1500 µmol m^{-2} s^{-1} PPFD after an increased step change in light intensity ($g_{sF;}$ **B**), and difference in g_s between 100 µmol m^{-2} s^{-1} PPFD and 1500 µmol m^{-2} s^{-1} PPFD (Δg_s; **C**) following the step increase in light intensity. All results for 4 independent lines of AtRieske FeS and WT tobacco plants (n=6-8). Different letters are used to indicate a significant difference from WT plants (P> 0.05) using the results of a Tukey post-hoc test.

Time constants to reach 63 % of final value for *A* (τ_A; Figure 3.13A) did not follow the same trend as τ_{gs} with all transgenic plants taking longer than the wild-type to increase τ_A. The final value for *A* was higher in all transgenic lines of AtRieske FeS (except line GCFeS 4.1) compared to the wild-type plants. The highest A_F observed was line GCFeS4.2, followed by line GCFeS4.22 (A_F; Figure 3.13B). The magnitude of change in *A* (ΔA; Figure 3.13C) between 100 µmol m^{-2} s^{-1} and 1500 µmol m^{-2} s^{-1} PPFD observed a variation between transgenic plants and wild-type plants. The highest being the wild-type at ~10 µmol m^{-2} $s^{-1}$and the lowest being GCFeS4.2 and GCFeS4.22 at ~8.5 µmol m^{-2} s^{-1}.

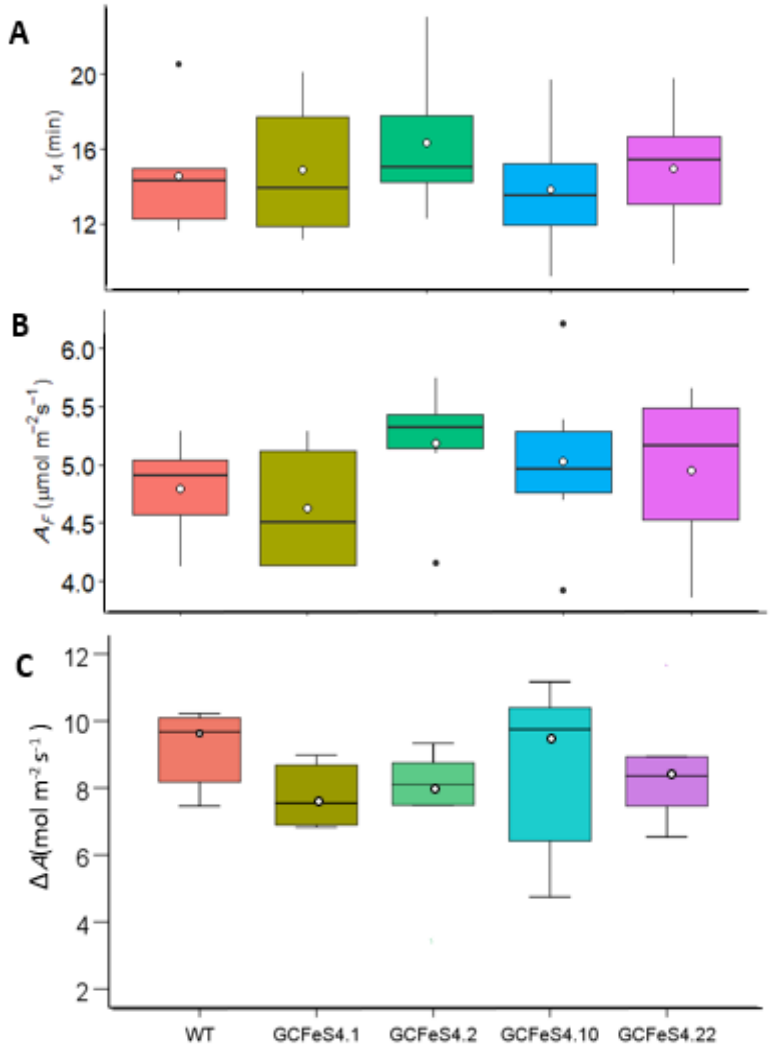

Figure 3.13 Time constants for the increases in *A* (τ_A; **A**) in minutes, the final value of the *A* response at 1500 μmol m^{-2} s^{-1} PPFD after an increased step change in light intensity (A_F; ***B***), and the difference in *A* between 100 μmol m^{-2} s^{-1} PPFD and 1500 μmol m^{-2} s^{-1} PPFD (ΔA; **C**) following the step increase in light intensity. All results for 4 independent lines of AtRieske FeS and WT tobacco plants. Error bars represent 95% confidence intervals using the results of a Tukey test (n=6-8).

3.2.5 Photosynthetic efficiencies in guard and mesophyll cells

High resolution chlorophyll fluorescence imaging was used to compare the photosynthetic efficiency of PSII in guard cell chloroplasts and mesophyll in leaves of plants overexpressing Rieske FeS and compared to wild-type plants at two different light intensities (61µmol m^{-2} s^{-1},130µmol m^{-2} s^{-1}, and 300µmol m^{-2} s^{-1} PPFD).

At low PPFD levels (61 µmol m^{-2} s^{-1}), there were significant differences between transgenic plants in *Fq′/Fm′* of guard and mesophyll cells compared to WT plants ($P < 0.05$). *Fq′/Fm′* values of guard cells and mesophyll were higher in all transgenic lines than WT plants. The GCFeS4.10 line showed the highest efficiencies, with guard cell and mesophyll *Fq′/Fm′* values of 0.50 and 0.49 respectively (Figure 3.14A).

A comparison between the *Fq′/Fm′* values of guard cells of AtRieske FeS lines and the WT showed that the GCFeS4.10 lines had significantly higher *Fq′/Fm′* values than the WT at PPFD 130µmol m^{-2} s^{-1} (Figure 3.14B).

At high PPFD levels (300µmol m^{-2} s^{-1}), there were significant differences between transgenic plants in *Fq′/Fm′* of guard and mesophyll cells compared to WT plants ($P < 0.05$). The *Fq′/Fm′* values of guard cells and mesophyll were higher in all transgenic lines than WT plants. The GCFeS4.10 line and GCFeS4.22 presented the highest efficiencies, with guard cell and mesophyll *Fq′/Fm′* values (Figure 3.14C). Moreover, no differences between *Fq′/Fm′* of guard and mesophyll cells in each plant.

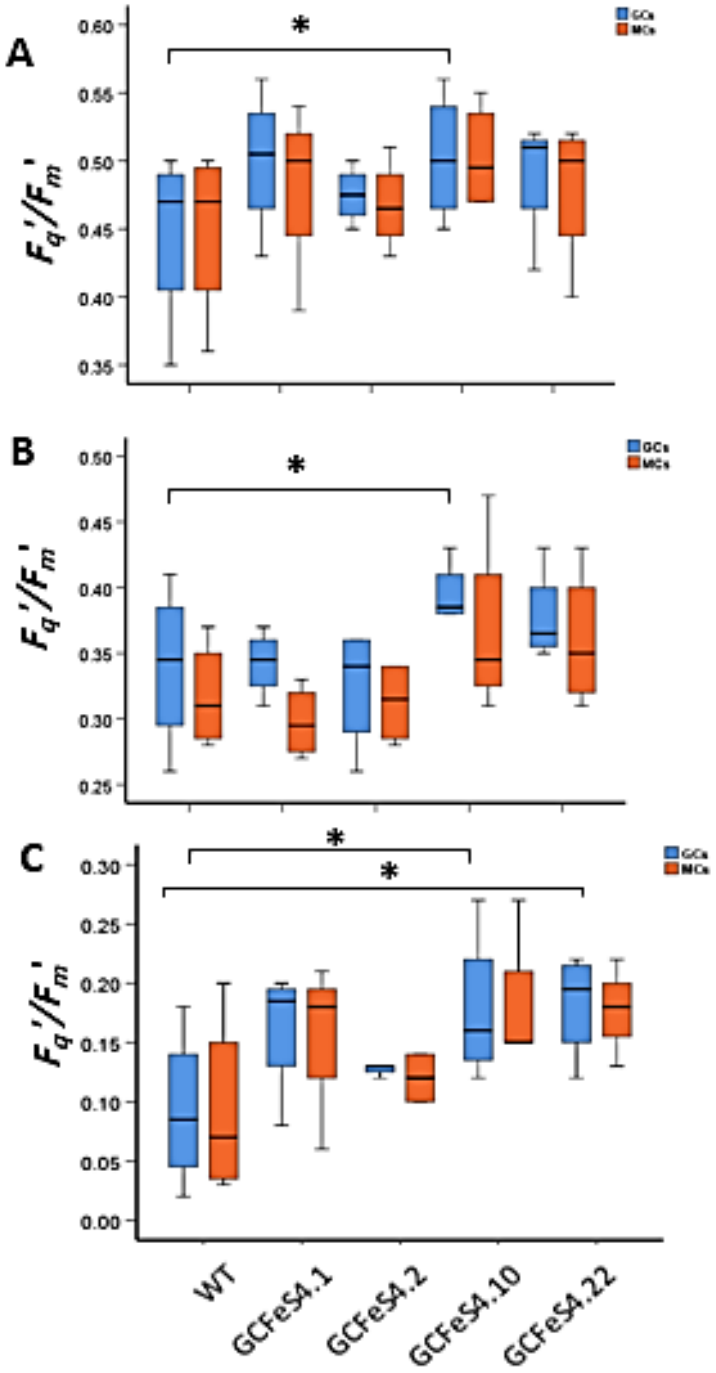

Figure 3.14 Comparison of guard cell and mesophyll cell photosynthetic efficiency (estimated by *Fq'/Fm'*) in leaves of wild-type (WT) and AtRieske FeS transgenic plants. Measurements were taken at three different light intensities: 61 µmol m^{-2} s^{-1}**(A),**130 µmol m^{-2} s^{-1} (**B**), 300 µmol m^{-2} s^{-1}(**C**). Mean values ± SE were indicated (n=4). Starts are used to indicate a significant difference from WT plants (P> 0.05) using the results of a Tukey post-hoc test following a two-way ANOVA.

3.2.6 Plant growth characteristics

In order to evaluate the effect of the overexpression of Rieske FeS (AtRieske FeS) on the growth and development of *Nicotiana tabacum*, the total leaf area (cm^2) and dry weight (g) were measured for all transgenic lines and the WT plants (Figure 3.15). The measurements were determined over the duration of the experiment and eight to ten biological replicates were included for each line. There was no significant difference in leaf area, although the GCFeS4.2 line achieved the highest leaf area (39.65 ± 1.39) of all the overexpression Rieske FeS plants (Figure 3.15A). On the other hand, a significant difference in dry weight (Figure 3.15) was also observed between the overexpression Rieske FeS plants and WT plants ($P < 0.0001$). The highest values were observed in line GCFeS4.2 (31.5 ± 0.95) and GCFeS4.1 (29.6 ± 0.59) was were significantly greater ($P < 0.0001$) than WT plants (21.1 ± 0.73). Line GCFeS4.10 (26.12 ± 0.95) also demonstrated significantly greater ($P < 0.01$) values of dry weight when compared to the wild-type plants (Figure 3.15B).

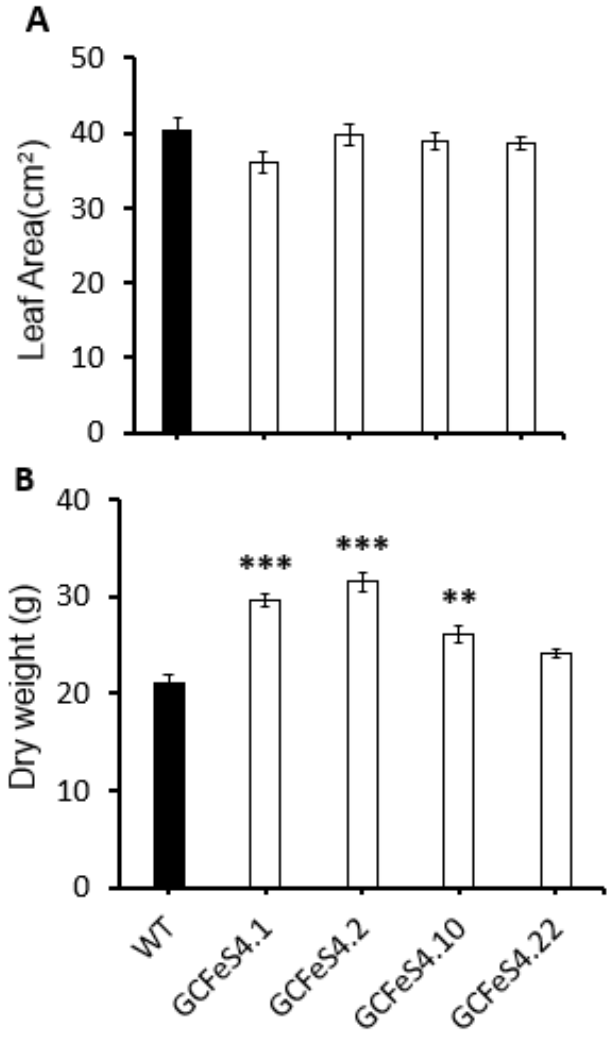

Figure 3.15 Leaf properties of the wild-type (WT) and AtRieske FeS transgenic plants of construct (4-pL2B-BAR-(pAGPase)-AtRieske) including: **(A)** leaf area and **(B)** dry weight. Plants were grown in an environmentally controlled greenhouse. Mean values ± SE were indicated (n=8 to 10). Asterisks (*) indicate significant differences ($P < 0.05$) using the results of a Tukey post-hoc test following a one-way ANOVA.

3.3 Discussion

Transgenic studies have shown that manipulation of enzymes of photosynthetic efficiency is a potential route for enhancing plant productivity (Lefebvre *et al.*, 2005; Feng *et al.*, 2009; Raines, 2011; Driever *et al.*, 2017a; Simkin *et al.*, 2017b). The work in this chapter identified transgenic tobacco plants with increased Rieske Fes gene in guard cells and explored the impact on whole photosynthetic capacity, operational assimilation rate as well as stomatal behaviour and guard cell specific photosynthetic efficiency.

It is evident from the Rieske FeS protein that the activity of the cytochrome b_6f complex is a key determinant of the rate of electron transport (Price *et al.*, 1998; Ruuska *et al.*, 2000; Yamori *et al.*, 2011a, 2011b). It has previously been established that if a plant overexpresses Rieske FeS, it will benefit from a superior quantum yield of both PSI and PSII photochemistry from the early growth stages (Baker, 2008). Moreover, overexpressing Rieske FeS results in heightened levels of the proteins related to ATP synthase as well as both PSI and PSII (Simkin *et al.*, 2017a). Using chlorophyll fluorescence imaging, our findings of transgenic plants with overexpression of cytochrome b_6f (Rieske FeS) in guard cells showed a small decrease in *Fq'/Fm'* which suggests that increases in the protein in the guard cells lead to decreases in PSII efficiency in the whole leaf. This could possibly due to an unbalance of the components of the electron transport chain. It has also been proposed that cyclic electron transport occurs in the guard cells (Lysenko, 2012), and therefore increasing the cytochrome b_6f complex in the guard cells does not help to promote this activity in the whole leaf.

Interestingly, the results of the high-resolution imaging with a microscope showed that the increase in Rieske FeS resulted in the increased *Fq'/Fm'* in guard cells when compared to guard cells of WT. This finding agrees with previous research that has focused on the role of Rieske FeS in PSII efficiency. In transgenic Arabidopsis thaliana plants, overexpression of the Rieske FeS protein in entire plants indicated an increase in the amounts of other cyt b_6f subunits and positive effects PSII efficiency (Simkin *et al.*, 2017a). Studies on transgenic tobacco plants show that cyt b_6f determines the rate of electron flow through the electron transport chain (Price *et al.*, 1995; Yamori *et al.*, 2011a). Therefore, these results suggest that the manipulation of Rieske FeS in guard cells might be of importance for stomatal behaviour. Our results of thermal imaging showed that leaf temperature (a proxy measure of stomatal behaviour) was not affected in plants overexpression of the Rieske FeS, whereas stomatal conductance that measured by porometry was significantly higher in overexpression of the Rieske FeS compared with wild type. These findings suggest that thermal screening may not be sensitive enough to reveal the small but significant differences in stomatal conductance (Vialet-Chabrand & Lawson, 2019). The change in stomatal conductance as demonstrated by the porometry measurements support the hypothesis that the electron transport chain plays a key role in stomatal responses and that manipulating electron flow in guard cells could be a potential target for manipulating stomatal behaviour.

Furthermore, a growth analysis conducted to examine the effect of the increased Rieske FeS in guard cells on plant growth revealed that the shoot biomass in overexpression Rieske FeS plants significantly increased by 5%-10%, and these

changes were due to both an increase in stem and leaf dry weights (Figure 3.15B). In transgenic Arabidopsis expressing algal cytochrome $(Cyt)_{c6}$, Chida *et al.*, (2007) observed that increases in electron transport can lead to an increase in improvements in plant growth in terms of height, root and leaf lengths. Similar findings were also shown when Yadav *et al.*, (2018) introduced the *Cytochrome* c_6 (*UfCyt* c_6) gene from *Ulva fasciata* Delile in tobacco. These authors showed that the expression of this enzyme can accelerate plants growth and better morphology/greenish color of plants at different time periods.

Previous studies have shown that increased stomatal conductance (g_s) leads to improved photosynthesis whilst increased WUE has been obtained in plants with lower g_s (Antunes *et al.*, 2012, 2017; Penfield *et al.*, 2012; Daloso *et al.*, 2016b). However, some findings suggest that manipulation of main genes that control the *A*– g_s trade-off leads to improve *A* and WUE in plants (Kelly *et al.*, 2013; Lugassi *et al.*, 2015). Our findings that changes in the kinetic responses of g_s and *A* to changes in PPFD but limited effects on assimilation rates (*A*) indicate that manipulating electron transport in guard cells could be a potential target for manipulating g_s behaviour in dynamic environment to improve photosynthesis and water use efficiency (W_i).

Moreover, the results obtained from analyses of the A/C_i response curves have shown that overexpression of Rieske FeS in guard cells has shown to impact negatively on carbon assimilation in the mesophyll. These findings suggested that the photosynthesis rates can be affected by the altered expression of Rieske FeS in guard cells. It is difficult to explain the decrease in photosynthesis in the transgenic plants as any alterations in expression should have been limited to the

guard cells. However, the promotor used for guard cell specific expression has been suggested to be “leaky” in certain situation or plant species (Rusconi *et al.*, 2013). Rusconi *et al.*, (2013) have found that a promoter has limitations between dicots and monocots, as the MYB60 promoter isolated from Arabidopsis failed to drive expression in rice (Oryza sativa) whereas was active in guard cells of Solanaceae species (tobacco and tomato). Furthermore, even if the specificity of the promotor was questioned, overexpression of Rieske Fe S and alterations to the cytochrome b_6f complex have shown positive effects on photosynthetic processes and plant performance (Simkin *et al.*, 2017a; Ermakova *et al.*, 2019). Stomatal behaviour can also influence photosynthetic rates, however increased g_s removes diffusional constraints and increases *A* but often at the expense of water use efficiency through increased transpiration (Lawson *et al.*, 2010; Lawson & Blatt, 2014; Lawson & Vialet-Chabrand, 2019) and therefore these findings cannot explain the lowered photosynthetic capacity.

Overall, these results indicate that stomata responded to manipulation of chloroplast metabolism in the guard cell and that these responses could elucidate mesophyll-stomatal interactions and could provide signal(s) that coordinate mesophyll CO_2 demands with stomatal responses.

CHAPTER 4

The effect of alter expression levels of the Sedoheptulose-1, 7-bisphosphatase (SBPase) on guard cell photosynthesis and stomatal behaviour

4.1 Introduction

Although there has been debate in the past regarding whether or not guard cell chloroplasts contain functional Calvin cycle enzymes but there is now consensus that the Calvin cycle enzymes are present and functional in guard cell chloroplasts (Lawson, 2009). It has been established by Daloso *et al.*, (2015) that guard cells have the ability to fix CO_2 via both Rubisco and phosphoenolpyruvate carboxylase (PEPc), however, it is unknown what contribution each individual pathway makes in terms of amount of carbon fixation and/or the production of sucrose.

The regulation of guard cells is complex and so is the role that sucrose plays in this process. Indeed, it has been suggested that sucrose can act as an osmoticum for guard cell function (Talbott & Zeiger, 1996; Daloso *et al.*, 2016a) and/or as a signalling molecule to co-ordinate photosynthesis and transpiration (Outlaw & De Vlieghere-He, 2001). Earlier studies proposed that sucrose in guard cells served as an osmolyte because it was known that increasing the stomatal aperture was accompanied by an increase in sucrose levels (Talbott & Zeiger, 1993, 1996; Amodeo *et al.*, 1996). More recently, research has indicated that sucrose can act as a substrate during light-induced opening of the stomata (Antunes *et al.*, 2012; Daloso *et al.*, 2015, 2016b), and also may play a role in stomatal closure (Kelly *et al.*, 2013; Lugassi *et al.*, 2015). Moreover, research has confirmed that the accumulation of mesophyll-derived sucrose in the guard cell apoplast can reduce stomatal aperture (Outlaw & De Vlieghere-He, 2001; Kang *et al.*, 2007).

There are three possible sources of sucrose found in guard cells: the primary source of sucrose is photosynthesis which takes place in mesophyll cells. There are certain similarities between guard cells and sink cells, including low rates of

photosynthesis (Gotow *et al.*, 1988), the high activity of sucrose synthase, and increased expression of sucrose synthase 3, as well as guard cells having different hexose transporters (Daloso *et al.*, 2015, 2017). Sucrose produced in the mesophyll can be taken up into the guard cells from the apoplastic space (Kang *et al.*, 2007). However, guard cells have the ability to create sucrose as a result of photosynthesis and starch breakdown within the chloroplasts (Lawson, 2009; Daloso *et al.*, 2015). However, it is unknown what proportion of the sucrose present in guard cells derives from mesophyll cells and what proportion is produced internally. Several studies have contributed important evidence that the breakdown of starch, sucrose and triacylglycerols in guard cells has a significant role in stomatal movements (Daloso *et al.*, 2015; Horrer *et al.*, 2016; McAusland *et al.*, 2016). In addition, there is also evidence to suggest that stomatal closure is governed by the presence of sucrose in the apoplast space (Kang *et al.*, 2007).

Transgenic plants with differing abilities to produce sucrose in the guard cells may allow a better understanding of the source of sucrose as well as the function it performs in stomatal movements. Several previous research studies have successfully manipulated the genes of guard cells by using guard cell specific promoters (such as KST1) or guard cell enriched promotors (AGPase). Using such promotors rather than generic ones prevent undesired pleotropic changes in sink tissues or mesophyll cells, especially when manipulating genes associated with sugar (Plesch *et al.*, 2001; Kelly *et al.*, 2017). It is known that the movement of the stomata can be manipulated in transgenic plants by altering the metabolism of guard cell sugar. For instance, Antunes *et al.*, (2017) confirmed that there are lower levels of sucrose in tobacco plants that have lower expression of Sucrose Transporter 1 (SUT1) within guard cells and these plants had lower steady state

stomatal conductance values. In addition, it is known that transgenic Arabidopsis and tomato plants with increased hexokinase (HXK) expression within the guard cells had reduced stomatal aperture, less transpiration and more WUE under drought conditions (Kelly *et al.*, 2019). Conversely, when sucrose synthase 3 (StSUS3) was overexpressed, g_s increased and resulted in higher *A* as well as greater plant growth (Daloso *et al.*, 2016b). Furthermore, it is known that Arabidopsis plants that lack enzymes associated with starch degradation (BAM1 and AMY3) or hexose transporters (STP1 and STP4) have altered metabolism and reduced sugar in guard cell which resulted in slower light-induced stomatal opening (Flütsch *et al.*, 2020a, 2020b). More recently, Freire et al., (2021) have concluded that there is slower stomatal opening and reduced whole plant transpiration in transgenic tobacco plants that have reduced expression of guard cell sucrose synthase 2 (NtSUS2).

Antisense and overexpression approaches are methods to manipulate Calvin-Benson Cycle enzymes and have a great impact on plants performance (Lefebvre *et al.*, 2005; Lawson, 2009; Raines, 2011; Simkin *et al.*, 2015; Driever *et al.*, 2017b). Therefore, it is the Calvin-Benson Cycle enzymes that genetic engineers manipulated in an attempt to enhance the rate of photosynthesis (Raines, 2003, 2011). One of the most important enzymes associated with the fixation of photosynthetic carbon in the Calvin cycle is Sedoheptulose-1, 7-bisphosphatase (SBPase). Compared to other Calvin-Benson Cycle enzymes, SBPase has a high control co-efficient on photosynthesis and therefore total carbon fixation (Ding *et al.*, 2016). It has been established in several modelling studies that the importance of the SBPase enzyme in the Calvin-Benson Cycle is because of its ability to

regulate and its localisation between the regenerative of RuBP and assimilatory (biosynthesis of sucrose and starch) stages of the cycle (Raines *et al.*, 1999; Feng *et al.*, 2007; Rosenthal *et al.*, 2011). Poolman et al., (2000) provided evidence that SBPase and Rubisco are responsible for controlling flux in the Calvin-Benson Cycle, that depended on the environmental growth conditions of plants. Moreover, it has been confirmed that transgenic manipulation of SBPase enzyme or alternative RuBP regeneration enzymes can influence plant biomass, rate of growth and rate of photosynthesis (Lefebvre *et al.*, 2005; Uematsu *et al.*, 2012). Plants overexpressing SBPase, for example, in transgenic tomato, tobacco, and *Arabidopsis thaliana* (Arabidopsis) have been reported to have increased photosynthetic carbon assimilation and plants biomass (Lefebvre *et al.*, 2005; Simkin *et al.*, 2015; Ding *et al.*, 2016; Driever *et al.*, 2017b). More specifically, when studying tobacco plants, Lefebvre et al., (2005) demonstrated that there was accumulation of starch and sucrose as well as increased rates of photosynthetic CO_2 assimilation, that resulted in increased biomass by 30%. Meanwhile, in a separate study, biomass yields were found to be significantly higher as a result of increasing the activity of SBPase under an open-air elevation of CO_2 (Rosenthal *et al.*, 2011). Further support for these results also comes from work on wheat where up to 40% increase in grain yield and the rate of photosynthesis were found when SBPase activity was increased (Driever *et al.*, 2017b). Using antisense SBPase tobacco plants, Lawson *et al.*, (2008) explored the relationship between CO_2 assimilation rate and stomatal conductance in response to step changes in normal mixed blue/red light, and red light alone and found antisense SBPase plants had a greater rate of stomatal opening and final stomatal conductance compared to wild type. However, interesting developments have been observed

in SBPase antisense plants and in response to manipulation of other metabolic pathways (Lawson *et al.*, 2006; Raines & Paul, 2006).

Transgenic tobacco (*Nicotiana tabacum*) plants with different expression levels of SBPase specifically in guard cells were used to investigate and study the effect of altered SBPase expression (overexpression and antisense) on stomatal function, photosynthesis, and growth rates under controlled greenhouse conditions.

4.2 Results

4.2.1 Screening for primary transgenics

As mentioned in section 2.2, to verify the BASTA-resistant seedlings. Transgenic tobacco seeds for two different expressions of SBPase (overexpression of SBPase) and (antisense of SBPase) were germinated on MS media containing BASTA herbicide (0.51 mM). Figure 4.1 shows the selection of BASTA resistant transgenics and demonstrates that WT seedlings completely died on media containing BASTA. Seedlings were selected that were BASTA resistant and planted in soil for further analysis.

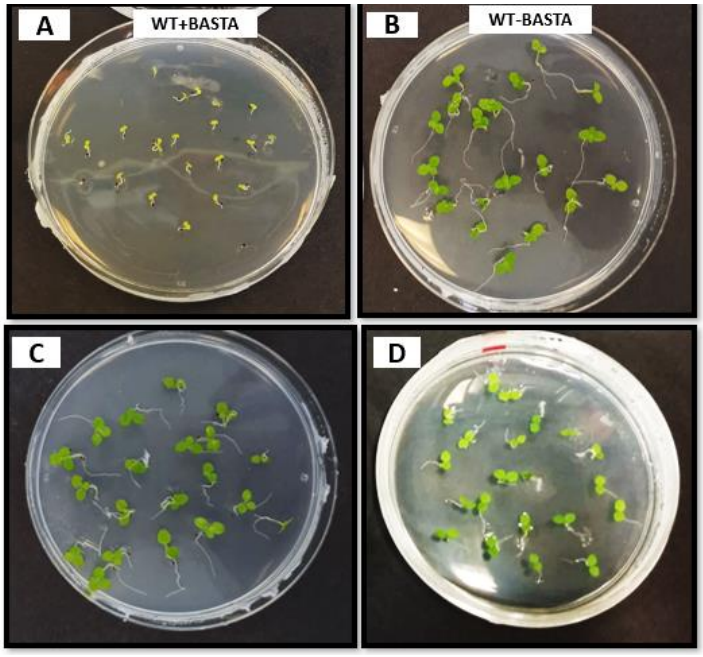

Figure 4.1 Herbicide (BASTA) screening of transgenic seeds and wild type seeds. (A) WT seedlings with BASTA, (B) WT seedlings without BAST, (C) transgenic overexpression SBPase seedlings, and (D) transgenic antisense SBPase seedlings. Plants were grown in controlled environment conditions (22°C, 8h light/16h dark).

4.2.2 Molecular Biology techniques

4.2.2.1 DNA analysis of T3 generation plants

As mentioned in the previous chapter, PCR analysis was performed to confirm the presence of the transgene for each line. To identify transgenic tobacco plants with antisense SBPase expression (ASNtSBPase) and overexpression of SBPase (AtSBPase),10 independent lines were screened using an insertion specific primer for ASNtSBPase gene and AtSBPase gene. Out of these 10 lines, four independent lines of antisense SBPase and three independent lines of overexpression SBPase were selected and then discussed in this chapter.

The results of PCR screening showed that several positive bands were identified at approximately 1269bp for the ASNtSBPase gene (Figure 4.2), and 1182bp for the AtSBPase gene (Figure 4.3) compared to the WT plants which had no bands. After the PCR analysis, only plants that showed a positive band were selected from each line, and the seeds collected for the next generation.

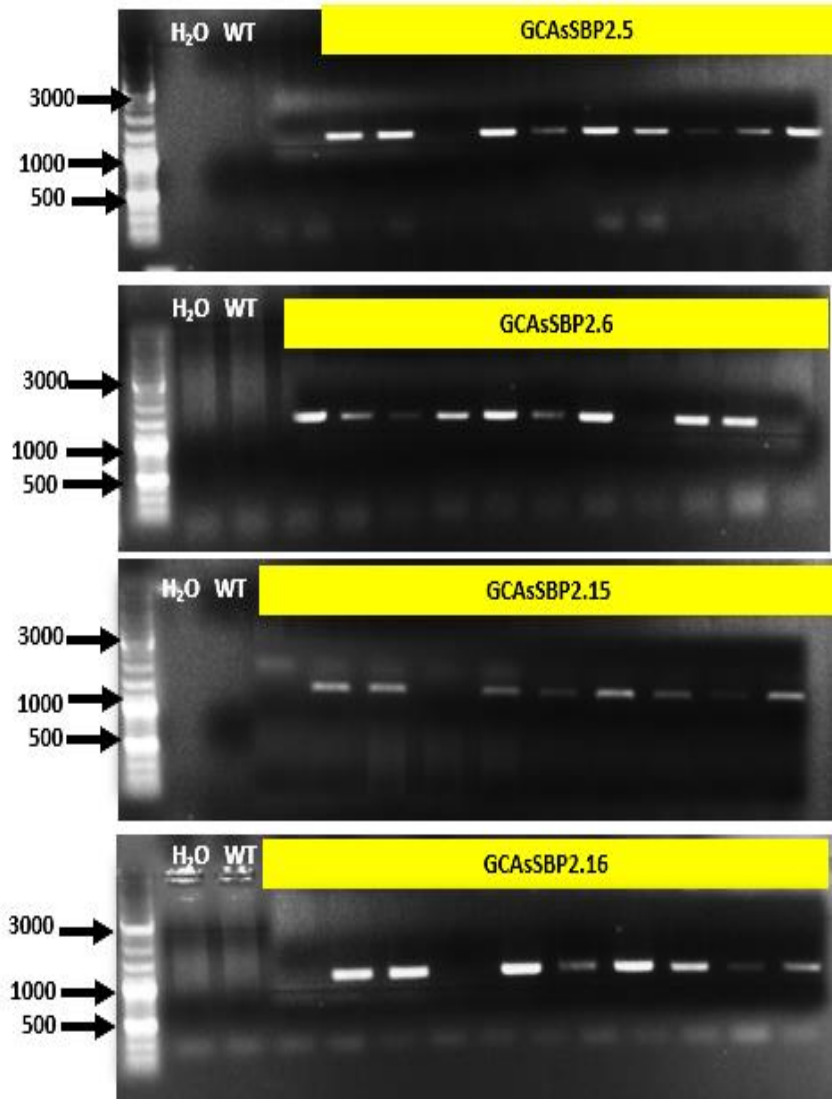

Figure 4.2 Genomic DNA screening of transformants for the presence of the transgene. PCR analysis was used to confirm the presence of construct (2-pL2B-BAR-(pAGPase)-ASNtSBPase) at approximately 1269 bp. Yellow bars represent the names of independents lines.

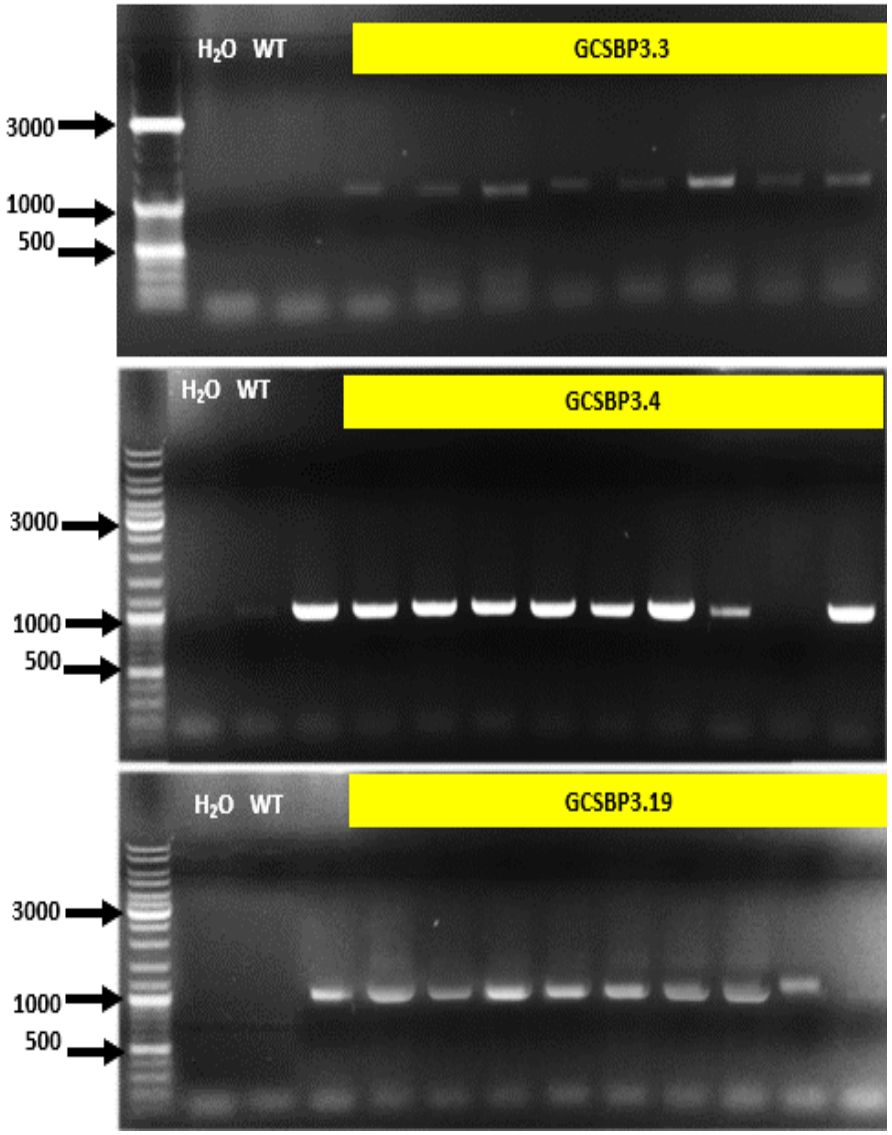

Figure 4.3 Genomic DNA screening of transformants for the presence of the transgene. PCR analysis was used to confirm the presence of construct (3-pL2B-BAR-(pAGPase)-AtSBPase) at approximately 1182 bp. Yellow bars represent the names of independents lines.

4.2.2.2 Gene expression analysis of transgenic tobacco plants using qPCR

The expression level of SBPase genes for each construct in transgenic tobacco plants was checked by qPCR analysis in all positive transformants. Four independent lines of antisense SBPase (GCAsSBP2.5, GCAsSBP2.6, GCAsSBP2.15, and GCAsSBP2.16), and three independent lines of overexpression SBPase (GCSBP3.3, GCSBP3.4, and GCSBP3.19) were checked and selected.

For each construct, total RNA was extracted from epidermal peel enrichment preps taken from four biological replicates from each independent line. In the next step, cDNA was produced for use in the quantification of the expression of the gene of interest transcript using qPCR.

Figure 4.4A indicates that some antisense lines do indeed show a reduction in ASNtSBPase gene expression levels compared to wild-type plants. The comparison between the four mutant lines revealed that the GCAsSBP2.16 line had the lowest values of ASNtSBPase gene expression (0.6 ± 0.34) which were significantly lower ($P < 0.05$) than wild-type (1.1 ± 0.01). For plants overexpressing SBPase, the majority of the AtSBPase plants tested showed an increase in expression levels compared to wild-type plants. The three transgenic lines shown that the GCSBP3.3 line and GCSBP3.4 line had the highest values of AtSBPase gene expression (17.9 ± 11.36) and (18.1± 2.51) respectively, which were significantly greater ($P < 0.05$) than wild-type (3.61 ± 2.56) (Figure 4.4B). A comparison of gene expressions between mesophyll and guard cells in WT and transgenic lines can be found in Appendix C.

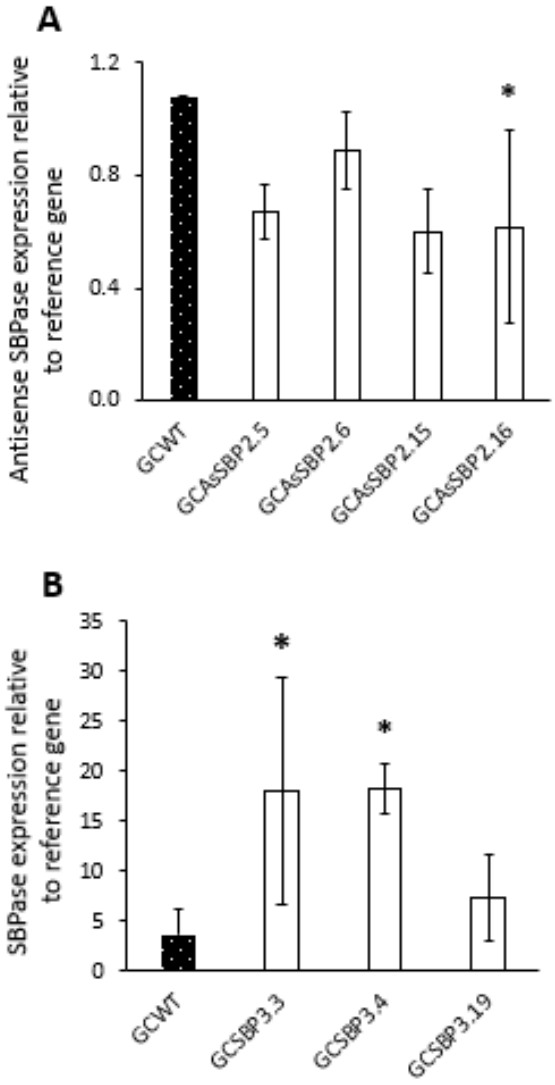

Figure 4.4 Quantitative PCR (qPCR) analysis. The expression of antisense SBPase of construct (2-pL2B-BAR-(pAGPase)- ASNtSBPase) **(A)** and the expression of SBPase of construct (3-pL2B-BAR-(pAGPase)- AtSBPase) **(B)** in tobacco plants. RNA was extracted from extractions of epidermal peel enrichments. ASNtSBPase and AtSBPase genes were amplified using specific primers (Chapter 2, Table 2.2). The expression was normalised against the reference gene (CER2 &GORK). Data are the means with standard error (n = 3 to 4). Asterisks (*) indicate significant differences ($P < 0.05$).

4.2.3 Plant phenotyping techniques

4.2.3.1 Thermal imaging and stomatal conductance

To identify phenotype in stomatal behaviour between transgenic plants differences in leaf temperature were measured and thermal images were obtained with a thermal imager as described in method 2.8.1. In both genotypes, there were no detectable differences in leaf temperature at different times of day (morning, mid-day, and afternoon) compared with wild-type plants (Figure 4.5). Although the leaf temperature was responded to change in the light intensities, where the increased light led to a decrease in leaf temperature and vice versa. The same results were found when these measurements were conducted on Rieske FeS plants in the previous chapter.

Furthermore, a leaf porometer was used to measure stomatal conductance (g_s) for each genotype and compared with wild-type plants. In antisense SBPase plants, there were found to be significant differences ($F_{(5,99)} = 6.466$, $P < 0.001$), with the greatest values of g_s observed in line GCAsSBP2.5 (117.9 ± 8.39) and line GCAsSBP2.16 (102.6 ± 5.28) both of which were significantly greater ($P < 0.001$) than the values observed for wild-type plants (70.5 ± 6.5) (Figure 4.6A). While SBPase overexpressing plants also demonstrated that the values of g_s were significantly different ($F_{(5,99)} = 4.319$, $P < 0.001$), g_s values were lower than wild-type plants except for line GCSBP3.3. The lowest values of g_s were achieved for line GCSBP3.4 (73.5 ± 7.22) when compared with wild-type plants (90.9 ± 9.73) (Figure 4.6B).

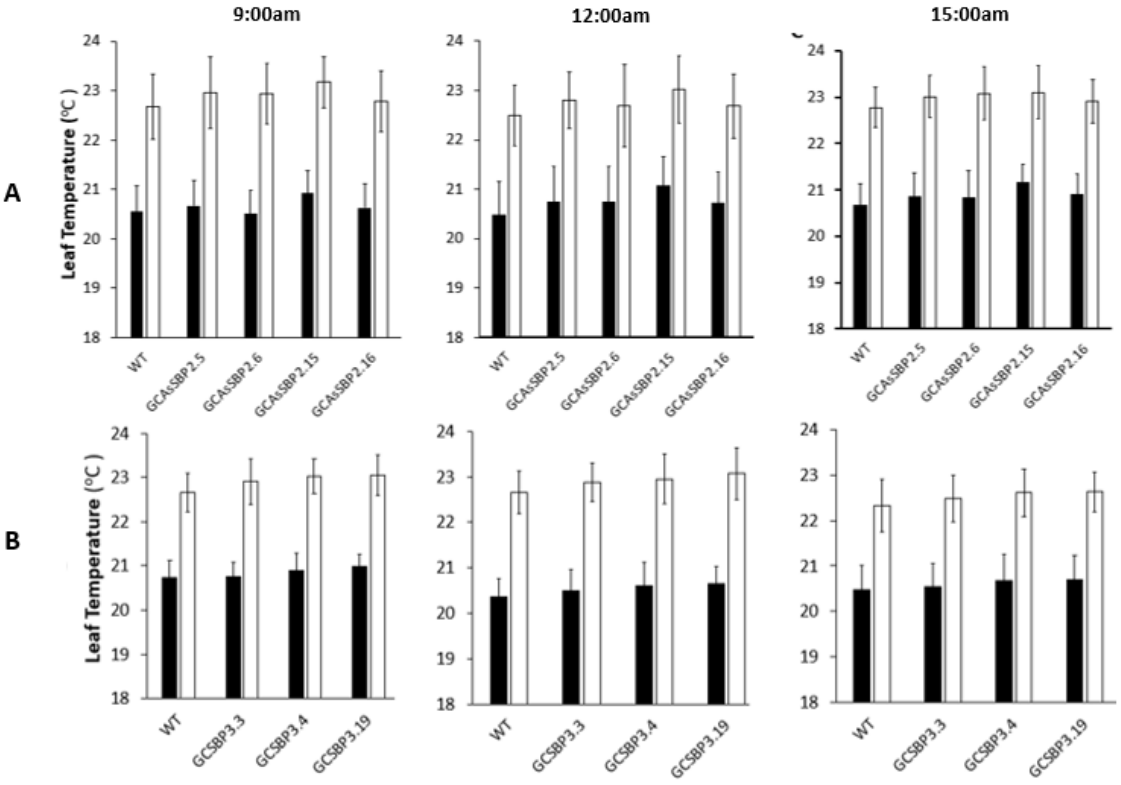

Figure 4.5 A comparison of leaf temperatures between wild-type (WT), transgenic plans. Construct (2-pL2B-BAR-(pAGPase)-ASNtSBPase) **(A)** and construct (3-pL2B-BAR-(pAGPase)-AtSBPase) **(B)** were made at low light intensity at 130µmol m^{-2} s^{-1} (White bars) and at 600µmol m^{-2} s^{-1} high light intensity (Black bars). The measurements were taken during the daytime period. Plants were grown in controlled environment conditions (22°C, 8h light/16h dark cycle). Mean values ± SE were indicated (n=20).

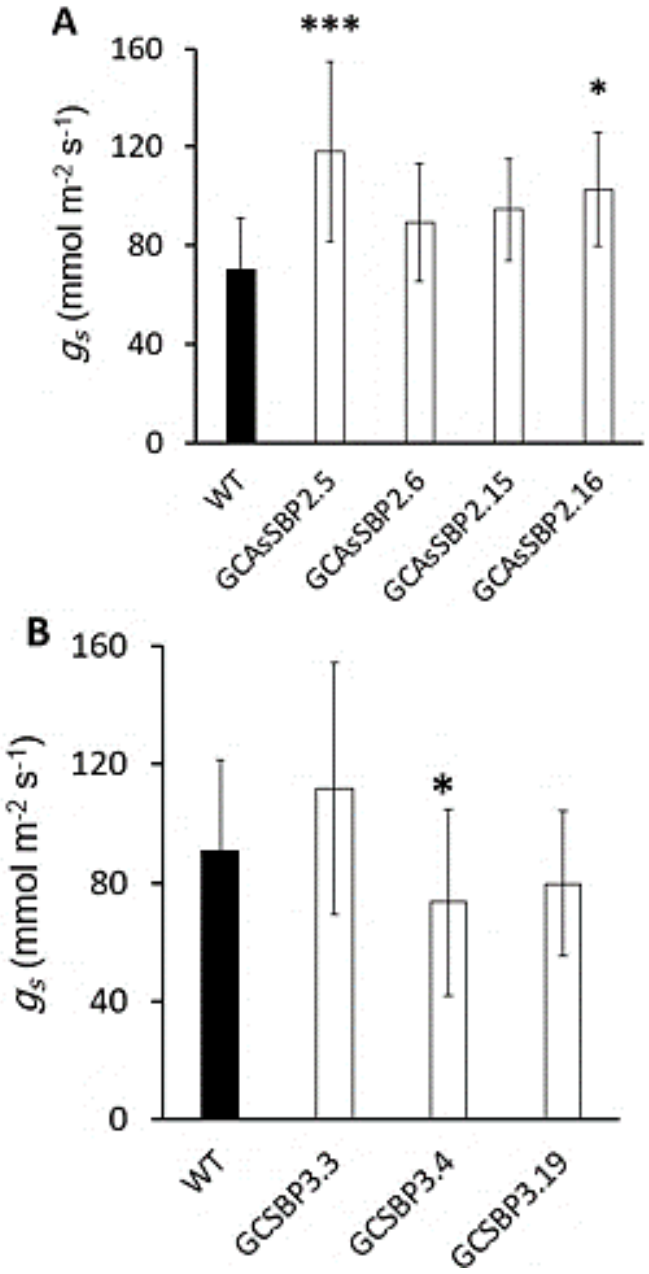

Figure 4.6 Stomatal conductance (g_s) of wild-type (WT) and transgenic plants. **(A)** construct (2-(pL2B-BAR-(pAGPase) ASNtSBPase), and **(B)** construct (3-pL2B-BAR-(pAGPase)-AtSBPase) were measured. Plants were grown in controlled environment conditions (22°C, 8h light/16h dark cycle). Mean values ± SE were indicated (n=20). A significant difference was observed between lines and asterisks are used to indicate a significant difference from WT plants (P> 0.05).

4.2.3.2 Chlorophyll fluorescence of PSII operative efficiency

The operating efficiency of PSII (*Fq'/Fm'*) for each genotype was compared with wild-type plants. The experiment was conducted on young seedlings of 14–21 days of growth subjected to two different light intensities. Transgenic plants of antisense SBPase (ASNtSBPase) showed no significant differences between wild type and transgenic plants at 200 µmol m^{-2} s^{-1} and 800 µmol m^{-2} s^{-1} (Figure 4.7). Similarly, *Fq'/Fm'* of wild type plants and transgenic plants overexpression SBPase (AtSBPase) showed no significant differences in *Fq'/Fm'* between transgenic plants when compared with wild-type plants at 200 µmol m^{-2} s^{-1} and 800 µmol m^{-2} s^{-1} (Figure 4.8).

To further explore the impact of altered expression levels of SBPase photosynthetic efficiency during a light induction and relaxation was assessed in transgenic lines and wild-type plants as described in method 2.8.2. In antisense SBPase plants, *Fq'/Fm'* values had a tendency to be lower at all PPFDs in the transgenic lines compared to the WT plants. However, there was no significant difference between values for transgenic plants and WT (Figure 4.9). In the light-adapted state at PPFD 500 µmol m^{-2} s^{-1}, there was a decline for *Fq'/Fm'* values in the transgenic lines, and markedly in line GCAsSBP2.16 which had the lowest values of *Fq'/Fm'* compared to the WT control. (Figure 4.10A). In the dark-adapted state, some transgenic lines showed a decrease in *Fv/Fm* values than others and also line GCAsSBP2.16 had more reduction than WT plants (Figure 4.10B).

In plants overexpressing guard cell SBPase (AtSBPase), the response of *Fq′/Fm′* to increasing PPFD showed that the operating efficiency of PSII (*Fq′/Fm′*) was not significant difference compared with wild-type plants (Figure 4.11). In the light-adapted state at PPFD 500 µmol m^{-2} s^{-1}, there was a decline for *Fq′/Fm′* values in all transgenic lines and line GCSBP3.4 had the lowest values of *Fq′/Fm′* compared to the WT control. (Figure 4.12A). Moreover, *Fv/Fm* values in the dark-adapted state were lower in all lines of AtSBPase compared to the WT control. The lowest values of *Fv/Fm* were observed for line GCSBP3.19 (Figure 4.12B).

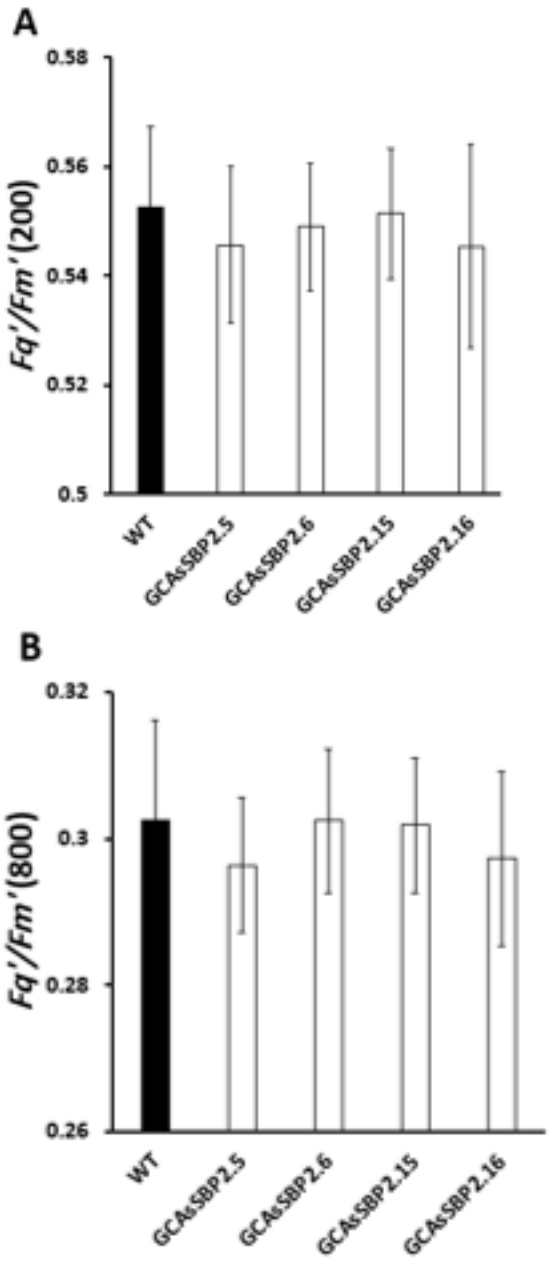

Figure 4.7 Photosynthetic efficiency of wild-type (WT) and ASNtSBPase transgenic plants (construct (2-pL2B-BAR-(pAGPase)- ASNtSBPase) at two different light intensities. The operating efficiency of PSII (*Fq'/Fm'*) was determined at: **(A)** 200μmol m^{-2} s^{-1} and **(B)** 800μmol m^{-2} s^{-1}. Plants were grown in controlled environment conditions (22°C, 8h light/16h dark cycle). Mean values ± SE were indicated (n=10).

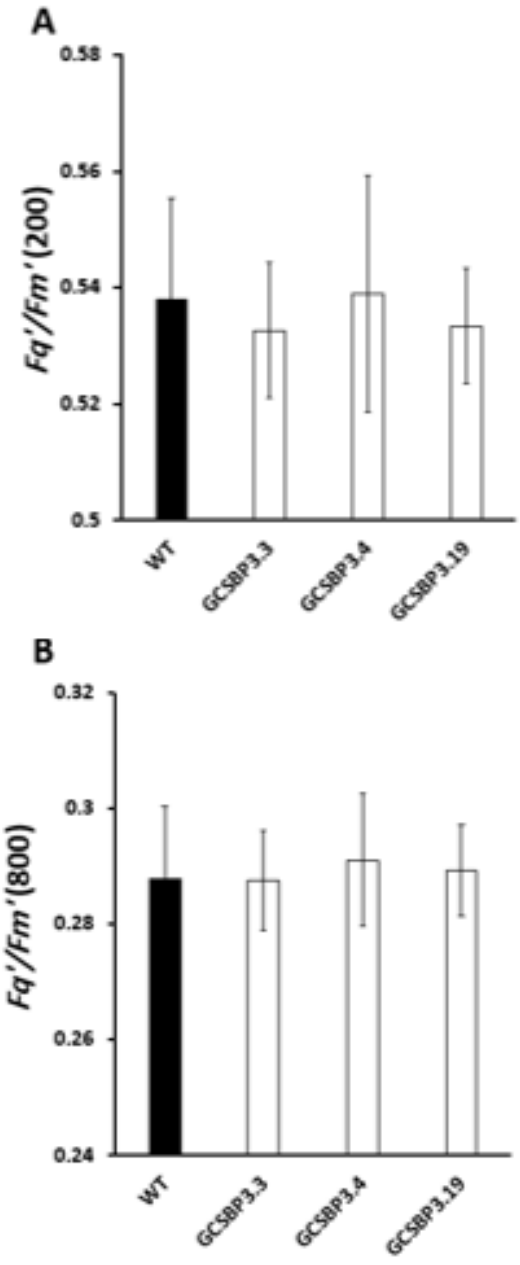

Figure 4.8 Photosynthetic efficiency of wild-type (WT) and AtSBPase transgenic plants of construct (3-pL2B-BAR-(pAGPase)- AtSBPase) at two different light intensities. The operating efficiency of PSII (*Fq'/Fm'*) was determined at: **(A)** 200μmol m^{-2} s^{-1} and **(B)** 800μmol m^{-2} s^{-1}. Plants were grown in controlled environment conditions (22°C, 8h light/16h dark cycle). Mean values ± SE were indicated (n=10).

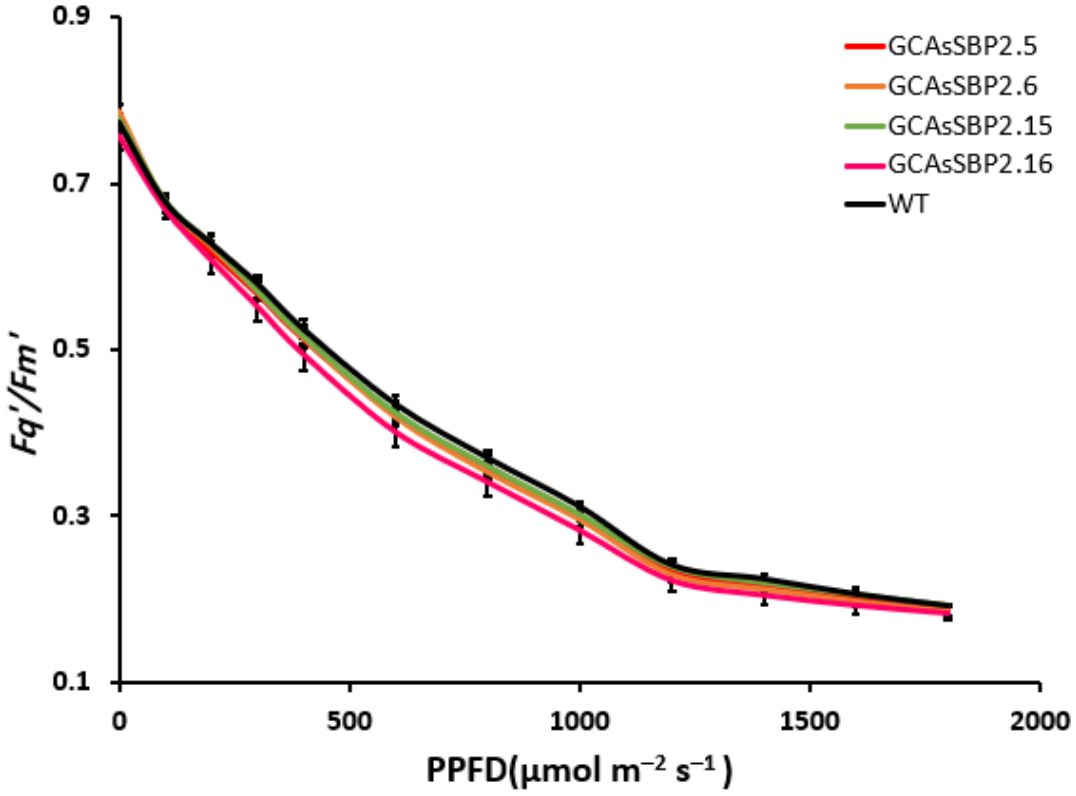

Figure 4.9 PSII operating efficiency of the light response curves of wild-type (WT) and ASNtSBPase transgenic plants of (construct 2-pL2B-BAR-(pAGPase)-ASNtSBPase). The chlorophyll fluorescence was used to determine *Fq'/Fm'* at different light intensities:100, 200, 300, 400, 600, 800, 1000, 1200, 1400, 1600, and 1800µmol m^{-2} s^{-1}. Plants were grown in controlled environment conditions (22°C, 8h light. 16h dark cycle). Mean values ± SE were indicated (n=10).

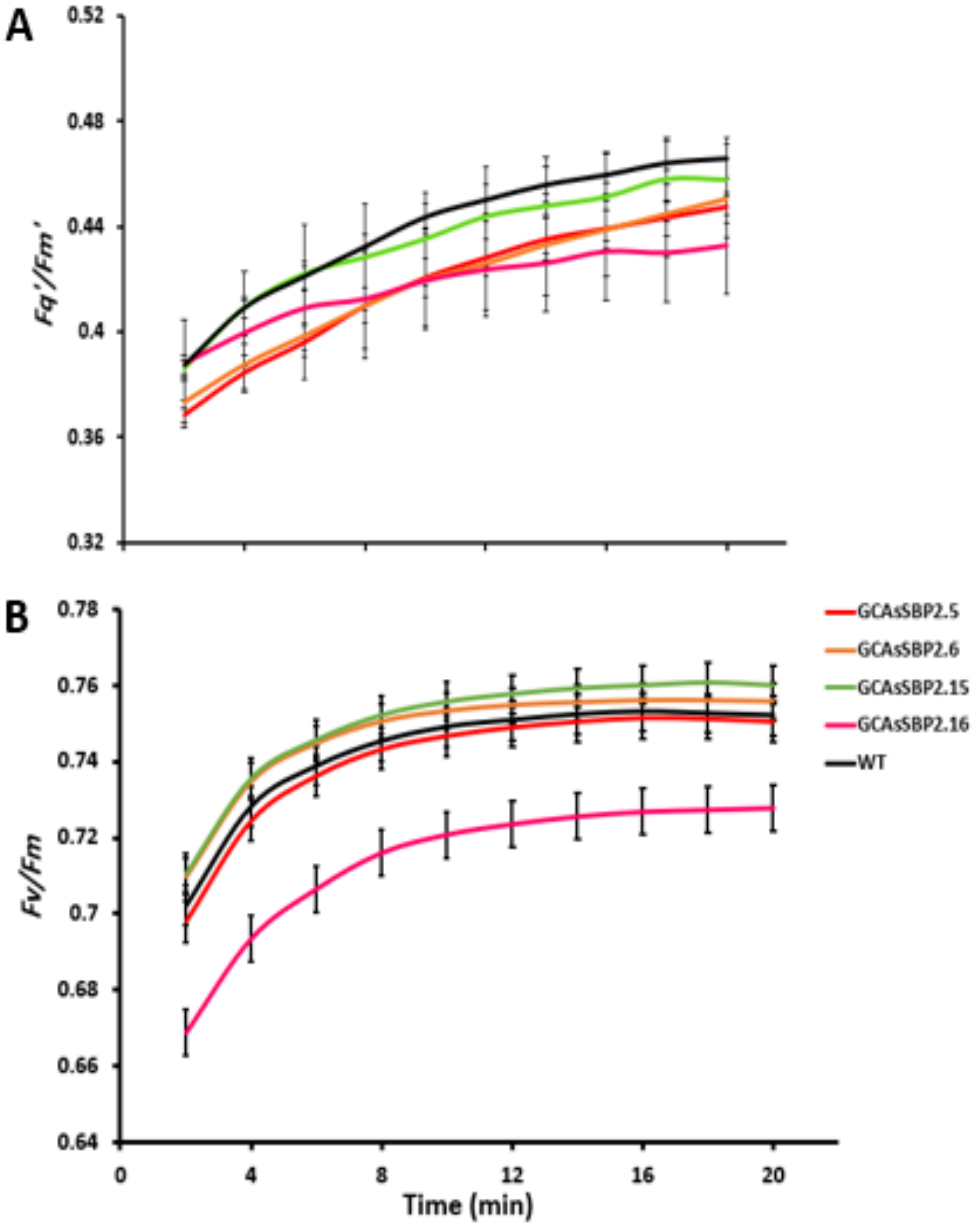

Figure. 4.10 PSII operating efficiency, *Fq'/Fm'*, at PPFD 500µmol m^{-2} s^{-1}**(A),** and the maximum quantum efficiency of PSII photochemistry, *Fv'/Fm'*, at PPFD 0µmol m^{-2} s^{-1} **(B)** were estimated. ASNtSBPase tobacco and WT seedlings were grown in controlled environment conditions (22°C, 8h light. 16 h dark cycle). Error bars represent mean ± SE (n=10).

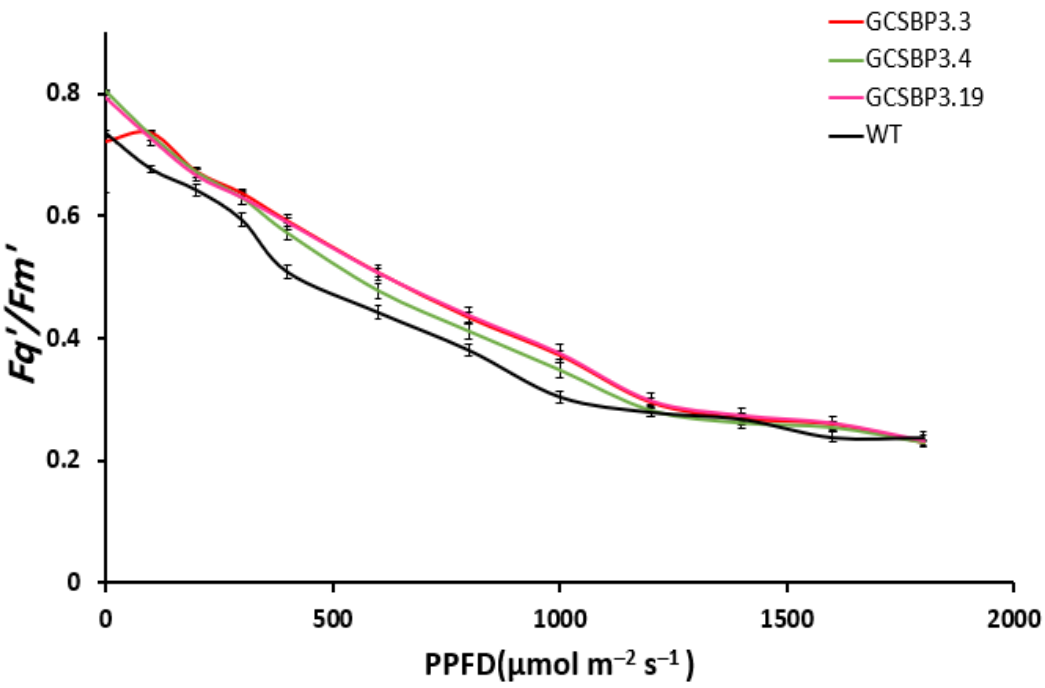

Figure 4.11 PSII operating efficiency of the light response curves of wild-type (WT) and AtSBPase transgenic plants of construct 3-pL2B-BAR-(pAGPase)-AtSBPase. The chlorophyll fluorescence was used to determine *Fq'/Fm'* at different light intensities:100, 200, 300, 400, 600, 800, 1000, 1200, 1400, 1600, and 1800µmol m^{-2} s^{-1}. Plants were grown in controlled environment conditions (22°C, 8h light. 16h dark cycle). Mean values ± SE were indicated (n=10).

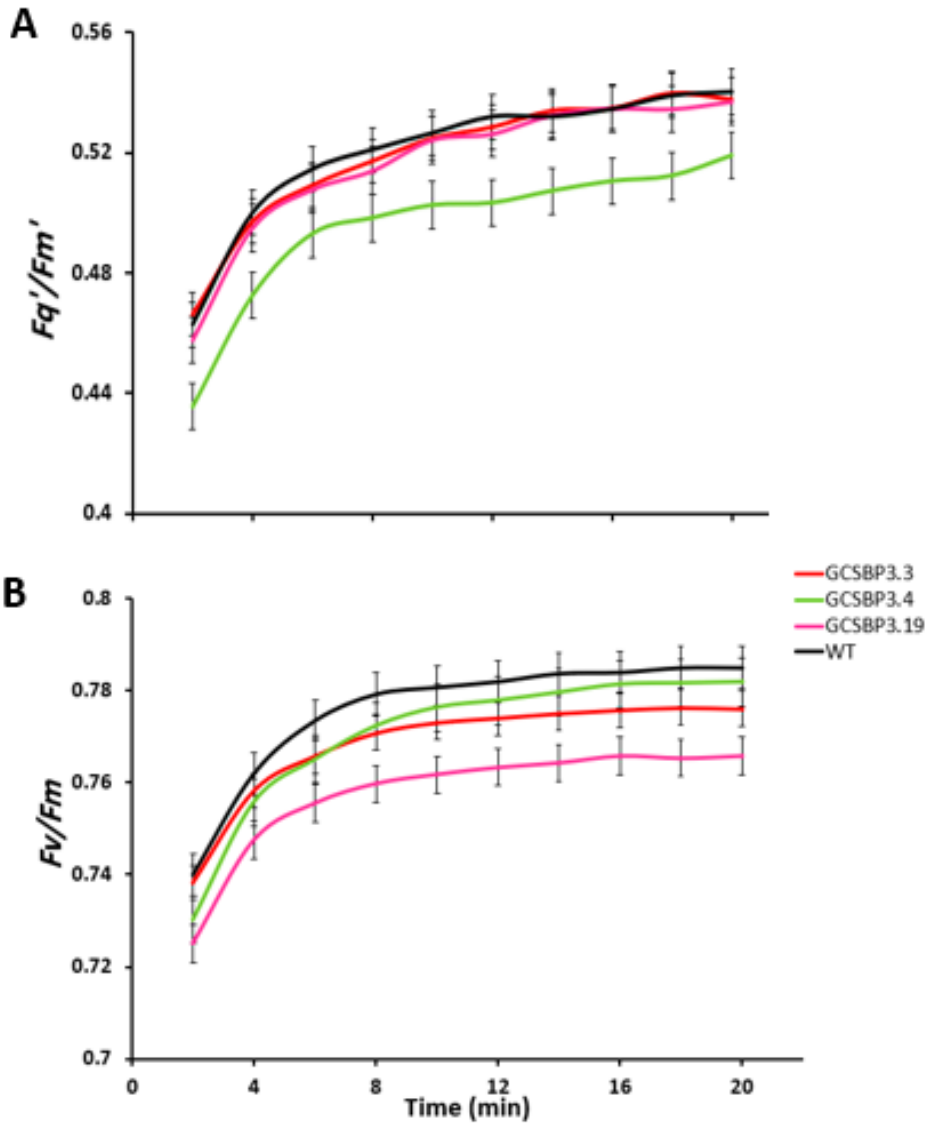

Figure. 4.12 PSII operating efficiency, *Fq'/Fm'*, at PPFD 500µmol m^{-2} s^{-1}**(A),** and the maximum quantum efficiency of PSII photochemistry, *Fv/Fm*, at PPFD 0 µmol m^{-2} s^{-1} **(B)** were estimated. AtSBPase tobacco and WT seedlings were grown in controlled environment conditions (22°C, 8h light. 16 h dark cycle). Error bars represent mean ± SE (n=10).

4.2.4 Leaf gas exchange

4.2.4.1 Intracellular CO_2 (A/C_i) response curves

To identify the effects of a decrease or increase in the levels of SBPase in guard cells on mesophyll photosynthetic capacity, the response of photosynthetic rates to changes in intercellular CO_2 concentrations (A/C_i) was measured under a light-saturated level of 1500 mmol m^{-2} s^{-1}. The results obtained from the A/C_i response analysis revealed that in transgenic plants with antisense SBPase, the photosynthetic response to increasing CO_2 was higher in all transgenic lines than WT plants. Line GCAsSBP2.6 achieved the greatest values of A compared with wild-type at C_i levels in the range between 50 µmol m^{-2} s^{-1} to 1,500 µmol m^{-2} s^{-1} (Figure 4.13).

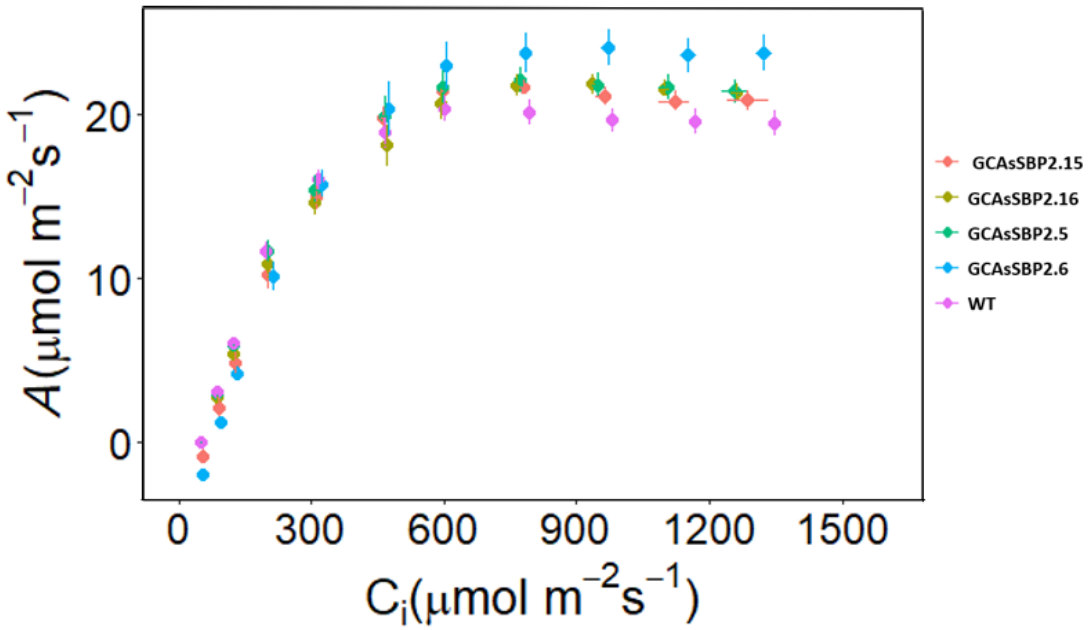

Figure 4.13 The response of net CO_2 assimilation (A) to intercellular [CO_2] (C_i) between 50 µmol m^{-2} s^{-1} and 1500 µmol m^{-2} s^{-1} under saturating PPFD (1500 µmol m^{-2} s^{-1}) for 4 independent lines of antisense SBPase and WT tobacco plants. Error bars represent mean ± SE (n = 6 to 8).

As mentioned in the previous chapter, the A/C_i curves were used to calculate Vc_{max}, J_{max}, and A_{max} at 1500 µmol m^{-2} s^{-1} CO_2 and under 1500 µmol m^{-2} s^{-1} PPFD (Figure 4.14). The results of antisense SBPase plants showed no significant differences in terms of the maximum rate of carboxylation (Vc_{max}) compared to wild-type plants. However, there was a trend toward line GCAsSBP2.6 having higher levels of Vc_{max} (68.7± 6.39) compared to WT (Figure 4.14A). In contrast, values of the maximum rate of electron transport for RuBP regeneration (J_{max}), were significantly higher ($P < 0.001$) in all transgenic plants compared to WT plants (Figure 4.14B). The highest value of J_{max} was found in line GCAsSBP2.6 (130.29± 7.38). The light and CO_2 saturated rate of CO_2 assimilation (A_{max}) was measured to assess the impact of the expression of SBPase on photosynthetic capacity. Values of A_{max} were significantly higher ($P < 0.01$) in all transgenic plants compared to WT plants, with the highest values observed in line GCAsSBP2.6 (24.58 ± 0.74) which were significantly greater ($P < 0.01$) than wild-type which had the lowest values of A_{max} (20.61 ± 0.54) (Figure 4.14C).

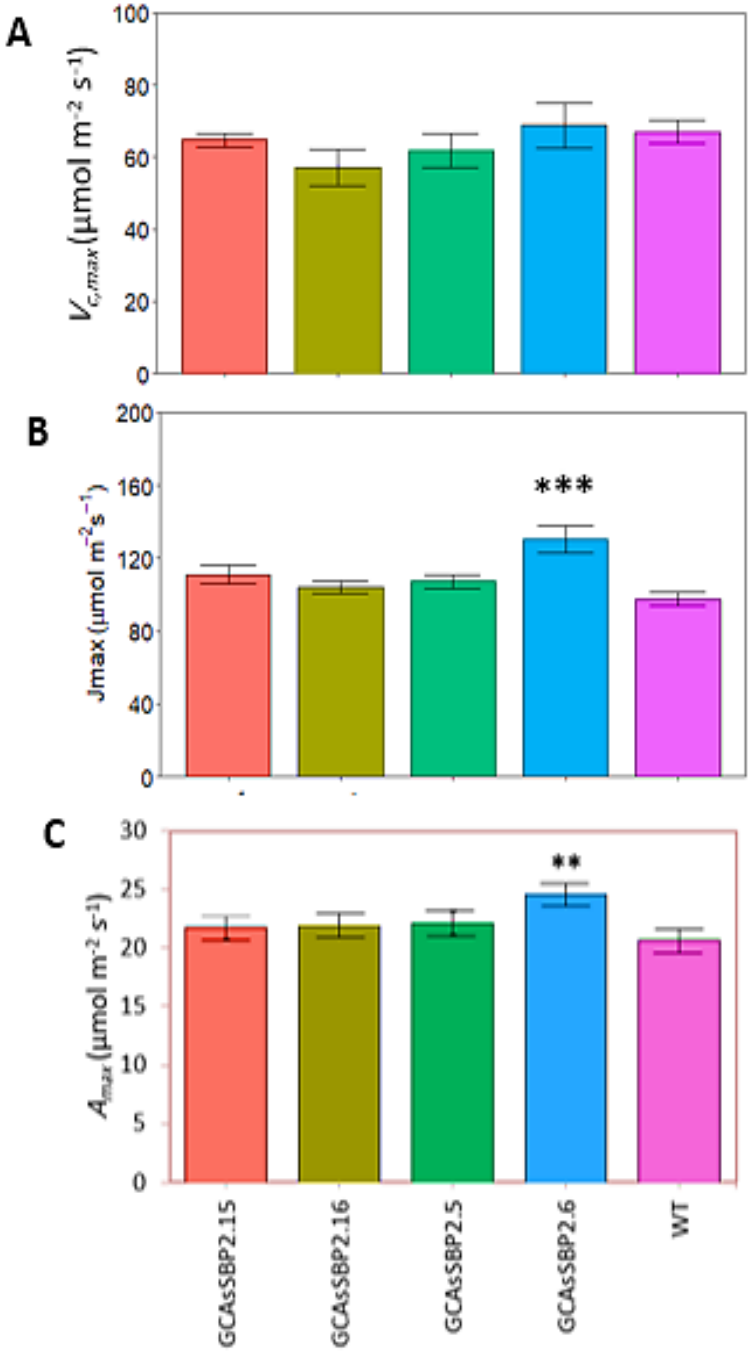

Figure 4.14 The maximum rate of carboxylation (Vc_{max}; **A**) and maximum rate of electron transport (J_{max}; **B**) estimated from the response of A to C_i, and the light and CO_2 saturated rate of photosynthesis (A_{max}; **C**) determined for the four independent lines of ASNtSBPase and WT tobacco plants. Error bars represent mean ± SE (n=6 to 8). A significant difference was observed between lines and asterisks are used to indicate a significant difference from WT plants (P> 0.05).

Transgenic plants overexpressing SBPase obtained higher rates CO_2 assimilation, except line GCSBP3.4, when compared to wild-type plants. The highest values of *A* were observed for line GCSBP3.3 and line GCSBP3.19 compared with wild-type at C_i levels in the range between 50 µmol m^{-2} s^{-1} to 1,500 µmol m^{-2} s^{-1} (Figure 4.15).

A further analysis of the A/C_i curves showed that Vc_{max} values were significant difference between plants ($P < 0.05$), with the lowest values of Vc_{max} observed for line GCSBP3.4 (34.06± 4.05) which were significantly lower ($P < 0.05$) than wild-type (43.71 ± 3.68) (Figure 4.16A). Similarly, J_{max} values were significantly different between the plants ($P < 0.05$). The lowest values of J_{max} were calculated for line GCSBP3.4 (72.4 ± 7.23), however only this line was found to be significantly lower ($P < 0.05$) than WT plants (Figure 4.16B). The light and CO_2 saturated rate of CO_2 assimilation (A_{max}) significantly different between the plants ($P < 0.05$), and line GCSBP3.4 demonstrated the lowest values of A_{max} (14.88± 1.45) (Figure 4.16C).

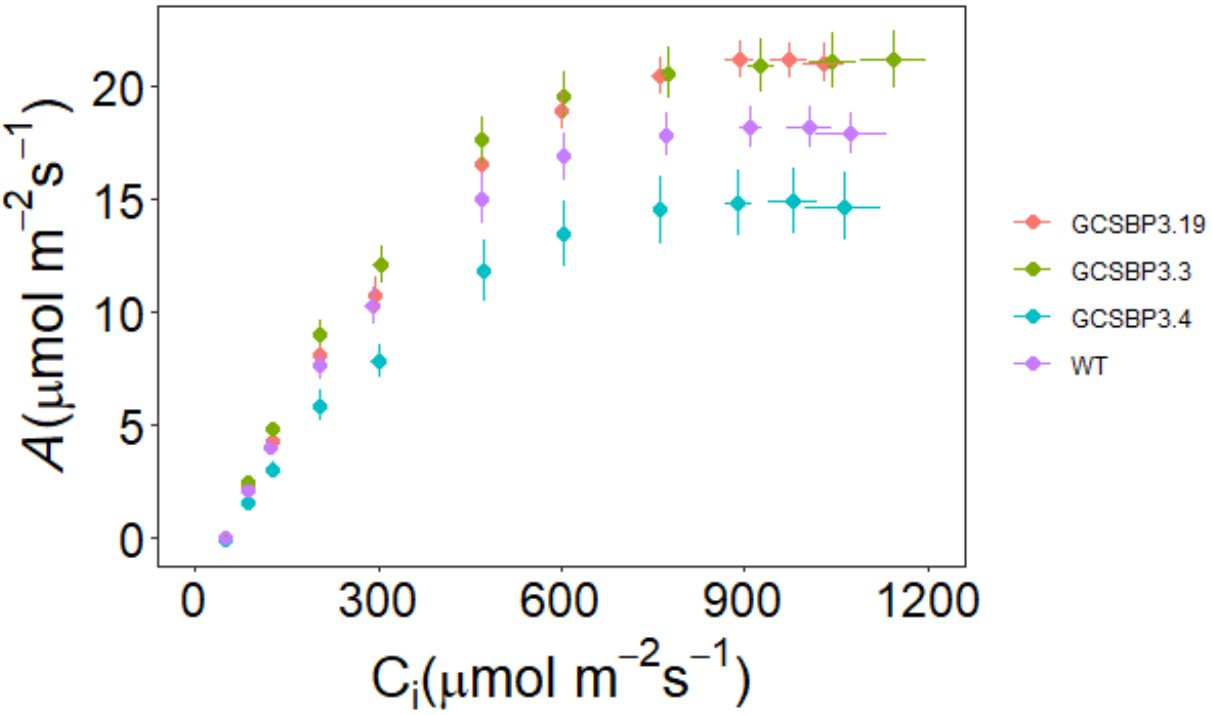

Figure 4.15 The response of net CO_2 assimilation (*A*) to intercellular [CO_2] (C_i) between 50 µmol m^{-2} s^{-1} and 1500 µmol m^{-2} s^{-1} under saturating PPFD (1500 µmol m^{-2} s^{-1}) for three independent lines of overexpressing SBPase and WT tobacco plants. Error bars represent mean ± SE (n = 6 to 8).

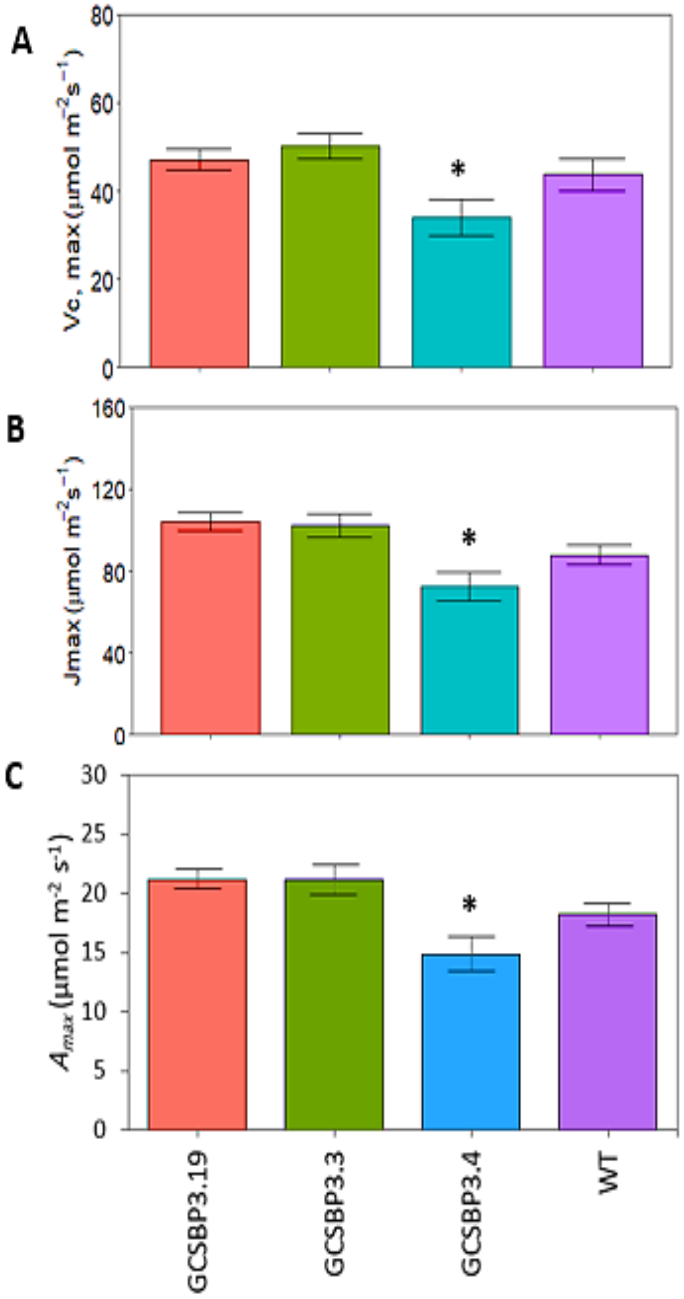

Figure 4.16 The maximum rate of carboxylation (Vc_{max}; **A**) and maximum rate of electron transport (J_{max}; **B**) estimated from the response of *A* to C_i, and the light and CO_2 saturated rate of photosynthesis (A_{max}; **C**) determined for the three independent lines of AtSBPase and WT tobacco plants. Error bars represent mean ± SE (n=6 to 8). A significant difference was observed between lines and asterisks are used to indicate a significant difference from WT plants (P> 0.05).

4.2.4.2 Kinetic responses of g_s and A to a step change in PPFD

To investigate whether altering expression levels of SBPase in the guard cells affect stomatal and photosynthetic response, leaves were subjected to a step increase in PPFD (100-1500 µmol m^{-2} s^{-1}). Plants were first stabilised to an initial PPFD of 100 µmol m^{-2} s^{-1} (and 400 ppm [CO_2]) and then subjected to a step increase in light intensity to approximately 1500 µmol m^{-2} s^{-1} for 1h (Figure 4.18). Gas exchange parameters were measured for each genotype, including: stomatal conductance (g_s; Figure 4.17 A+B), net CO_2 assimilation (A; Figure 4.17 C+D), and intrinsic water use efficiency (W_i; Figure 4.17 E+F) calculated from the values of A and g_s ($W_i = A/g_s$).

Both genotypes demonstrated different responses to the step-change in PPFD from 100 to 1500 µmol m^{-2} s^{-1}. When PPFD was increased to 1500 µmol m^{-2} s^{-1}, an increase in A and g_s was observed, and the most pronounced increases in g_s occurred for the antisense SBPase plants compared to overexpression SBPase plants. Line GCAsSBP2.6 achieved steady state g_s under 1500 µmol m^{-2} s^{-1} PPFD, whilst other lines of antisense SBPase failed to reach steady state g_s under 1500 µmol m^{-2} s^{-1} PPFD (Figure 4.17A). In contrast, all overexpressing SBPase lines achieved steady state under 1500 µmol m^{-2} s^{-1} PPFD, although the g_s response was much slower (Figure 4.18B).

In response to the increase in PPFD, it was observed that all plants increased *A*, however, antisense SBPase plants demonstrated higher rates of *A* compared to overexpression SBPase plants. In the antisense SBPase plants *A* increased from 15.2 to 21.3 µmol m^{-2} s^{-1} (Figure 4.17C), while overexpressing SBPase lines increased *A* in the range 8.8 to 14.3 µmol m^{-2} s^{-1} (Figure 4.17D). A slow increase in *A* in overexpression SBPase lines was synchronized with the response of g_s at the, indicating a potential limitation of *A* by g_s. However, *A* had reached near steady state levels in both genotypes.

As observed with the g_s and *A* response data, intrinsic water use efficiency (W_i) decreased over the course of the step increase in light intensity (Figure 4.17E + F). In antisense SBPase plants, line GCAsSBP2.6 had the lower values of W_i during the measurement period, which were largely driven by the higher values of g_s at this time period (Figure 4.17E). In overexpression SBPase plants, line GCSBP3.4 displayed slightly higher levels of W_i following a step increase in PPFD, predominantly driven by the slow decrease in g_s over the same time period (Figure 4.17F).

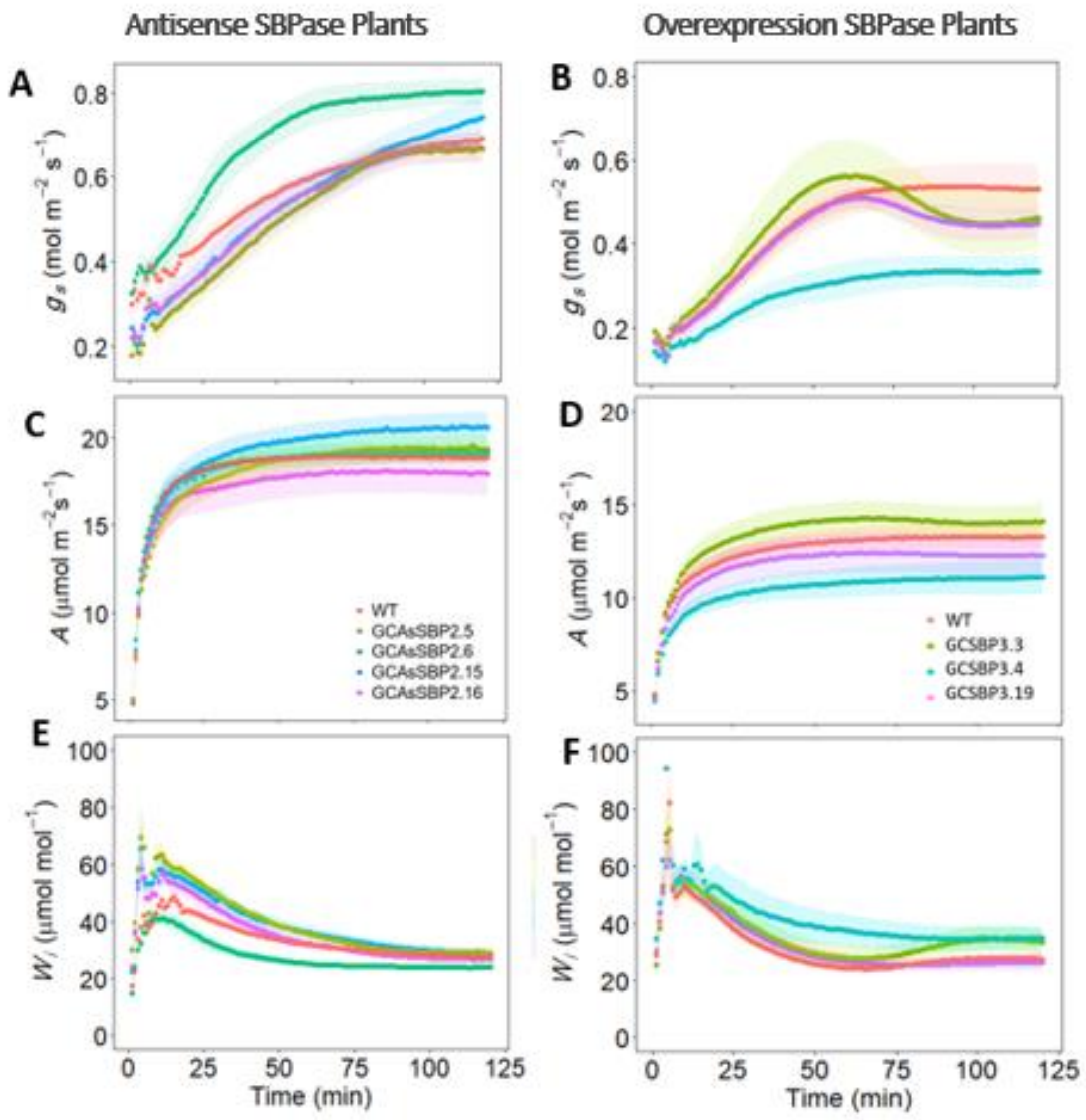

Figure. 4.17 Temporal response of stomatal conductance (g_s; **A+B**), net CO_2 assimilation (A; **C+D**), and intrinsic water use efficiency (Wi; **E+F**), to a step increase in light intensity (from 100 µmol m^{-2} s^{-1} for 10 min to 1500 µmol m^{-2} s^{-1} for 60 min) for WT and transgenic tobacco plants (ASNtSBPase & AtSBPase). Gas exchange parameters (g_s and A) were recorded at 30s intervals, leaf temperature maintained at 25°C, and leaf VPD at 1 ± 0.2 KPa. The data represent mean ± SE (n=6-8).

4.2.4.3 Speed of g_s response to a step change in light intensity

Stomatal responses to a step increase in PPFD were used to determine the influence of altering the expression levels of SBPase in the guard cells on the rapidity of the g_s and A responses when subjected to a step increase in light intensity. Figure 4.18 highlights the time constants for the increases in g_s (τ_{gs}; Figure 4.18A+B), the final value of the g_s response at 1500 µmol m^{-2} s^{-1} PPFD (g_{sF}; Figure 4.18C+D), and the magnitude of change in g_s between steady state values at 100 PPFD to 1500 PPFD (Δg_s; Figure 4.18E+F). While, figure 4.19 displays the time constants to reach 63 % of the final value for A (τ_A; Figure 4.19A+B), the final value of the A response at 1500 µmol m^{-2} s^{-1} PPFD (A_F; Figure 4.19C+D), and finally the magnitude of change in A between steady state values at 100 PPFD to 1500 PPFD (ΔA; Figure 4.19E+F).

Time constants for stomatal opening (τ_{gs}) in response to a step increase in light were significantly slower ($P<0.05$) in plants antisense SBPase (except line GCAsSBP2.6) compared with WT plants (τ_{gs}; Figure 4.18A), whereas no significant differences ($P = 0.965$) were observed in the total time taken for the stomata to open between overexpression SBPase lines compared to WT plants (τ_{gs}; Figure 4.18B). The final value of g_s (g_{sF}) were higher in antisense SBPase lines (except line GCAsSBP2.16) compared to WT plants (g_{sF}; Figure 4.18C). The highest g_{sF} observed was line GCAsSBP2.15, followed by line GCAsSBP2.6. In overexpression SBPase plants, the final value of g_s (g_{sF}) was lower (except line

GCSBP3.19) compared with WT plants (g_{sF}; Figure 4.18D). The magnitude of change in g_s (Δg_s) between steady state values at 100 PPFD to 1500 PPFD was higher in the transgenic antisense SBPase lines compared to WT plants, and the highest values were line GCAsSBP2.5 (Δg_s; Figure 4.18E). In contrast, the magnitude of change in g_s between steady state values at 100 PPFD to 1500 PPFD (Δg_s; Figure 4.18F) was lower in the transgenic lines of overexpression SBPase when compared to WT plants.

Time constants to reach 63 % of final value for *A* (τ_A) were significantly slower ($P<0.05$) in antisense SBPase plants (except line GCAsSBP2.6) compared to WT plants. (τ_A; Figure 4.19A), whereas no significant differences were observed in τ_A between overexpression SBPase lines compared to WT plants (τ_A; Figure 4.19B). The final value of *A* (A_F) at 1500 µmol m^{-2} s^{-1} PPFD was significantly ($P< 0.05$) higher in antisense SBPase lines compared to WT plants (A_F; Figure 4.19C). No differences was observed in the final value of *A* between overexpression SBPase lines compared to WT plants (A_F; Figure 4.19D). The magnitude of change in *A* (ΔA) between 100 µmol m^{-2} s^{-1} - 1500 µmol m^{-2} s^{-1} PPFD displayed a conserved variation in antisense SBPase lines between approx. 12 and 14 µmol m^{-2} s^{-1} (ΔA; Figure 4.19E). While, in the overexpression SBPase plants, ΔA presented a larger variation compared to WT plants, with the highest being GCSBP3.3 at ~ 9 µmol m^{-2} s^{-1} and the lowest being GCSBP3.4 at ~ 6 µmol m^{-2} s^{-1} (ΔA; Figure 4.19F)

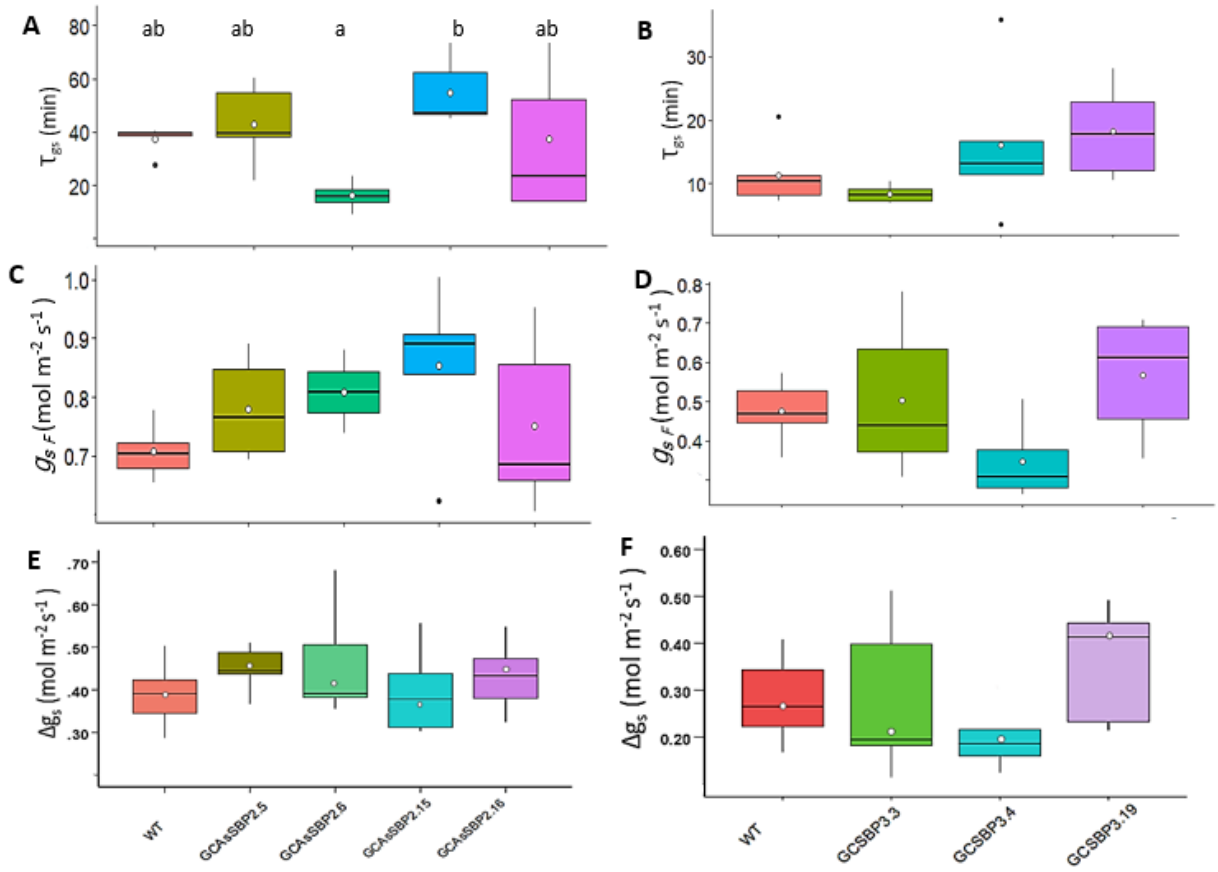

Figure 4.18 Time constants for the increases in gs (τ_{gs}; **A+B**) in minutes, the final value of the g_s response at 1500 µmol m^{-2} s^{-1} PPFD after an increased step change in light intensity (g_sF; **C+D**), and difference in g_s between 100 µmol m^{-2} s^{-1} PPFD and 1500 µmol m^{-2} s^{-1} PPFD (Δg_s; **E+F**) following the step increase in light intensity. All results for 4 independent lines of ASNtSBPase, three independent lines of AtSBPase, and WT tobacco plants. Error bars represent 95% confidence intervals using the results of a Tukey test (n=6-8).

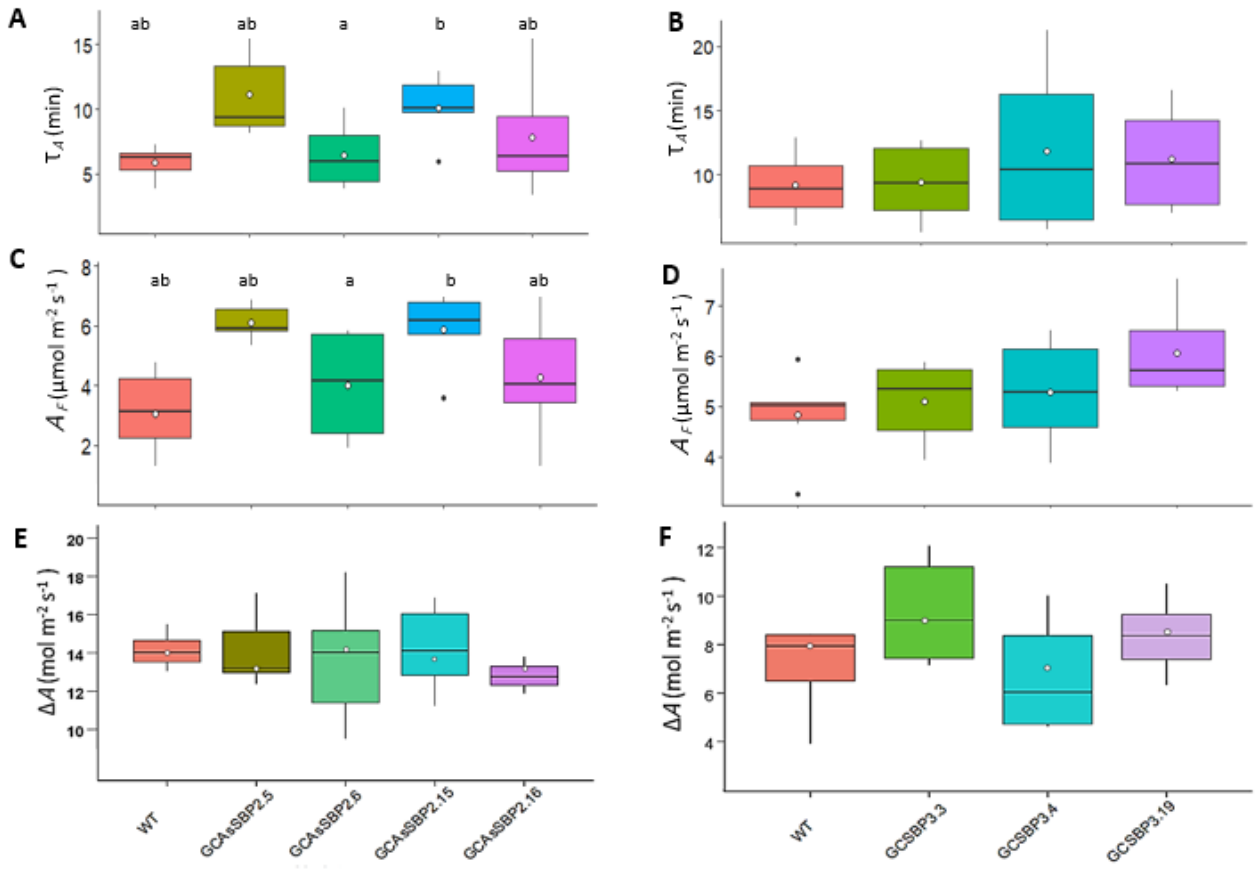

Figure 4.19 Time constants for the increases in *A* (τ_A; **A+B**) in minutes, the final value of the *A* response at 1500 µmol m^{-2} s^{-1} PPFD after an increased step change in light intensity (A_F; **C+D**), and the difference in *A* between 100 µmol m^{-2} s^{-1} PPFD and 1500 µmol m^{-2} s^{-1} PPFD (ΔA; **E+F**) following the step increase in light intensity All results for 4 independent lines of ASNtSBPase, three independent lines of AtSBPase, and WT tobacco plants. Error bars represent 95% confidence intervals using the results of a Tukey test (n=6-8).

4.2.5 Photosynthetic efficiencies in guard and mesophyll cells

To investigate the effect of altered levels of SBPase expression in guard cells on mesophyll and guard cell quantum efficiency of PSII photochemistry, high resolution chlorophyll fluorescence imaging was used as described in method 2.11. *Fq′/Fm′* estimated the quantum efficiency of photosystem II at three different light intensities (61 µmol m^{-2} s^{-1},130 µmol m^{-2} s^{-1}, and 300 µmol m^{-2} s^{-1}PPFD).

At low PPFD levels (61 µmol m^{-2} s^{-1}), there were significant differences between antisense SBPase plants (ASNtSBPase) in *Fq′/Fm′* of guard and mesophyll cells compared to WT plants ($P < 0.01$). *Fq′/Fm′* values of guard cells and mesophyll were higher in all transgenic lines than WT plants. Line GCAsSBP2.15 showed the highest efficiencies, with guard cell and mesophyll *Fq′/Fm′* values of 0.56 and 0.55 respectively (Figure 4.20A). By contrast, no statistically significant difference in *Fq′/Fm′* of guard and mesophyll cells of overexpression SBPase plants compared to WT plants was found (Figure 4.20B).

At moderate light intensity (130 µmol m^{-2} s^{-1}), the *Fq′/Fm′* values of guard cells and mesophyll cells of antisense SBPase lines were significantly decreased (except line GCAsSBP2.15) compared to WT plants. The lowest values of *Fq′/Fm′* for both guard and mesophyll cells were observed for line GCAsSBP2.16 (Figure 4.20C). While a comparison between the *Fq′/Fm′* of guard and mesophyll cells of overexpression of SBPase (AtSBPase) plants showed that no significant differences between transgenic lines compared to WT plants (Figure 4.20D). Whilst at high PPFD levels (300 µmol m^{-2} s^{-1}), both genotypes were slightly higher

in *Fq'/Fm'* values of guard and mesophyll cells compared to WT plants, but no significant increase was recorded when compared to WT plants (Figure 4.20E+F). However, Line AsSBP2.16 showed a significant difference in *Fq'/Fm'* of guard cells compared to mesophyll cells (Figure 4.20E).

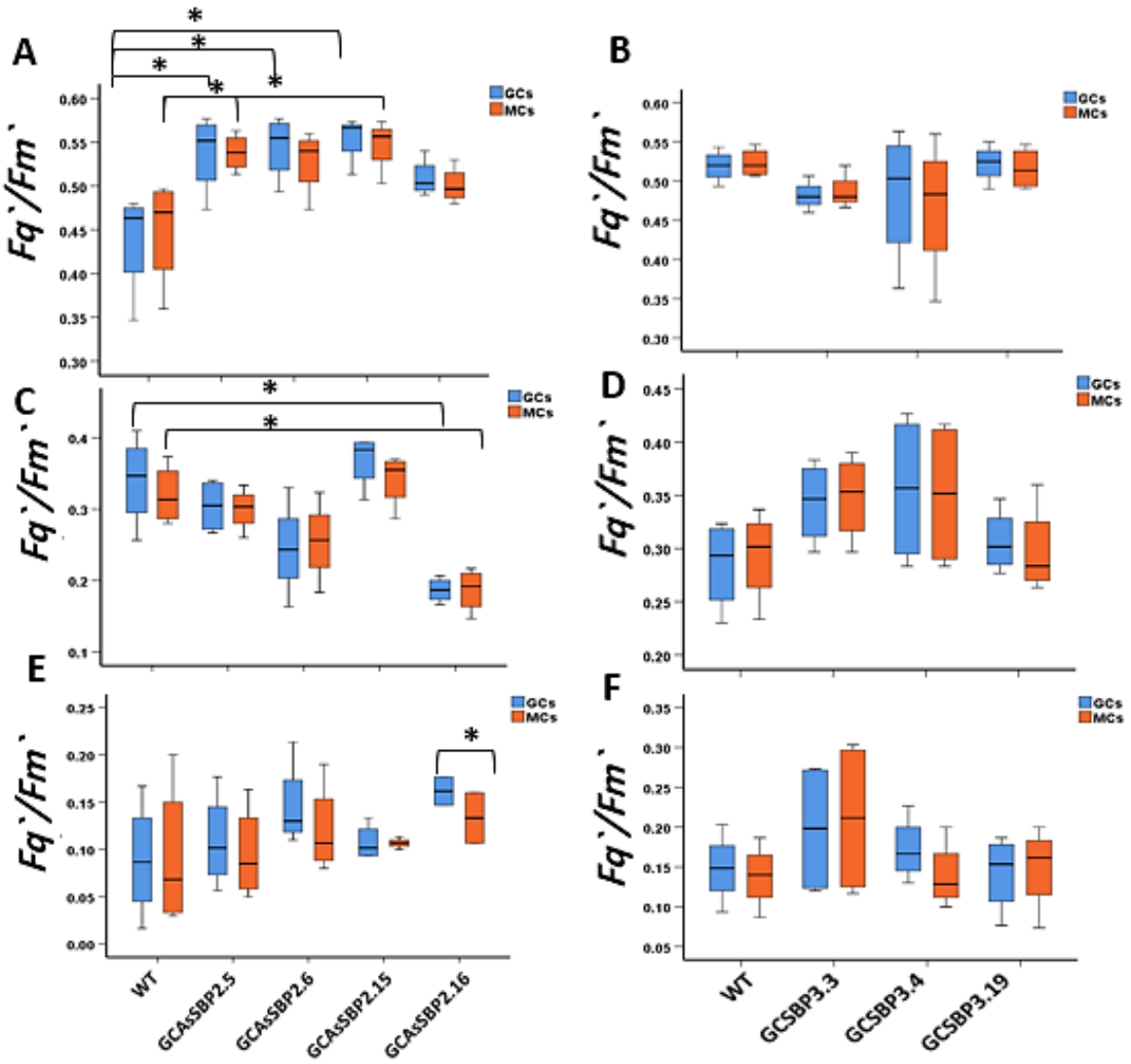

Figure 4.20 Variation (box and whisper plots displaying distribution of biological replicates) and mean (central black line) of photosynthetic efficiency (estimated by *Fq'/Fm'*) of wild-type (WT) and transgenic tobacco plants (ASNtSBPase and AtSBPase) (n=4). Measurements were taken at three different light intensities: 61 µmol m^{-2} s^{-1} (**A+B**),130 µmol m^{-2} s^{-1} (**C+D**), 300 µmol m^{-2} s^{-1} (**E+F**). Starts are used to indicate a significant difference from WT plants (P> 0.05) using the results of a Tukey post-hoc test following a two-way ANOVA.

4.2.6 Plant growth characteristics

To assess the effect of different expression levels of SBPase on the growth and development of *Nicotiana tabacum* plants, the leaf area (cm^2) and dry weight (g) were measured on all transgenic and WT plants using method 2.12.1. The measurements were determined over the duration of the experiment on plants grown in an environmentally controlled greenhouse.

The results of leaf area revealed that the antisense SBPase plants had significantly greater area ($P<0.001$) compared to the WT plants. The highest value of leaf area was recorded to line GCAsSBP2.5 (40.25±0.41) (Figure 4.21A). While no significant differences were observed between overexpression SBPase lines compared to WT plants for leaf area (Figure 4.21B).

For dry weight, antisense SBPase plants were significantly lower ($P<0.05$) compared to the WT plants, with the lowest ($P < 0.001$) dry weight values observed in line GCAsSBP2.6 (22.7±0.75) and line GCAsSBP2.15 (22.8±0.63) (Figure 4.21C). In contrast, plants with overexpression SBPase had a significantly higher dry weight than the WT plants, and markedly in line GCSBP3.19 which had the highest values of dry weight (38.1±3.28) compared to the WT plants (Figure 4.21D).

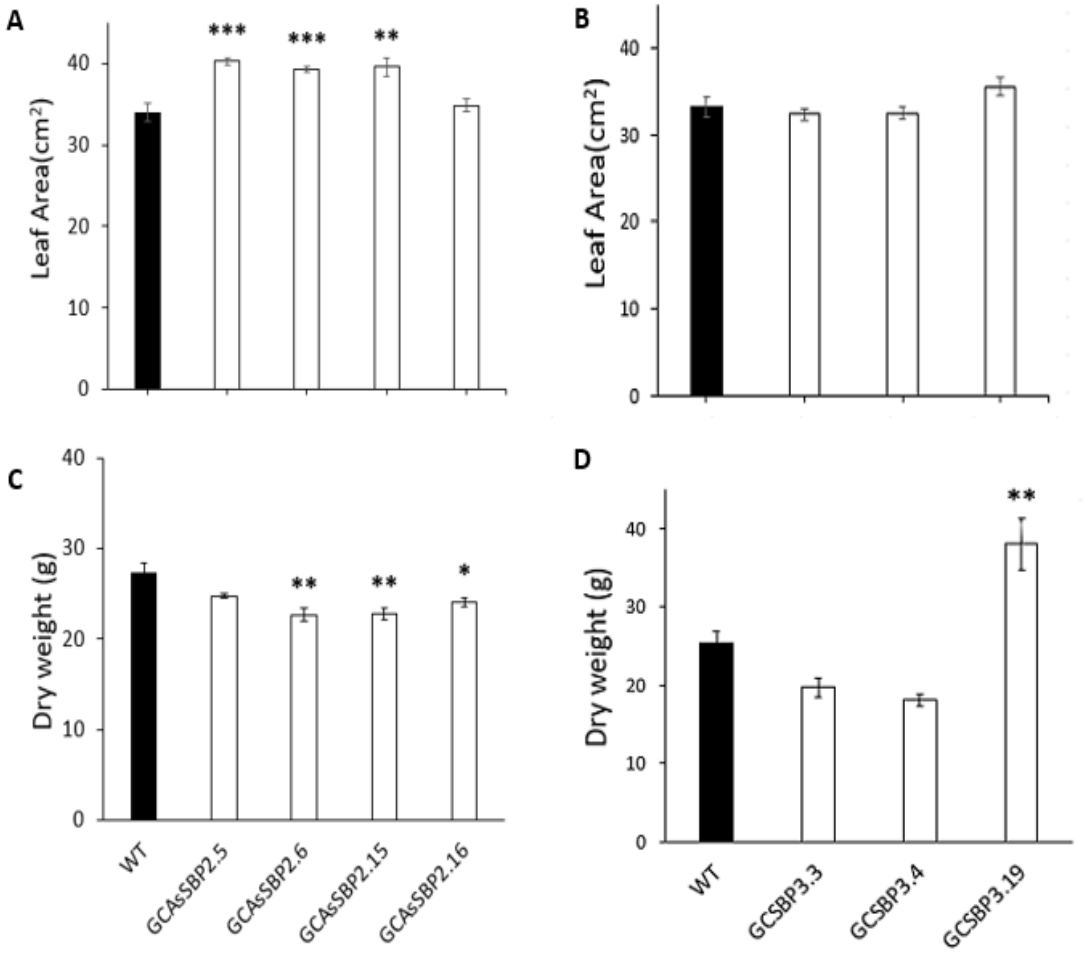

Figure 4.21 Leaf properties of transgenic tobacco plants (ASNtSBPase & AtSBPase) and WT plants, including: **(A+B)** leaf area and **(C+D)** dry weight. Plants were grown in an environmentally controlled greenhouse. Mean values ± SE were indicated (n=8 to 10). A significant difference was observed between lines and asterisks are used to indicate a significant difference from WT plants (P> 0.05).

4.3 Discussion

As previously discussed, several studies have manipulated enzymes involved in the Calvin-Benson cycle in model plants (Tobacco and Arabidopsis) to create transgenic plants with either higher or lower enzyme levels and test what effect this has in terms of photosynthesis and the production of biomass (Lefebvre *et al.*, 2005; Feng *et al.*, 2007, 2009; Rosenthal *et al.*, 2011; Araus *et al.*, 2014). The findings initially reported by Lefebvre *et al.*, (2005) were subsequently verified by a series of experiments demonstrating that the increase was maintained from one generation to the next and irrespective of whether low or high light was used (Simkin *et al.*, 2015). Subsequently, tobacco plants confirmed that increasing the rate of SBPase activity brought about a significantly higher yield of biomass when grown under an open-air elevation of CO_2 (Rosenthal *et al.*, 2011). Meanwhile, research conducted by Simkin *et al.*, (2017a) based on Arabidopsis supported these findings, confirming that CO_2 assimilation increased, the rate of development improved and there was a 42% increase in biomass. Furthermore, Ding *et al.*, (2016) demonstrated that there was an accumulation of starch, sucrose and biomass in tomatoes, thereby confirming that SBPase has the ability to control carbon flows in the CB cycle for various species. Therefore, the findings of these studies indicated that the enzyme, sedoheptulose 1,7-bisphosphatase (SBPase) displays a high flux control over carbon fixation, relative to other enzymes in the cycle. Consequently, this enzyme has been widely studied by researchers attempting to enhance rates of photosynthesis in plants (Raines, 2003, 2011). The current chapter presents data relating to transgenic tobacco (*Nicotiana tabacum*) plants that have varying levels of SBPase expression in guard cells and no change

in mesophyll cells. This research attempted to establish what effect SBPase has on stomata response and metabolism and the role of CC in guard cell function.

Transgenic tobacco plants with reduced or increased SBPase gene expressions were identified and confirmed in guard cells. First, the existence of SBPase in T2 generation was confirmed using PCR. As a result, several lines were shown to contain the construct of antisense SBPase in four independent lines and the construct of overexpression SBPase in three independent lines compared to the WT plants. Next, the SBPase genes expression was quantified using q-PCR to determine the extent of gene expression in the guard cells compared to the guard cells of wild- type plants. When stomatal conductance measurements were taken using porometry, it was found that antisense SBPase plants had significantly higher stomatal conductance. Meanwhile, there was significantly lower stomatal conductance in the overexpression of SBPase relative to wild type plants. As such, this suggests that the greatest effect in terms of stomatal behaviour is realised by manipulation of Calvin cycle enzymes, such as SBPase, in guard cells. This agrees with work Kelly *et al.*, (2013) who concluded that the speed at which stomata close can be increased by increasing whole plant expression of hexokinase (a sugar-phosphorylating enzyme that plays a role in the sensing of sugar). In addition, it has been shown that stomata responded to changes in HXK1 expression under the control of the guard cell specific promoter KST1, which has been shown to drive guard cell-specific expression in *Citrus sinensis*, *Arabidopsis thaliana*, and *Solanum lycopersicum* (Kelly *et al.*, 2013; Lugassi *et al.*, 2015). This indicates that HXK and sucrose could be responsible for bringing about the closing of stomata when rates of photosynthesis are elevated (Kelly *et al.*, 2013). Moreover, it has also been suggested that the accumulation of sucrose may

provide the signal that causes a decline in g_s during periods of high photosynthetic rates (Kang *et al.*, 2007) and is responsible for the decrease in g_s reported later in the day (Lawson et al., 2014).

High resolution chlorophyll fluorescence imaging confirmed that the operating efficiency of PSII (*Fq'/Fm'*) in mesophyll cells is impacted in transgenic plants that altered expression of SBPase in guard cells. Lawson *et al.* (2008) demonstrated that antisense tobacco plants with a range of SBPase activities resulted in a decrease in the quantum efficiency of photosystem II electron transport in both mesophyll and guard cells compared to the wild-type plants when using high resolution chlorophyll a fluorescence imaging. However, our findings showed apparent substantial variation in the guard cell *Fq'/Fm'* when the two transgenics were subjected to different light intensities. Unexpected results were observed for guard cell *Fq'/Fm'* in the antisense SBPase plants. Decreased expression of SBPase led to increasing *Fq'/Fm'* in guard cells, irrespective of whether the light intensity was high or low. Meanwhile, a reduction in SBPase brought about a reduction in guard cell *Fq'/Fm'* relative to the WT when the intensity of light was moderate. Conversely, increasing SBPase brought about an increase in guard cell *Fq'/Fm'* for two levels of light intensities. As such, the results for SBPase overexpression lines are similar to those reported in the literature on tobacco plants (Lefebvre *et al.*, 2005; Rosenthal *et al.*, 2011). Therefore, this infers that the SBPase enzyme could influence the movement of stomata which either directly influence mesophyll photosynthesis or provides some sort of signal to the mesophyll.

The current study sought to investigate what effects altered expression of SBPase levels specifically in guard cells has on stomatal function and the impact on mesophyll carbon assimilation. When saturated with CO_2, sizeable reductions in guard cell expression of SBPase resulted in a significant increase in CO_2 assimilation rates. Conversely, plants overexpressing SBPase with greater expression of SBPase transcript the rate of CO_2 assimilated was declined. $V_{c,max}$ and J_{max} were also clearly affected as a result of changes in the expression level of SBPase in guard cells. As such it appears that photosynthetic capacity is influenced by the manipulation of Calvin cycle activity in guard cells. It has previously been established that the activity of Calvin-Benson cycle enzymes is low in guard cells (Hampp *et al.*, 1982; Reckmann *et al.*, 1990). Moreover, due to the role of SBPase in the Calvin cycle, it is probable that efforts to manipulate the guard cell photosynthesis enzymes could affect how the stomata respond as a result of the effect exerted on guard cell metabolism, thus affecting the assimilation of carbon.

One interesting observation is that the leaf area of antisense SBPase plants was significantly increased in most of those lines compared to WT plants (Figure 4.20A+C), and the shoot biomass was significantly decreased (Figure 4.20D). In contrast, the dry weight significantly increased in one line of overexpressed SBPase (GCSBP3.19). Thus, these findings suggested that changes in some pathways in guard cells such as Calvin cycle activity seem to have an impact on plants development. Our findings of kinetics responses of g_s and A to changes in the PPFD revealed that, in general, antisense SBPase plants have higher g_s and this result led to increases in A, whilst plants overexpression guard cell SBPase showed the opposite with general decrease in both g_s and A. However, some lines

did show higher g_s values (e.g. line GCAsSBP2.6) that did not result in a higher *A*. These findings, indicating that maximal g_s is not necessarily required for plants to achieve high *A* (Kelly, 2019), although this may depend on the growth environment (Matthews et al., 2018).

CHAPTER 5

General Discussion

5.1 Overall aim and main findings

Whilst the functioning of stomata is an event at the micro-level within a leaf, its impact extends to the global scale in terms of how it affects water and carbon cycles. Indeed, just 0.3-5.0% of a leaf's surface comprises stomata yet they are responsible for 95% of water and CO_2 gaseous fluxes in terrestrial ecosystems. Moreover, it has been estimated that plants take up 60% of all precipitation falling on the terrestrial biosphere and transpire this through stomatal pores (Morison *et al.*, 2008b). The manipulation of guard cell specific metabolism is important for determining the role of the guard cell chloroplasts in stomatal function and the possible role in the signal transduction processes that effectively control stomatal conductance (Lawson *et al.*, 2002, 2003; Lawson, 2009). The photosynthetic enzymes which play a role in carbon metabolism can be manipulated to control the photosynthetic rate of a plant, thereby helping to enhance crop yields (Lefebvre *et al.*, 2005; Lawson, 2009; Raines, 2011; Simkin *et al.*, 2015; Driever *et al.*, 2017b).

The overarching aim of the current study was to clarify a possible role of guard cell chloroplasts in stomatal behaviour as well as the coordination that links mesophyll and guard cells metabolism by genetic engineering plants with guard cell specific perturbation in metabolism. Here transgenic tobacco (*Nicotiana tabacum*) plants with altered expression levels of the Calvin cycle enzyme Sedoheptulose-1,7, bis-phosphatase (SBPase), and the electron transport protein, Rieske FeS specifically in guard cells were used. The impact of these manipulations on photosynthesis and stomatal behaviour was examined. There

were two reasons for selecting these particular genes. Firstly, it has yet to be confirmed whether stomatal responses are influenced by either guard cell Calvin cycle activity or guard cell electron transport or both (Lawson, 2009; Lawson *et al.*, 2014). Secondly, it is possible that guard cell photosynthesis could provide the mechanism that coordinate stomatal responses with those of the underlying mesophyll (Lawson *et al.*, 2002, 2003).

Rieske FeS and SBPase enzymes have not yet been the subject of enough studies in the empirical literature concerning guard cells. Therefore, the current study has adopted a transgenic approach in an attempt to clarify the role that these enzymes play in stomatal function and mesophyll photosynthesis. To achieve this, three genotypes of tobacco plants were used: overexpression Rieske FeS, antisense SBPase, and overexpression SBPase. Gene expression was verified and confirmed in guard cells and each genotype has varying levels of gene expression. As a result of growth analysis, it was possible to observe that transgenic overexpressed Rieske FeS and SBPase plants (especially those that experience the greatest increase in SBPase levels) have a markedly different level of biomass production. Meanwhile, plants that experience lower levels of SBPase have lower levels of shoot biomass. Such findings support those in the empirical literature concerning how these genes are manipulated in the mesophyll cells (Chida *et al.*, 2007; Simkin *et al.*, 2017a; Yadav et al. 2018), thereby indicating that yields could be increased by overexpressing Rieske FeS protein. In addition, previous research has established that the biomass of plants can be controlled by manipulating the SBPase enzyme (Lefebvre *et al.*, 2005; Uematsu *et al.*, 2012). However, it is important to note that it was not in the guard cells that SBPase and

Rieske FeS were manipulated but rather in the mesophyll cells. The current study also established that a small reduction in the operating efficiency of photosystem II (*Fq'/Fm*') was observed for whole plants at the various genotypes. Based on these results, we suggest that it will not be possible to stimulate such activity across the entire leaf by manipulating the enzymes found in the guard cells.

5.2 Impact of Increased Rieske FeS protein on photosynthetic efficiency of PSII electron transport.

It is known that electron transport is governed by cytb_6f and the amount of cytb_6f is believed to be controlled by the abundance of Rieske FeS subunit (Simkin *et al.*, 2017a). It is the position of Rieske FeS amidst the complex that determines the function it serves in terms of regulating electron transport. As such, the activity of PSII can be controlled by accelerating the rate of electron transport via overexpressing Rieske FeS (Ermakova *et al.*, 2019).

In the current study, increased Rieske FeS in guard cells brought about changes in the photosynthetic efficiency of both mesophyll and guard cells, with a more pronounced effect being observed in the guard cells. As such, it is apparent that guard cells with increased levels of Rieske FeS achieved greater PSII quantum yields at high light intensities and this suggests that a higher portion of the light absorbed is used for electron flow at PSII reaction centres. It has been shown that guard cells are able to obtain ATP by means of electron transport. The products of electron transport (ATP) are required for guard cells to achieve photosynthetic electron transport and this could indicate that ATP effectively regulates the activity of ion transport and guard cell photosynthesis (Goh *et al.*, 2002). Previous studies

in the mesophyll cells reported overexpression of the Rieske FeS protein has positive effects PSII electron transport rate in transgenic Arabidopsis thaliana plants, this led to increase in biomass and seed yield (Simkin *et al.*, 2017a). Therefore, a potential route for improving photosynthetic electron flow through the Cyt b_6f complex is the of the Rieske FeS protein.

5.3 Influence of altering expression levels of SBPase on guard cell quantum efficiency of PSII

As mentioned previously, SBPase plays a significant role in enabling photosynthetic carbon to be fixed in the Calvin cycle because it is required for controlling both photosynthesis and the production of sucrose. Research has confirmed that changing the level of SBPase influences the Calvin cycle's ability to regenerate RuBP, thereby demonstrating how important SBPase is to the functioning of the Calvin cycle (Raines, 2003). Previous research has confirmed that SBPase activity is correlated with the quantum efficiency of PSII electron transport (*Fq'/Fm'*) in whole plants (Baroli *et al.*, 2008; Lawson *et al.*, 2008). The current research revealed differences in the results for antisense SBPase plants depending on the intensity of light they received. When exposed to moderate light, reducing SBPase caused the guard cell *Fq'/Fm'* to also decline. When SBPase was increased, the result was an upturn in guard cell *Fq'/Fm'* for two levels of light intensities. This finding provides further support for the opinion that guard cell Calvin cycle activity serves as a significant sink for ATP and NADPH generated as a result of photosynthetic electron transport (Cardon & Berry, 1992; Lawson *et al.*, 2002, 2003; von Caemmerer *et al.*, 2004). It has previously been established that there was an impact on mesophyll and guard cell quantum efficiency of PSII

photochemistry due to reductions in SBPase activity in transgenic antisense tobacco plants. In fully expanded leaves, photosynthetic capacity was decreased in both mesophyll and guard cells by approximately 20% and this reduction in photosynthesis was greatest in heightened light intensity (Lawson *et al.*, 2008).

5.4 Influence of increased Rieske FeS protein on stomatal and photosynthetic behaviour

When examining the effect of increasing Rieske FeS has on the response of g_s and A, and therefore W_i, it was clear that the g_s response to changes in the PPFD was impacted. This adjustment led to changes in the speed of g_s response as well as altering the magnitude of change in g_s after the light was applied. Meanwhile, the assimilation rates (A) and water use efficiency (W_i) were lower. In addition, the time required for g_s to increase in response to changes in PPFD has a significant bearing on carbon gain as well as the conservation of water. For instance, it is typically the case that greater magnitudes of g_s and more timely responses enhance carbon gain but are detrimental to water use efficiency (Lebaudy *et al.*, 2008; McAusland *et al.*, 2016). It has been confirmed in the empirical literature that enhancing stomatal conductance (g_s) increases the rate of photosynthesis, while it is typically plants that have relatively low g_s that experience increased levels of WUE. However, some researchers have concluded that manipulating certain genes responsible for regulating the A– g_s trade-off results in plants with improved A and WUE (Kelly *et al.*, 2013; Lugassi *et al.*, 2015).

Another finding obtained from analyses of the A/C_i curves has shown that overexpression of Rieske FeS in guard cells has been shown to impact negatively

on carbon assimilation in the mesophyll. Whilst it is known that transgenic plants experience a reduction in photosynthesis, it is not apparent why this is the case because it would be expected that changes in expression should be constrained to the guard cells. One possible explanation is that the promoter involved in guard cell-specific expression leaks in some species of plant and in specific situations (Rusconi *et al.*, 2013). There are two distinct types of promoters responsible for driving expression in guard cells. The first type of promotor is responsible for exclusive guard cell expression, whereas the second type brings about preferred expression along with further low expression in various tissues including veins and roots (Kelly *et al.*, 2017) as was the case here. Even if questions have been raised regarding the promotor's specificity, it is apparent that changes made to the cytochrome b_6f complex as well as Rieske FeS overexpression are beneficial in terms of how plant growth and development (Simkin *et al.*, 2017a; Ermakova *et al.*, 2019). Simkin *et al.*, (2017a) observed an increase in dry weight, leaf area and up to 51% increase in seed yield in some lines of Arabidopsis by the overexpression of the Rieske FeS protein. The rate of photosynthesis is affected by the way in which stomata behave but heightened levels of g_s mitigate any diffusional limitations and boost A, albeit frequently at the cost of less efficient water use because the rate of transpiration increases (Lawson *et al.*, 2010; Lawson & Blatt, 2014; Lawson & Vialet-Chabrand, 2019). Consequently, it is not possible for these results to clarify why it is that the photosynthetic capacity is reduced.

5.5 The impact of manipulation of the Calvin cycle activity on stomatal responses and photosynthetic CO_2 assimilation

To understand whether altered expression of SBPase in guard cells can impact stomatal conductance and thus CO_2 assimilation rate in mesophyll cells, the kinetic responses of g_s and *A* to changes in the PPFD were examined. The results indicate that antisense plants typically experience heightened levels of g_s, thereby bringing about increased levels of *A*. The findings were stronger in these plants than in SBPase plants for *A* and g_s. The results support the findings of the empirical literature which indicated that suppressing the stomatal conductance (g_s) results in less CO_2 taken up, thereby reducing the rate of photosynthesis (Jones, 2013; Lawson & Blatt, 2014; Flexas, 2016). It is also known that plants are capable of achieving elevated *A* without g_s being maximised (Kelly *et al.*, 2019). Therefore, the results of the current study indicate that line GCAsSBP2.6 and a number of others in antisense plants have heightened levels of g_s without a correspondingly high level of *A*. One of the aims of the research was to establish whether altering the level of SBPase in guard cells affects the rate at which carbon is assimilated in mesophyll cells. When saturated with CO_2, significant reductions in SBPase result in a marked increase in CO_2 assimilation rates and this could be due to increased levels of g_s. Moreover, increased levels of gs could be due to reduced ATP consumption by the Calvin cycle in antisense plants therefore that ATP might be available for guard cells osmoregulation. Tominaga *et al.*, (2001) showed that guard cells provided ATP to the cytosol which was used for H^+ pumping by the plasma membrane H^+-ATPase and opening of stomata. While reducing stomatal conductance with increased SBPase could be due to changes in carbohydrate

status which are important in guard cells movement. Previous studies have revealed that a clear correlation was apparent between SBPase activity and increased carbohydrate (starch and sucrose) accumulation, the levels of starch and sucrose increased up to 50% in lines with the highest SBPase activity comparison with wild type plants(Lefebvre *et al.*, 2005; Ding *et al.*, 2016). On the other hand, if there is a high level of SBPase activity in plants known to overexpress SBPase, there is a lower rate of CO_2 assimilation. In addition, alterations in guard cell SBPase expression influence both J_{max} and Vc_{max}. Accordingly, it could be suggested that the rate of CO_2 assimilation (A) could be reduced by increasing SBPase levels in guard cells, and *vice versa*. It has been confirmed in the empirical literature by studying transgenic plants with reduced SBPase activity that SBPase makes a significant contribution to regulating the flow of carbon in the Calvin cycle, and that the rate of photosynthesis has been shown to be sensitive to reductions in the levels of the enzymes SBPase (Harrison *et al.*, 1998; Raines *et al.*, 2000). It has been reported that heightened levels of AtHXK1 expression have the effect of suppressing the stomatal conductance in Arabidopsis plants. As such, this indicates that the way in which stomatal function is regulated could be governed by changes in the enzymes of guard cells (Kelly *et al.*, 2012). In addition, it is known that increased levels of SBPase activity stimulate transgenic tobacco plants to experience elevated rates of photosynthesis (Lefebvre *et al.*, 2005), whilst improving photosynthesis against stresses in transgenic rice plants (Feng *et al.*, 2007, 2009). Based on this, it appears that SBPase plays an important role in the Calvin cycle in terms of the rate of photosynthesis and how carbon is partitioned into end products in certain environmental conditions.

5.6 Conclusion and future works

In order for plants to utilise water as efficiently as possible, it is necessary to achieve a good balance between the rate of mesophyll photosynthesis and how stomata behave. In the future, it is anticipated that there will be less water available as well as higher temperature (IPPC, 2013) and this insight must be taken into consideration when utilising mesophyll and stomatal targets to improve crop productivity so that sufficient fuel and food can be produced for the increasing global population. The current study attempted to analyse and clarify a number of matters relating to transgenic tobacco plants with genetic modification to guard cells expression of key enzymes. For instance, it sought to confirm the role played by chloroplasts in guard cells and what effect these changes have in terms of mesophyll photosynthesis. The current study has demonstrated that there is considerable scope to manipulate the metabolism of guard cells or certain traits of stomata to explain the interaction between stomata and the mesophyll. It is possible that the behaviour of stomata could be altered as a result of single or multiple enzyme transformations, thereby improving how efficiently water is used by plants and enhancing the rate of photosynthesis. In conclusion, whilst numerous efforts have been made in the empirical literature to confirm the mesophyll signal, this has not been possible to date. Future research should examine such genotypes and specify numerous positive independent lines with a wide range of expressions to select lines offering heightened levels of expression. This will allow to investigate the influence of changes in SBPase and Rieske in these plants on stomatal function and mesophyll photosynthesis. It would also be useful to establish how such plants respond to changes in the prevailing conditions

such as water stress and the concentration of O_2 and CO_2. Perhaps it would be more advantageous to further investigate the signal transduction pathways and mechanisms that support the close correlation between stomatal conductance and mesophyll photosynthetic rates.

It would be useful to apply the current research using wheat (*Triticum aestivum L*.). Wheat is the most important crop in Saudi Arabia and is grown in diverse environmental conditions.In the past decade, there has been marginal increase in wheat productivity, especially under environments relatively favorable for growth and development of wheat (Chatrath *et al.*, 2017). As such, it is distinctly possible that productivity could be significantly enhanced in the coming years when presented with adverse growing conditions including extreme weather warming, drought and increased temperatures and CO_2 levels (Joshi *et al.*, 2007). For plants to adapt to climate change, physiological and genetic modifications of photosynthetic apparatus like stomata are needed to increase performance and yield.

References

Ainsworth EA, Rogers A (2007) The response of photosynthesis and stomatal conductance to rising [CO2]: Mechanisms and environmental interactions. *Plant, Cell and Environment*, **30**, 258–270.

Amodeo G, Talbott LD, Zeiger E (1996) Use of potassium and sucrose by onion guard cells during a daily cycle of osmoregulation. *Plant and Cell Physiology*, **37**, 575–579.

Antunes WC, Provart NJ, Williams TCR, Loureiro ME (2012) Changes in stomatal function and water use efficiency in potato plants with altered sucrolytic activity. *Plant, Cell and Environment*, **35**, 747–759.

Antunes WC, de Menezes Daloso D, Pinheiro DP, Williams TCR, Loureiro ME (2017) Guard cell-specific down-regulation of the sucrose transporter SUT1 leads to improved water use efficiency and reveals the interplay between carbohydrate metabolism and K+accumulation in the regulation of stomatal opening. *Environmental and Experimental Botany*, **135**, 73–85.

Araus JL, Li J, Parry MAJ, Wang J (2014) Phenotyping and other breeding approaches for a New Green Revolution. *Journal of Integrative Plant Biology*, **56**, 422–424.

Asai N, Nakajima N, Tamaoki M, Kamada H, Kondo N (2000) Role of malate synthesis mediated by phosphoenolpyruvate carboxylase in guard cells in the regulation of stomatal movement. *Plant & cell physiology*, **41**, 10–15.

Azoulay-Shemer T, Palomares A, Bagheri A et al. (2015) Guard cell photosynthesis is critical for stomatal turgor production, yet does not directly mediate CO2- and ABA-induced stomatal closing. *Plant Journal*, **83**, 567–581.

Bacon MA (2009) *Water use efficiency in plant biology.*

Baker NR (2008) Chlorophyll Fluorescence: A Probe of Photosynthesis In Vivo. *Annual Review of Plant Biology*, **59**, 89–113.

Ball JT, Berry JA (1988) Ci/Cs ratio: a basis for predicting stomatal control of photosynthesis. In: *Carnegie Institution of Washington Yearbook*, pp. 88–92.

Baroli I, Price GD, Badger MR, von Caemmerer S (2008) The Contribution of Photosynthesis to the Red Light Response of Stomatal Conductance. *Plant Physiology*, **146**, 737–747.

Beer C, Ciais P, Reichstein M et al. (2009) Temporal and among-site variability of inherent water use efficiency at the ecosystem level. *Global Biogeochemical Cycles*, **23**, 1–13.

Black CC, Osmond CB (2003) Crassulacean acid metabolism photosynthesis: 'Working the night shift'. *Photosynthesis Research*, **76**, 329–341.

Blatt MR, Brodribb TJ, Torii KU (2017) Small pores with a big impact. *Plant Physiology*, 467–469.

Boyer JS (1982) Plant Productivity and Environment. *Science*, **218**, 443–448.

Braun HJ, Atlin G, Payne T (2010) Multi-location testing as a tool to identify plant response to global climate change. In: *Climate Change and Crop Production*, pp. 115–138.

Von Braun J, Rosegrant MW, Pandya-Lorch R, Cohen MJ, Cline SA, Brown MA, Bos MS (2005) *New risks and opportunities for food security scenario analyses for 2015 and 2050*. 1-39 pp.

Buckley TN (2017) Modeling stomatal conductance. *Plant Physiology*, **174**, 572–582.

Buckley TN, Mott KA (2013) Modelling stomatal conductance in response to environmental factors. *Plant, Cell & Environment*, **36**, 1691–1699.

Busch FA (2014) Opinion: The red-light response of stomatal movement is sensed by the redox state of the photosynthetic electron transport chain. *Photosynthesis Research*, **119**, 131–140.

von Caemmerer S, Evans JR (2010) Enhancing C3 Photosynthesis. *Plant Physiology*, **154**, 589–592.

von Caemmerer S, Lawson T, Oxborough K, Baker NR, Andrews TJ, Raines CA (2004) Stomatal conductance does not correlate with photosynthetic capacity in transgenic tobacco with reduced amounts of Rubisco. *Journal of Experimental Botany*, **55**, 1157–1166.

Cardon ZG, Berry J (1992) Effects of O2 and CO2 concentration on the steady-state fluorescence yield of single guard cell pairs in intact leaf discs of tradescantia albiflora: evidence for Rubisco-mediated CO2 fixation and photorespiration in guard cells. *Plant physiology*, **99**, 1238–1244.

Carter R, Woolfenden H, Baillie A et al. (2017) Stomatal Opening Involves Polar, Not Radial, Stiffening Of Guard Cells. *Current Biology*.

Casson S, Gray JE (2008) Influence of environmental factors on stomatal

development. *New Phytologist*, **178**, 9–23.

Casson SA, Hetherington AM (2010) Environmental regulation of stomatal development. *Current Opinion in Plant Biology*, **13**, 90–95.

Chatrath R, Mishra B, Ortiz Ferrara G, Singh SK, Joshi AK (2017) Challenges to wheat production in South Asia. In: *Euphytica*, pp. 447–456.

Chen ZH, Chen G, Dai F et al. (2017) Molecular Evolution of Grass Stomata. *Trends in Plant Science*, 124–139.

Chida H, Nakazawa A, Akazaki H et al. (2007) Expression of the algal cytochrome c6 gene in Arabidopsis enhances photosynthesis and growth. *Plant and Cell Physiology*, 48: 948–957.

Daloso DM, Antunes WC, Pinheiro DP et al. (2015) Tobacco guard cells fix CO2by both Rubisco and PEPcase while sucrose acts as a substrate during light-induced stomatal opening. *Plant Cell and Environment*, **38**, 2353–2371.

Daloso DM, dos Anjos L, Fernie AR (2016a) Roles of sucrose in guard cell regulation. *New Phytologist*, **211**, 809–818.

Daloso DM, Williams TCR, Antunes WC, Pinheiro DP, Müller C, Loureiro ME, Fernie AR (2016b) Guard cell-specific upregulation of sucrose synthase 3 reveals that the role of sucrose in stomatal function is primarily energetic. *New Phytologist*, **209**, 1470–1483.

Daloso DM, Medeiros DB, dos Anjos L, Yoshida T, Araújo WL, Fernie AR (2017) Metabolism within the specialized guard cells of plants. *New Phytologist*, **216**, 1018–1033.

Ding F, Wang M, Zhang S, Ai X (2016) Changes in SBPase activity influence photosynthetic capacity, growth, and tolerance to chilling stress in transgenic tomato plants. *Scientific Reports*, **6**, 1–14.

Driever SM, Simkin AJ, Alotaibi S et al. (2017a) Increased SBPase activity improves photosynthesis and grain yield in wheat grown in greenhouse conditions. *Philosophical Transactions of the Royal Society B: Biological Sciences*, **372**, 20160384.

Driever SM, Simkin AJ, Alotaibi S et al. (2017b) Increased SBPase activity improves photosynthesis and grain yield in wheat grown in greenhouse conditions. *Philosophical Transactions of the Royal Society B: Biological Sciences*, **372**, 20160384.

Eckert M, Kaldenhoff R (2000) Light-induced stomatal movement of selected Arabidopsis thaliana mutants. *Journal of Experimental Botany*, **51**, 1435–1442.

Edwards D, Kerp H, Hass H (1998) Stomata in early land plants: an anatomical and ecophysiological approach. *Journal of Experimental Botany*, **49**, 255–278.

Eisenach C, Chen ZH, Grefen C, Blatt MR (2012) The trafficking protein SYP121 of Arabidopsis connects programmed stomatal closure and K+ channel activity with vegetative growth. *Plant Journal*, **69**, 241–251.

Engle KM, Mei T-S, Wasa M, Yu J-Q (2008) Structure of the Cytochrome b6 f Complex: Quinone Analogue Inhibitors as Ligands of Heme cn. *Accounts of Chemical Research*, **45**, 788–802.

Ermakova M, Lopez-Calcagno P, Raines C, Furbank R, von Caemmerer S (2019) Overexpression of the Rieske FeS protein of the Cytochrome b 6 f complex

increases C 4 photosynthesis. *bioRxiv*, 1–32.

Evert R (2006) *Esau's Plant anatomy: meristems, cells, and tissues of the plant body: their structure, function, and development*. John Wiley Sons p.

FAO (2015) Food and Agriculture Organisation of the United Nations. (2015) How to feed the world in 2050 [Web Document]. *Rome; Italy Accessed on: http://www.fao.org/fileadmin/templates/wsfs/docs/expert_paper/How_to_Feed_the_World_in_2050.pdf*, **Last acces**, 20/12/2017.

Farquhar GD, Raschke K (1978) On the Resistance to Transpiration of the Sites of Evaporation within the Leaf. *PLANT PHYSIOLOGY*, **61**, 1000–1005.

Farquhar GD, Sharkey TD (1982) Stomatal Conductance and Photosynthesis. *Annual Review of Plant Physiology*, **33**, 317–345.

Feng L, Han Y, Liu G et al. (2007) Overexpression of sedoheptulose-1,7-bisphosphatase enhances photosynthesis and growth under salt stress in transgenic rice plants. *Functional Plant Biology*, **34**, 822–834.

Feng L, Li H, Jiao J, Li D, Zhou L, Wan J, Li Y (2009) Reduction in SBPase activity by antisense RNA in transgenic rice plants: Effect on photosynthesis, growth, and biomass allocation at different nitrogen levels. *Journal of Plant Biology*, **52**, 382–394.

Fischer RA (1968) Stomatal opening: role of potassium uptake by guard cells. *Science*, **160**, 784–785.

Fischer RA, Edmeades GO (2010) Breeding and cereal yield progress. *Crop Science*, **50**, S-85-S-98.

Fischer RA, Hsiao TC (1968) Stomatal Opening in Isolated Epidermal Strips of Vicia faba. II. Responses to KCl Concentration and the Role of Potassium Absorption. *Plant physiology*, **43**, 1953–8.

Fischer RA, Rees D, Sayre KD, Lu ZM, Condon AG, Larque Saavedra A (1998) Wheat yield progress associated with higher stomatal conductance and photosynthetic rate, and cooler canopies. *Crop Science*, **38**, 1467–1475.

Fitzsimons PJ, Weyers JDB (1986) Volume changes of Commelina communis guard cell protoplasts in response to K+, light and CO2. *Physiologia Plantarum*, **66**, 463–468.

Flexas J (2016) Genetic improvement of leaf photosynthesis and intrinsic water use efficiency in C3 plants: Why so much little success? *Plant Science*, **251**, 155–161.

Flütsch S, Santelia D (2021) Starch Metabolism in Guard Cells and its Impact on Stomatal Function. *New Phytologist*.

Flütsch S, Nigro A, Conci F et al. (2020a) Glucose uptake to guard cells via STP transporters provides carbon sources for stomatal opening and plant growth. *EMBO reports*, **21(8)**.

Flütsch S, Wang Y, Takemiya A et al. (2020b) Guard cell starch degradation yields glucose for rapid stomatal opening in Arabidopsis. *Plant Cell*.

Foulkes MJ, Scott RK, Sylvester-Bradley R (2002) The ability of wheat cultivars to withstand drought in UK conditions: Formation of grain yield. *Journal of Agricultural Science*, **138**, 153–169.

Foulkes MJ, Sylvester-Bradley R, Weightman R, Snape JW (2007) Identifying physiological traits associated with improved drought resistance in winter wheat. *Field Crops Research*, **103**, 11–24.

Franks PJ, Farquhar GD (2007) The Mechanical Diversity of Stomata and Its Significance in Gas-Exchange Control. *Plant Physiology*, **143**, 78–87.

Franks PJ, Bonan GB, Berry JA, Lombardozzi DL, Holbrook NM, Herold N, Oleson KW (2018) Comparing optimal and empirical stomatal conductance models for application in Earth system models. *Global Change Biology*, **24**, 5708–5723.

Frechilla S, Zhu J, Talbott LD, Zeiger E (1999) Stomata from npq1, a zeaxanthin-less Arabidopsis mutant, lack a specific response to blue light. *Plant & cell physiology*, **40**, 949–954.

Frechilla S, Talbott LD, Zeiger E (2002) The CO2 response of Vicia guard cells acclimates to growth environment. *Journal of Experimental Botany*, **53**, 545–550.

Freire FBS, Bastos RLG, Bret RSC et al. (2021) Mild reductions in guard cell sucrose synthase 2 expression leads to slower stomatal opening and decreased whole plant transpiration in Nicotiana tabacum L. *Environmental and Experimental Botany*, **184**.

Gehlen J, Panstruga R, Smets H et al. (1996) Effects of altered phosphoenolpyruvate carboxylase activities on transgenic C3 plant Solanum tuberosum. *Plant Molecular Biology*, **32**, 831–848.

Godfray HCJ, Beddington JR, Crute IR et al. (2010) The Challenge of Food Security. *Science*, **327**, 812–818.

Goh CH, Dietrich P, Steinmeyer R, Schreiber U, Nam HG, Hedrich R (2002) Parallel recordings of photosynthetic electron transport and K+-channel activity in single guard cells. *Plant Journal*, **32**, 623–630.

Gotow K, Taylor S, Zeiger E (1988) Photosynthetic Carbon Fixation in Guard Cell Protoplasts of Vicia faba L . 1. 700–705.

Guilioni L, Jones HG, Leinonen I, Lhomme JP (2008) On the relationships between stomatal resistance and leaf temperatures in thermography. *Agricultural and Forest Meteorology*.

Hampp R, Outlaw WH, Tarczynski MC (1982) Profile of basic carbon pathways in guard cells and other leaf cells of Vicia faba L. *Plant physiology*, **70**, 1582–1585.

Hanjra MA, Qureshi ME (2010) Global water crisis and future food security in an era of climate change. *Food Policy*, **35**, 365–377.

Harrison EP, Willingham NM, Lloyd JC, Raines CA (1998) Reduced sedoheptulose-1,7-bisphosphatase levels in transgenic tobacco lead to decreased photosynthetic capacity and altered carbohydrate accumulation. *Planta*, **204**, 27–36.

Harrison MT, Tardieu F, Dong Z, Messina CD, Hammer GL (2014) Characterizing drought stress and trait influence on maize yield under current and future conditions. *Global Change Biology*, **20**, 867–878.

Hetherington AM, Woodward FI (2003) The role of stomata in sensing and driving environmental change. *Nature*, **424**, 901–908.

Hipkins MF, Fitzsimons PJ, Weyers JDB (1983) The primary processes of

photosystem II in purified guard-cell protoplasts and mesophyll-cell protoplasts from Commelina communis L. *Planta*, **159**, 554–560.

Hiyama A, Takemiya A, Munemasa S et al. (2017) Blue light and CO2 signals converge to regulate light-induced stomatal opening. *Nature Communications*, **8**, 1284.

Horrer D, Flütsch S, Pazmino D et al. (2016) Blue light induces a distinct starch degradation pathway in guard cells for stomatal opening. *Current Biology*, **26**, 362–370.

Hosy E, Vavasseur A, Mouline K et al. (2003) The Arabidopsis outward K+ channel GORK is involved in regulation of stomatal movements and plant transpiration. *Proceedings of the National Academy of Sciences*, **100**, 5549–5554.

Hudson GS, Evans JR, von Caemmerer S, Arvidsson YB, Andrews TJ (1992) Reduction of ribulose-1,5-bisphosphate carboxylase/oxygenase content by antisense RNA reduces photosynthesis in transgenic tobacco plants. *Plant physiology*, **98**, 294–302.

Huxman TE, Monson RK (2003) Stomatal responses of C3, C3-C4 and C4 Flaveria species to light and intercellular CO2 concentration: Implications for the evolution of stomatal behaviour. *Plant, Cell and Environment*, **26**, 313–322.

Inoue S, Kinoshita T (2017) Blue Light Regulation of Stomatal Opening and the Plasma Membrane H $^{+}$ -ATPase. *Plant Physiology*, **174**, 531–538.

IPPC (2007) Summary for Policymakers. In Climate Change. *New York Cambridge University Press*, 996.

Jones HG (2013) *Plants and microclimate: A quantitative approach to environmental plant physiology*.

Joshi AK, Mishra B, Chatrath R, Ortiz Ferrara G, Singh RP (2007) Wheat improvement in India: Present status, emerging challenges and future prospects. In: *Euphytica*, pp. 431–446.

Kang Y, Outlaw WH, Andersen PC, Fiore GB (2007) Guard-cell apoplastic sucrose concentration - A link between leaf photosynthesis and stomatal aperture size in the apoplastic phloem loader Vicia faba L. *Plant, Cell and Environment*, **30**, 551–558.

Keenan TF, Gray J, Friedl MA et al. (2014) Net carbon uptake has increased through warming-induced changes in temperate forest phenology. *Nature Climate Change*, **4**, 598–604.

Kellogg EA (2001) Evolutionary History of the Grasses. *PLANT PHYSIOLOGY*, **125**, 1198–1205.

Kelly G, David-Schwartz R, Sade N, Moshelion M, Levi A, Alchanatis V, Granot D (2012) The pitfalls of transgenic selection and new roles of AtHXK1: A high level of AtHXK1 expression uncouples hexokinase1 dependent sugar signaling from exogenous sugar. *Plant Physiology*, **159**, 47–51.

Kelly G, Moshelion M, David-Schwartz R et al. (2013) Hexokinase mediates stomatal closure. *Plant Journal*, **75**, 977–988.

Kelly G, Lugassi N, Belausov E et al. (2017) The Solanum tuberosum KST1 partial promoter as a tool for guard cell expression in multiple plant species. *Journal of Experimental Botany*, **68**, 2885–97.

Kelly G, Egbaria A, Khamaisi B, Lugassi N, Attia Z, Moshelion M, Granot D (2019) Guard-Cell Hexokinase Increases Water-Use Efficiency Under Normal and Drought Conditions. *Frontiers in Plant Science*, **10**, 1499.

Kim T-H, Bohmer M, Hu H, Nishimura N, Schroeder JI (2010) Guard cells signal transduction network: advances in understanding abscisic acid CO2, and Ca2+ signalling. *Annual Review of Plant Biology*, **61**, 561–591.

Kinoshita T, Doi M, Suetsugu N, Kagawa T, Wada M, Shimazaki KI (2014) phot1 and phot2 mediate blue light regulation of stomatal opening. *Nature*, **414**, 656– 660.

Kirchhoff H, Horstmann S, Weis E (2000) Control of the photosynthetic electron transport by PQ diffusion microdomains in thylakoids of higher plants. *Biochimica et Biophysica Acta - Bioenergetics*, **1459**, 148–168.

Kirchhoff H, Li M, Puthiyaveetil S (2017) Sublocalization of Cytochrome b6f Complexes in Photosynthetic Membranes. *Trends in Plant Science*.

Kramer PJ, Boyer JS (1995) Stomata and Gas Exchange. *Water relations of plants and soils*, 257–282.

Kurisu G, Zhang H, Smith JL, Cramer WA (2003) Structure of the cytochrome b6f complex of oxygenic photosynthesis : tuning the cavity . Science 302 , 1009- Structure of the Cytochrome b 6 f Complex of Oxygenic Photosynthesis : Tuning the. 1009–1014.

Laanemets K, Wang YF, Lindgren O et al. (2013) Mutations in the SLAC1 anion channel slow stomatal opening and severely reduce K+ uptake channel activity via enhanced cytosolic [Ca2+] and increased Ca2+ sensitivity of K+ uptake channels. *New Phytologist*, **197**, 88–98.

Laporte MM, Shen B, Tarczynski MC (2002) Engineering for drought avoidance: expression of maize NADP-malic enzyme in tobacco results in altered stomatal function. *Journal of Experimental Botany*, **53**, 699–705.

Lawson T (2009) Guard Cell Photosyn and Stomatal Function. *New Phytologist*, 13–34.

Lawson T, Blatt MR (2014) Stomatal Size, Speed, and Responsiveness Impact on Photosynthesis and Water Use Efficiency. *Plant Physiology*, **164**, 1556–1570.

Lawson T, Vialet-Chabrand S (2019) Speedy stomata, photosynthesis and plant water use efficiency. *New Phytologist*, 93–98.

Lawson T, Oxborough K, Morison JIL, Baker NR (2002) Responses of photosynthetic electron transport in stomatal guard cells and mesophyll cells in intact leaves to light, CO2, and humidity. *Plant Physiology*, **128**, 52–62.

Lawson T, Oxborough K, Morison JIL, Baker NR (2003) The responses of guard and mesophyll cell photosynthesis to Co2, O2, light, and water stress in a range of species are similar. *Journal of Experimental Botany*, **54**, 1743–1752.

Lawson T, Bryant B, Lefebvre S, Lloyd JC, Raines CA (2006) Decreased SBPase activity alters growth and development in transgenic tobacco plants. *Plant, Cell and Environment*, **29**, 48–58.

Lawson T, Lefebvre S, Baker NR, Morison JIL, Raines CA (2008) Reductions in mesophyll and guard cell photosynthesis impact on the control of stomatal responses to light and CO2. *Journal of Experimental Botany*, **59**, 3609–3619.

Lawson T, Caemmerer S Von, Baroli I (2010) Photosynthesis and Stomatal

Behaviour. *Nature*, **194**, 266–304.

Lawson T, Kramer DM, Raines CA (2012) Improving yield by exploiting mechanisms underlying natural variation of photosynthesis. *Current Opinion in Biotechnology*, **23**, 215–220.

Lawson T, Simkin AJ, Kelly G, Granot D (2014) Mesophyll photosynthesis and guard cell metabolism impacts on stomatal behaviour. *New Phytologist*, **203**, 1064–1081.

Lebaudy A, Hosy E, Simonneau T, Sentenac H, Thibaud JB, Dreyer I (2008) Heteromeric K+ channels in plants. *Plant Journal*, **54**, 1076–1082.

Lefebvre S, Lawson T, Fryer M, Zakhleniuk OV, Lloyd JC, Raines C a (2005) Increased sedoheptulose-1, 7-bisphosphatase activity in transgenic tobacco plants stimulates photosynthesis and growth from an early stage in development. *Plant Physiology*, **138**, 451–460.

Li L, Zhang Q, Huang D (2014) A review of imaging techniques for plant phenotyping. *Sensors (Switzerland)*, **14**, 20078–20111.

Lodge RJ, Dijkstra P, Drake BG, Morison JIL (2001) Stomatal acclimation to increased CO2concentration in a Florida scrub oak species Quercus myrtifolia Willd. *Plant, Cell and Environment*, **24**, 77–88.

Long SP, Marshall-Colon A, Zhu XG (2015) Meeting the global food demand of the future by engineering crop photosynthesis and yield potential. *Cell*, **161**, 56–66.

Lu P, Zhang SQ, Outlaw WH, Riddle KA (1995) Sucrose: a solute that accumulates in the guard-cell apoplast and guard-cell symplast of open stomata. *FEBS*

Letters, **362**, 180–184.

Lu P, Outlaw Jr WH, Smith BG, Freed G a. (1997) A new mechanism for the regulation of stomatal aperture size in intact leaves (accumulation of mesophyll-derived sucrose in the guard-cell wall of Vicia faba). *Plant physiology*, **114**, 109–118.

Lugassi N, Kelly G, Fidel L et al. (2015) Expression of Arabidopsis Hexokinase in Citrus Guard Cells Controls Stomatal Aperture and Reduces Transpiration. *Frontiers in Plant Science*, **6**.

Lurie S (1977) Photochemical properties of guard cell chloroplasts. *Plant Science Letters*, **10**, 219–223.

Lysenko V (2012) Fluorescence kinetic parameters and cyclic electron transport in guard cell chloroplasts of chlorophyll-deficient leaf tissues from variegated weeping fig (Ficus benjamina L.). *Planta*, **235**, 1023–1033.

MacRobbie EAC, Lettau J (1980) Potassium content and aperture in ‘intact’ stomatal and epidermal cells of Commelina communis L. *The Journal of Membrane Biology*, **56**, 249–256.

Maggio A, van Criekinge T, Malingreau JP (2015) *Global Food Security 2030 Assessing trends with a view to guiding*. 1-45 pp.

Maherali H, Reid CD, Polley HW, Johnson HB, Jackson RB (2002) Stomatal acclimation over a subambient to elevated CO 2 gradient in a C 3 / C 4 grassland. *Plant, Cell and Environment*, **2**, 557–566.

Marten I, Deeken R, Hedrich R, Roelfsema MRG (2010) Light-induced modification

of plant plasma membrane ion transport. *Plant Biology*, **12**, 64–79.

Matthews JS, Vialet-Chabrand SR, Lawson T (2018) Acclimation to fluctuating light impacts the rapidity and diurnal rhythm of stomatal conductance. *Plant Physiology*, pp.01809.2017.

Matthews JSA, Vialet-Chabrand S, Lawson T (2020) Role of blue and red light in stomatal dynamic behaviour. *Journal of Experimental Botany*, 2253–2269.

Mawson BT, Zeiger E (1991) Blue light-modulation of chlorophyll a fluorescence transients in guard cell chloroplasts. *Plant physiology*, **96**, 753–60.

Mcausland L, Antunes WC, de Menezes Daloso D et al. (2017) Guard cell-specific down-regulation of the sucrose transporter SUT1 leads to improved water use efficiency and reveals the interplay between carbohydrate metabolism and K+accumulation in the regulation of stomatal opening. *Plant Physiology*, **164**, 1556–1570.

McAusland L, Vialet-Chabrand S, Davey P, Baker NR, Brendel O, Lawson T (2016) Effects of kinetics of light-induced stomatal responses on photosynthesis and water-use efficiency. *New Phytologist*, **211**, 1209–1220.

Messinger SM, Buckley TN, Mott KA (2006) Evidence for involvement of photosynthetic processes in the stomatal response to CO_2. *Plant physiology*, **140**, 771–778.

Morison JIL, Baker NR, Mullineaux PM, Davies WJ (2008a) Improving water use in crop production. *Philosophical Transactions of the Royal Society B: Biological Sciences*, 639–658.

Morison J, Baker N, Mullineaux P, Davies W (2008b) Improving water use in crop production. *Philosophical Transactions of the Royal Society B: Biological Sciences*, **363**, 639–658.

Mott KA (1988) Do Stomata Respond to CO2 Concentrations Other than Intercellular? *Plant Physiology*, **86**, 200–203.

Müller-Röber B, La Cognate U, Sonnewald U, Willmitzer L (1994) A truncated version of an ADP-glucose pyrophosphorylase promoter from potato specifies guard cell-selective expression in transgenic plants. *Plant Cell*, 601–612.

Müller-Röber B, Ellenberg J, Provart N et al. (1995) Cloning and electrophysiological analysis of KST1, an inward rectifying K+ channel expressed in potato guard cells. *The EMBO Journal*, **14**, 2409–2416.

Nelson SD, Mayo JM (1975) The occurrence of functional non-chlorophyllous guard cells in Paphiopedilum spp. *Canadian Journal of Botany*, **53**, 1–7.

Nilson SE, Assmann SM (2006) The Control of Transpiration. Insights from Arabidopsis. *Plant Physiology*, **143**, 19–27.

Nunes-Nesi A, Nascimento VDL, De Oliveira Silva FM, Zsögön A, Araújo WL, Sulpice R (2016) Natural genetic variation for morphological and molecular determinants of plant growth and yield. *Journal of Experimental Botany*.

Olsen RL, Pratt RB, Gump P, Kemper A, Tallman G (2002) Red light activates a chloroplast-dependent ion uptake mechanism for stomatal opening under reduced CO 2 concentrations in. *New Phytologist*, 497–508.

Outlaw WH (1983) Current concepts on the role of potassium in stomatal

movements. *Physiologia Plantarum*, **59**, 302–311.

Outlaw WH, Manchester J (1979) Guard cell starch concentration quantitatively related to stomatal aperture. *Plant physiology*, **64**, 79–82.

Outlaw WH, De Vlieghere-He X (2001) Transpiration rate. An important factor controlling the sucrose content of the guard cell apoplast of broad bean. *Plant physiology*, **126**, 1716–1724.

Outlaw J, William H (2003) Integration of Cellular and Physiological Functions of Guard Cells. *Critical Reviews in Plant Sciences*, **22**, 503–529.

Outlaw WH, Manchester J, Dicamelli CA, Randall DD, Rapp B, Veith GM (1979) Photosynthetic carbon reduction pathway is absent in chloroplasts of Vicia faba guard cells. *Proceedings of the National Academy of Sciences of the United States of America*, **76**, 6371–5.

Outlaw WH, Mayne BC, Zenger VE, Manchester J (1981) Presence of both photosystems in guard cells of Vicia faba L: implications for environmental signal processing. *Plant physiology*, **67**, 12–16.

Pearson CJ (1973) Daily changes in stomatal aperture and in carbohydrates and malate within epidermis and mesophyll of leaves of commelina cyanea and vicia faba. *Australian Journal of Biological Sciences*, **26**, 1035–1044.

Penfield S, Clements S, Bailey KJ, Gilday AD, Leegood RC, Gray JE, Graham IA (2012) Expression and manipulation of PHOSPHOENOLPYRUVATE CARBOXYKINASE 1 identifies a role for malate metabolism in stomatal closure. *Plant Journal*, **69**, 679–688.

Peterson KM, Rychel AL, Torii KU (2010) Out of the Mouths of Plants: The Molecular Basis of the Evolution and Diversity of Stomatal Development. *The Plant Cell*, **22**, 296–306.

Plesch G, Ehrhardt T, Mueller-Roeber B (2001) Involvement of TAAAG elements suggests a role for Dof transcription factors in guard cell-specific gene expression. *Plant Journal*, **28**, 455–464.

Poffenroth M, Green DB, Tallman G (1992) Sugar Concentrations in Guard Cells of Vicia faba Illuminated with Red or Blue Light1 Analysis by High Performance Liquid Chromatography. 1460–1471.

Poolman MG, Fell DA, Thomas S (2000) Modelling photosynthesis and its control. *Journal of Experimental Botany*, **51**, 319–328.

Preiss J (1991) Biology and molecular biology of starch synthesis and its regulation. *Oxford Surveys of Plant Molecular Cell Biology Vol 7*, 59–114.

Price G, Yu J, Caemmerer S et al. (1995) Chloroplast Cytochrome b6/f and ATP Synthase Complexes in Tobacco: Transformation With Antisense RNA Against Nuclear-Encoded Transcripts for the Rieske FeS and ATPδ Polypeptides. *Functional Plant Biology*, **22**, 285–297.

Price GD, Von Caemmerer S, Evans JR, Siebke K, Anderson JM, Badger MR (1998) Photosynthesis is strongly reduced by antisense suppression of chloroplastic cytochrome bf complex in transgenic tobacco. *Australian Journal of Plant Physiology*, **25**, 445–452.

Raines CA (2003) The Calvin cycle revisited. *Photosynthesis Research*, **75**, 1–10.

Raines CA (2006) Transgenic approaches to manipulate the environmental responses of the C3 carbon fixation cycle. *Plant, Cell and Environment*, **29**, 331–339.

Raines CA (2011) Increasing Photosynthetic Carbon Assimilation in C3 Plants to Improve Crop Yield: Current and Future Strategies. *Plant Physiology*, **155**, 36–42.

Raines CA, Paul MJ (2006) Products of leaf primary carbon metabolism modulate the developmental programme determining plant morphology. *Journal of Experimental Botany*, **57**, 1857–1862.

Raines CA, Lloyd JC, Dyer TA (1999) New insights into the structure and function of but neglected Calvin cycle enzyme. **50**, 1–8.

Raines CA, Harrison EP, Ölçer H, Lloyd JC (2000) Investigating the role of the thiol-regulated enzyme sedoheptulose-1,7-bisphosphatase in the control of photosynthesis. *Physiologia Plantarum*, **110**, 303–308.

Raschke K, Dittrich P (1977) [14C]Carbon-dioxide fixation by isolated leaf epidermes with stomata closed or open. *Planta*, **134**, 69–75.

Raven JA (2002) Selection pressures on stomatal evolution. *New Phytologist*, **153**, 371–386.

Ray DK, Foley JA (2013) Increasing global crop harvest frequency: Recent trends and future directions. *Environmental Research Letters*, **8**, 1–10.

Reckmann U, Scheibe R, Raschke K (1990) Rubisco activity in guard cells compared with the solute requirement for stomatal opening. *Plant physiology*,

92, 246–53.

Roelfsema MRG, Steinmeyer R, Staal M, Hedrich R (2001) Single guard cell recordings in intact plants: Light-induced hyperpolarization of the plasma membrane. *Plant Journal*, **26**, 1–13.

Roelfsema MRG, Hanstein S, Felle HH, Hedrich R (2002) CO2 provides an intermediate link in the red light response of guard cells. *Plant Journal*, **32**, 65–75.

Roelfsema MRG, Konrad KR, Marten H, Psaras GK, Hartung W, Hedrich R (2006) Guard cells in albino leaf patches do not respond to photosynthetically active radiation, but are sensitive to blue light, CO2 and abscisic acid. *Plant, Cell and Environment*, **29**, 1595–1605.

Rosenthal DM, Locke AM, Khozaei M, Raines CA, Long SP, Ort DR (2011) Over-expressing the C3photosynthesis cycle enzyme Sedoheptulose-1-7 Bisphosphatase improves photosynthetic carbon gain and yield under fully open air CO2fumigation (FACE). *BMC Plant Biology*, **11**.

Rusconi F, Simeoni F, Francia P et al. (2013) The Arabidopsis thaliana MYB60 promoter provides a tool for the spatio-temporal control of gene expression in stomatal guard cells. *Journal of Experimental Botany*, **64**, 3361–3371.

Ruuska SA, Andrews TJ, Badger MR, Lilley RM, Price GD, Caemmerer S von (1998) Rubisco activation is impaired in transgenic tobacco plants with reduced electron transport capacity. In: *Photosynthesis: mechanisms and effects. Volume V. Proceedings of the XIth International Congress on Photosynthesis, Budapest, Hungary, 17-22 August, 1998.*

Ruuska SA, Andrews TJ, Badger MR, Price GD, Von Caemmerer S (2000) The role of chloroplast electron transport and metabolites in modulating Rubisco activity in tobacco. Insights from transgenic plants with reduced amounts of cytochrome b/f complex or glyceraldehyde 3-phosphate dehydrogenase. *Plant Physiology*, **122**, 491–504.

Santelia D, Lawson T (2016) Rethinking Guard Cell Metabolism. *Plant Physiology*, **172**, 1371–1392.

Schnabl H (1981) The compartmentation of carboxylating and decarboxylating enzymes in guard cell protoplasts. *Planta*, **152**, 307–313.

Schnabl H, Raschke K (1980) Potassium chloride as stomatal osmoticum in Allium cepa L., a species devoid of starch in guard cells. *Plant physiology*, **65**, 88–93.

Schwartz A, Zeiger E (1984) Metabolic energy for stomatal opening. Roles of photophosphorylation and oxidative phosphorylation. *Planta*, **161**, 129–136.

Serrano EE, Zeiger E, Hagiwara S (1988) Red light stimulates an electrogenic proton pump in Vicia guard cell protoplasts. *Proceedings of the National Academy of Sciences of the United States of America*, **85**, 436–440.

Sharkey TD, Raschke K (1981) Effect of Light Quality on Stomatal Opening in Leaves of Xanthium strumarium L. *Plant physiology*, **68**, 1170–1174.

Shimazaki K, Okayama S (1990) Calvin Benson cycle enzimes in guard-cell protoplasts and their role in stomatal movement. *Biochemie und Physiologie der Pflanzen*, **186**, 327–331.

Shimazaki K-I, Zeiger E (1985) Cyclic and Noncyclic Photophosphorylation in

Isolated Guard Cell Chloroplasts from Vicia faba L. *Plant physiology*, **78**, 211–214.

Shimazaki K, Gotow K, Kondo N (1982) Photosynthetic Properties of Guard Cell Protoplasts from Vicia faba L . *Plant & Cell Physiology*, **23**, 871–879.

Shimazaki K, Terada J, Tanaka K, Kondo N (1989) Calvin-Benson Cycle Enzymes in Guard-Cell Protoplasts from Vicia faba L. *Plant physiology*, **90**, 1057–1064.

Shimazaki K, Doi M, Assmann SM, Kinoshita T (2007) Light Regulation of Stomatal Movement. *Annual Review of Plant Biology*, **58**, 219–247.

Simkin AJ, McAusland L, Headland LR, Lawson T, Raines CA (2015) Multigene manipulation of photosynthetic carbon assimilation increases CO2 fixation and biomass yield in tobacco. *Journal of Experimental Botany*, **66**, 4075–4090.

Simkin AJ, McAusland L, Lawson T, Raines CA (2017a) Over-expression of the RieskeFeS protein increases electron transport rates and biomass yield. *Plant Physiology*, pp.00622.2017.

Simkin AJ, Lopez-Calcagno PE, Davey PA et al. (2017b) Simultaneous stimulation of sedoheptulose 1,7-bisphosphatase, fructose 1,6-bisphophate aldolase and the photorespiratory glycine decarboxylase-H protein increases CO2 assimilation, vegetative biomass and seed yield in Arabidopsis. *Plant Biotechnology Journal*, **15**, 805–816.

Slingo JM, Challinor AJ, Hoskins BJ, Wheeler TR (2005) Introduction: food crops in a changing climate. *Philosophical Transactions of the Royal Society B: Biological Sciences*, **360**, 1983–1989.

Stevens RA, Martin ES (1978) Structural and functional aspects of stomata - I. Developmental studies in Polypodium vulgare. *Planta*, **142**, 307–316.

Stroebel D, Choquet Y, Popot JL, Picot D (2003) An atypical haem in the cytochrome b6f complex. *Nature*, **426**, 413–418.

Taiz L, Zeiger E (2010) *Plant Physiology 5th ed, Annals of Botany*. 60-61 pp.

Talbott L (1998) The role of sucrose in guard cell osmoregulation. *Journal of Experimental Botany*, **49**, 329–337.

Talbott LD, Zeiger E (1993) Sugar and Organic Acid Accumulation in Guard Cells of Vicia faba in Response to Red and Blue Light'. *Plant Physiol*, **102**, 1163–1.

Talbott LD, Zeiger E (1996) Central Roles for Potassium and Sucrose in Guard-Cell Osmoregulation. *Plant physiology*, **111**, 1051–1057.

Tallman G, Zeiger E (1988) Light quality and osmoregulation in vicia guard cells : evidence for involvement of three metabolic pathways. *Plant physiology*, **88**, 887–895.

Tanaka Y, Sugano SS, Shimada T, Hara-Nishimura I (2013) Enhancement of leaf photosynthetic capacity through increased stomatal density in Arabidopsis. *New Phytologist*, **198**, 757–764.

Taylor a R, Assmann SM (2001) Apparent absence of a redox requirement for blue light activation of pump current in broad bean guard cells. *Plant physiology*, **125**, 329–38.

Tichá I (1982) Photosynthetic characteristics during ontogenesis of leaves: 7. Stomata density and sizes. *Photosynthetica*, **16**, 375—471.

Tominaga M, Kinoshita T, Shimazaki K (2001) Guard-cell chloroplasts provide ATP required for H(+) pumping in the plasma membrane and stomatal opening. *Plant & cell physiology*, **42**, 795–802.

Tubiello FN, Soussana J-F, Howden SM (2007) Crop and pasture response to climate change. *Proceedings of the National Academy of Sciences*, **104**, 19686–19690.

Uematsu K, Suzuki N, Iwamae T, Inui M, Yukawa H (2012) Increased fructose 1,6-bisphosphate aldolase in plastids enhances growth and photosynthesis of tobacco plants. *Journal of Experimental Botany*, **63**, 3001–3009.

Unesco (2009) Water in a Changing World. *World Water*, **11**, 349.

Vialet-Chabrand S, Lawson T (2019) Dynamic leaf energy balance: Deriving stomatal conductance from thermal imaging in a dynamic environment. *Journal of Experimental Botany*, **70**, 2839–2855.

Vialet-Chabrand SRM, Matthews JSA, McAusland L, Blatt MR, Griffiths H, Lawson T (2017a) Temporal Dynamics of Stomatal Behavior: Modeling and Implications for Photosynthesis and Water Use. *Plant Physiology*, **174**, 603–613.

Vialet-Chabrand S, Matthews JSA, Simkin AJ, Raines CA, Lawson T (2017b) Importance of Fluctuations in Light on Plant Photosynthetic Acclimation. *Plant Physiology*, **173**, 2163–2179.

Wang P, Song CP (2008) Guard-cell signalling for hydrogen peroxide and abscisic acid. *New Phytologist*, **178**, 703–718.

Wang Y, Holroyd G, Hetherington AM, Ng CKY (2004) Seeing ‘cool’ and ‘hot’ -

Infrared thermography as a tool for non-invasive, high-throughput screening of Arabidopsis guard cell signalling mutants. *Journal of Experimental Botany*, **55**, 1187–1193.

Wang Y, Noguchi K, Terashima I (2011) Photosynthesis-dependent and -independent responses of stomata to blue, red and green monochromatic light: Differences between the normally oriented and inverted leaves of sunflower. *Plant and Cell Physiology*, **52**, 479–489.

Wang Y, Noguchi K, Ono N, Inoue SI, Terashima I, Kinoshita T (2014) Overexpression of plasma membrane H+-ATPase in guard cells promotes light-induced stomatal opening and enhances plant growth. *Proceedings of the National Academy of Sciences of the United States of America*, **111**, 533–538.

Webb AAR, Baker AJ (2002) Stomatal biology: new techniques, new challenges. *New Phytologist*, **153**, 365–369.

Willmer C, Fricker M (1996) Stomata. *2nd edn. London: Chapman & Hall.*

Wong SC, Cowan IR, Farquhar GD (1979) Stomatal conductance correlates with photosynthetic capacity. *Nature*, **282**, 424–426.

Wu W, Assmann SM (1993) Photosynthesis by guard cell chloroplasts of Vicia faba {L}.: Effects of factors associated with stomatal movement. *Plant and Cell Physiology*, **34**, 1015–1022.

Yadav SK, Khatri K, Rathore MS, Jha B (2018) Introgression of UfCyt c6, a thylakoid lumen protein from a green seaweed Ulva fasciata Delile enhanced photosynthesis and growth in tobacco. *Molecular Biology Reports*, **45**, 1745–1758.

Yamori W, Takahashi S, Makino A, Price GD, Badger MR, von Caemmerer S (2011a) The roles of ATP synthase and the cytochrome b6/f complexes in limiting chloroplast electron transport and determining photosynthetic capacity. *Plant Physiology*, **155**, 956–962.

Yamori W, Sakata N, Suzuki Y, Shikanai T, Makino A (2011b) Cyclic electron flow around photosystem i via chloroplast NAD(P)H dehydrogenase (NDH) complex performs a significant physiological role during photosynthesis and plant growth at low temperature in rice. *Plant Journal*, **68**, 966–976.

Yamori W, Kondo E, Sugiura D, Terashima I, Suzuki Y, Makino A (2016) Enhanced leaf photosynthesis as a target to increase grain yield : insights from transgenic rice lines with variable Rieske FeS protein content in the cytochrome b 6 / f complex. 80–87.

Yang Y, Costa A, Leonhardt N, Siegel RS, Schroeder JI (2008) Isolation of a strong Arabidopsis guard cell promoter and its potential as a research tool. *Plant Methods*, 1–15.

Zeiger E (2000) Sensory transduction of blue light in guard cells. *Trends in Plant Science*, **5**, 183–185.

Zeiger E, Armond P, Melis A (1980) Fluorescence properties of guard cell chloroplasts: evidence for linear electron transport and light harvesting pigments of photosystem I and II. *Plant physiology*, **67**, 17–20.

Zeiger E, Talbott LD, Frechilla S, Srivastava A, Zhu J (2002) The guard cell chloroplast: A perspective for the twenty-first century. *New Phytologist*, **153**, 415–424.

Zeiger1 E, Zhu J (1998) Role of zeaxanthin in blue light photoreception and the modulation of light–CO 2 interactions in guard cells. *Journal of Experimental Botany*, **49**, 433–442.

Zhao C, Liu B, Piao S et al. (2017) Temperature increase reduces global yields of major crops in four independent estimates. *Proceedings of the National Academy of Sciences of the United States of America*.

Zhu X-G, Long SP, Ort DR (2010) Improving Photosynthetic Efficiency for Greater Yield. *Annual Review of Plant Biology*, **61**, 235–261.

-Appendices

Appendix (A)

- The sequence of the homolog genes in tobacco and design primers for them.

Nitab4.5_0000697g0100.1 (Nt14-CER2)

TACAGTCAACAAAAATCCCCCTTACTTATAATCTTTTATCCTTCAACTTCTTTCCAAA
GAAAAAACCAACTCAATCAAAATAATCTCAAAAATAGAAAAAATTTAATTTCAAGAAA
TGGTGTCTTCAAAATCAGAAGCTGGTCTAATTTACAACATCAAGTTTTCCTCAGTTG
GACCAGCAAATGTAACAGGACAAGATGTAGTTTATGAGCCAAGTAATATGATTTAG
CCATGAAATTACACTACTTGAGAGGGATTTATTACTTTAATAGCCAAGCGTTTCAAG
ATGTAACCATATATAAAGTTAAGGAGCCAATATTTTCATGGTTTAGCCATTTTTATAT
GACAGCTGGTAGGTTTAGGAGAGCAGAATCTGGGAGGCCATATATAAAATGCAATG
ACTGTGGAGCTAGGTTTATTGAAGCACAATGTGATAAGACTTTGGAAGAATGGCTA
GAAATGAAAGATGCTTCTCTTGAGAAATTACTTGTTTCTAATCAAGTTCTTGGTCCT
GAGTTGACTTTCTCCCCTCCAATCCTCATACAGCATACAAAATTCAAATGTGGAGGA
ATTGCATTGGGCTTAAGTTGGGCCCATGTACTCGGAGATGTATTCTCAGCCACTGA
ATTTATTAACTTTTTGGGGAAAGTAGTTGGTGGATTCCAACCAGCCCGGCCCAATA
ACTTGGCCCATTTATTGACAAAAGCAAACCCAACCCAAACCCTGCAAAAGATCGTG
GAGGATCCACTTTCAATAAAACGGGTCGGACCAGTTGAAGATCATTGGATTGCCAA
CAATAGTTGCAAAATGGAGTCCTTTTCATTCTATATTACTGCCTCCAAATTGGGCCA
CTTGCAATCAAGAACAGAAATTCAAGGCCCATTTGAATCATTATGTGCTATTATTTG
GCAGTCCATTTCTAGAATTAGAGATGGGCCTGAGCCCAAAGTTGTGACCATTTGTA
AAAAGAGTGAGGAAAAGAAAGAAGGCCCCGTAGGAAACAATCAATTCATTGGTGTG
GTAAAGGTTGATCACTCAATTAGAGAAGCTAATCCTAGTGAATTAGCAAGGTTAATT
AAAAATGAGATTATCGACGAGCGATTAAAGATCGATGAAGCCATCGAAAAAGATCA
TGGAGTATCGGACGTGGTTGTTTACGGAGCAAATTTGACTTTCGTGAACGTGGAAG
GTGCTGATCTCTATGGATTTGACTGGGAGGGACACAAACCGATGAATGTAAGTTAC
CTAGTCGATGGAGTTGGCGATGCAGGAGCCGTCGTGGTGCTTCCGGCCGGGCCA
AATGATTCTAGCAAGGATGGTGATGAAGGAAGGGTTGTGACCATGACTTTGCCTGA
GGATGAGATAATGAAGTTGAAATATGAGCTAAACAAGGAATGGTCTATTGCTTGAA
GTTAAAATGTATTTGTTTCATTCTTGTTCCATAATTTTAATTTGGTGTGAGGTCCAAA
GACACTGTATTTAATAATTGCTTTATGTAATGCTATTTAGATATTAGCCAGTATTTATT
TTGTCATAAAATTTTAAATTAAAATTCGTAATTTCAAG

2-Nitab4.5_0000777g0090.1 (Nt13-GORK)

ATGTCGATGATGAGGAGAGAAGTAGAGGAAGAGAGGAATATTAGTAGAAGAGATTC
AGGCGCAGAGTATAAGATGGAGGATTTAACGAAACCGTCGAGAAGTAGTAGGCGA
TTCGCGTTAATGGAGAAGGAGCTAGGACTGGACTCCAGTACTCACTCCAGGTTTAG
CAGAGAAAACGTCATCAATGGCATCAAAGGCCTCTCCCAAGGTTCCGTTATTTATC
CCGATGACAGGTGGTACAAGATATGGGAGAAGTTTATCCTGATTTGGGCGATTTAT
TCATCTTTTTTTACTCCAATGGAGTTTGCATTCTTCACGGGATTGCCCAGGAAACTT
TTTCTCTTAGACATTTGTGGCCAAATAGCTTTTCTTGTCGACATAGTCGTGCAATTC
TTTGTAGCTTACAGAGATAGTCAGACCTACAAGATGGTGCATAAACGAACCCCTATT
GCTCTTCGGTACTTGAAAACTCATTTTATCTTGGATTTTCTCAGTTGCATGCCGTGG
GATAACATTTATAAGGCTGCTGGCAAAAAAGAGGGATTGAGATACCTTTTATGGATT
AGGTTATGCAGGGTGCGCCGAGTCAATGACTTTTTTCAGAAGATGGAGAAAGATAT
TCGGATCAATTTTCTCTTCACTAGGATATTAAAACTTATCGTTGTTGAACTCTATTGC
ACGCATACAGCAGCTTGCATCTTTTACTTTTTGGCTACCACTCTGCCTGAAGAGAAA
GAAGGTTACACATGGATTGGGAGTTTGACCCTGGGAGACTACAGTTATTCACACTT
TAGAGAGATTGATCTCTGGAGGCGATACATCACTTCTCTGTATTTTGCAATTGTCAC
TATGGCAACTGTGGGCTATGGTGACATACATGCAGTCAATCTGAGGGAAATGATAT
TCGTAATGGTTTATGTCTCTTTTGACATGATTCTTGGTGCTTATTTGATCGGTAATAT
GACAGCACTGATTGTCAAGGGATCAAAAACTGTCCGATACAGGGATAAAATGACAG
ATCTTATGAACTATATGAACAGAAATAGACTCGGAAGAGAAATTCGTACTCAAATTA
AAGATCACTTGCGATTACAATATGAAAGCGCTTACACTGATGCAGCTGTTCTTCAG
GACCTTCCCATCTCAATCCGTGCCAAGATATCCCAGACATTATATCAGTCTTGCATT
GAAAATATTCCTCTTTTCAGGGGCTGCTCCTCAGAATTCATAAGTCAAATTGTAACT
CGAGTGCGTGAAGAATTTTTCCTTCCAGGAGAAGTGATCATGGAACAAGGGCATGT
CATAGACCAACTTTATTTTGTCTGTCATGGTGTTCTGGAGGAAATTGGTATAGGGAA
AGATGGGTCAGAAGAGACAGTAGCACTTCTTGAGCCAAATAGCTCGTTTGGGGAAA
TATCCATTCTTTGCAACATTCCACAACCATATACTGTCCGTGTTTGTGAACTCTGCA
GACTCATACAGATTGATAAGCAATTGTTTTCAAATATTTTGGAGATCTACTTTCATGA
CGGGAGAAGAATTTTGACTAACTTATTAGAGGGAAAGGATTCTGATCTTCGTGTGA
AGCAAGTGGAGTCAGATATTACATTCCATATTGGGAAACAAGAGGCTGAGCTTGCT
TTGAAAGTGAATAGTGCAGCTTATCATGGTGATTTGCACCAGCTGAAGAGTCTGAT
CCGAGCTGGAGCTGATCCCAACAAGAAAGATTATGATGGAAGATCTCCTTTGCATC
TTGCAGCGTCCAGAGGATATGAAGACATCTCTCTTTTCCTTATCCAAGAAGGTGTT
GATCTCAATGCTTCAGACAATTTTGACAACACACCGCTGTTTGAAGCTATCAAGAAT
GGACACGATCGTGTTGCTTCATTACTTGTTAAGGAAGGTGCTTTCTTGAAGATCGA
AAATGCTGGTAGCTTTTTGTGTGTGTTGGTTGCAAAAGGGGATTCAGATCTACTAC
GAAGGCTGTTGTCCAATGGTATTGATCCAGACTCTAAAGACTATGATCACCGAACA
CCACTCCATGTAGCGGCTTCTCAAGGATTATTCACGATGGCAAGATTGCTTCTGGG
AGCTGGTGCTTCTGTTTTCTCAAAAGACAGATGGGGGAATACTCCATTTGATGAAG
CTAGACTAAGTGGAAACAATCAATTGACCAAGCTTATGGAAGAAGCAAAATCAACT
CAGATATCGGAATTCCCTATTGCTCCACACGAGATCTCAGAAAAAATGCACCCACG
GAAGTGTACTGTGTTTCATTTCCACCCATGGGAGCCCAAGGATCTCAGGAAACATG
GTGTTGTACTGTGGATACCTAAGAGTATGGAAGAGCTCGTTACTACAGCATCGGAA
CAACTCAACTTTCCATCTGGCTCTTGTATTTTATCAGAAGATGCAGGTAAAATACTT
GATATAGGTTTGATTTCTGATGGTCAGAAGTTGTACTTGATCAGTGAAACAACTTGA
GAGTACCTCGTCTATATATAGTTATATCCTGTGTAGCTTTGGGGTTTGTATA

Appendix (B)

- A comparison of gene expressions between mesophyll and guard cells in WT and transgenic lines.

- **Overexpression Rieske FeS lines**

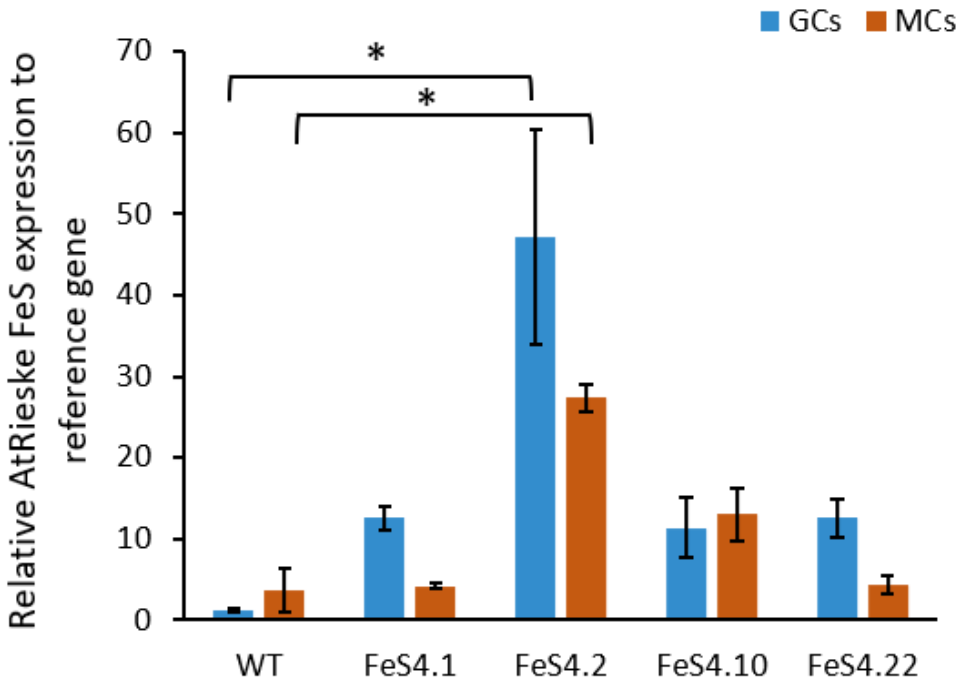

Appendix (C)

- A comparison of gene expressions between mesophyll and guard cells in WT and transgenic lines.

- **Antisense SBPase lines**

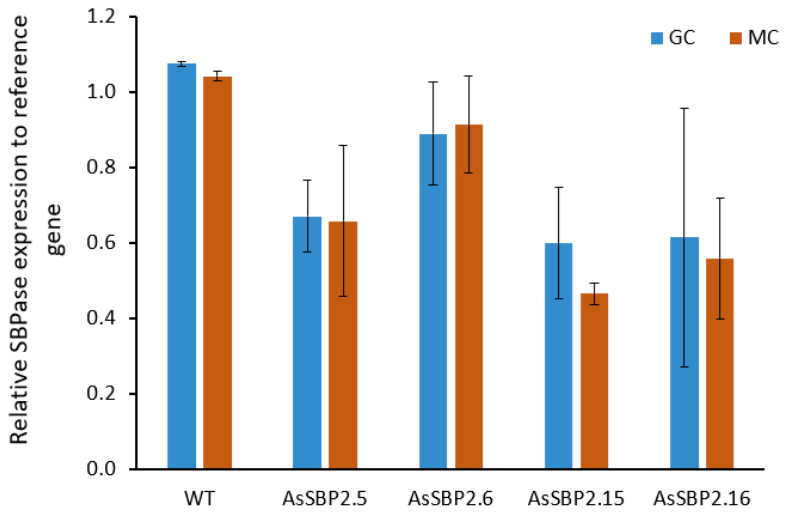

- **Overexpression SBPase lines**